Synthetic Studies of Novel Polymeric Materials for Optical Applications

Shuhei Yamada

Kyushu Institute of Technology

2011

PREFACE

The study in this thesis has been carried out under direction of Professor Kohji Yoshinaga in the Department of Materials Science, Graduate School of Engineering, Kyushu Institute of Technology. The study is concerned with synthesis and characterization of novel polymeric materials, aiming at applications for optical or electronic devices

The author wishes to express his sincerest gratitude to Professor Kohji Yoshinaga for his kind guidance, valuable suggestion throughout this work. The author wishes to thank sincerely Assistant Professor Emiko Mouri, Mr. Hiroyuki Karakawa, Dr. Kenichi Takizawa, Dr. Toshihiko Urakawa, Mr. Zhiguo Ma, Dr. Zhifeng Wang, and all the members of Yoshinaga's lab for hearty encouragement. The author also wishes to express his sincerest gratitude to Professor Shigeori Takenaka, Professor Ryuichi Shiratsuchi, and Professor Takahito Itoh of Mie University for their valuable suggestion and helpful advices.

The author would like to express his heartfelt thanks to Professor Hongsuk Suh of Pusan National University, Busan, Korea, for his kind invitation for collaborative studies on Organic Light Emitting Diode (OLED), his warm guidance, and encouragement, during the author's staying from June, 2009 to March, 2010. The author also wishes to express his heartfelt gratitude to Dr. Suhee Song, Mr. Seijung Park, Ms. Joo Young Shim, and all the members of Suh's lab for their valuable discussion, and warm encouragement. The author is also much obliged to Professor Jang Oo Lee and Mr. Jung Min Moon for warm encouragement and helpful advices.

Furthermore, the author deeply appreciates to Mr. Kohichi Okada, Mr. Kohji Kuramoto, and Mr. Sadayoshi Watanabe, for their kind and useful advices and hearty encouragement, during doctoral course in Kyushu Institute of Technology.

Finally, the author wishes to express his deep appreciation to his parents, Mr. Mitsuo Yamada, and Mrs. Miho Yamada for their continuous assistance and warm encouragement.

Shuhei Yamada

Department of Materials Science
Graduate School of Engineering
Kyushu Institute of Technology
March, 2011

CONTENTS

GENERAL INTRODUCTION

As the results of extensive research within the 20th century, polymeric materials[1] of today could be widely utilized for industrial products, such as plastic bottles, synthetic fibers, rubber, and so on. Immediate developments of these polymeric materials obviously have improved our standard of living. For past decades, considerable efforts have been devoted to developing functional polymeric materials for many kinds of applications. Especially, electronic materials, like organic light emitting diode (OLED), photovoltaic cell, and organic transistor are expected to play a key role as the promising materials in near-future technology.[2] Use of Polymeric materials have great advantage for fabrication of advanced functional electronic materials, because of their low density, ability to be shaped and molded at relatively low temperatures, and excellent impact resistance, compared to common materials such as inorganic metal. Therefore, in their materials, the parts and components, which have been generally made of metals, ceramics, or glasses, are redesigned with polymeric materials on a daily basis. However, although demands for utilizing polymeric materials in the field of advanced technology have been increasing, a lot of problems still remain in terms of functionalities. One of the important ways to overcome challenging themes is fusion and collaboration through some research fields.

Recently, needs of the optical materials with high refractive index have been increasing in the fields of highly reflective and antireflection coatings, in the areas of solar cell, liquid crystal displays, and ophthalmic lenses.[3] In order to enhance refractive index, so far, some polymer materials containing sulfur atoms, aromatic rings, metallic elements, and halogen atoms have been developed. However, it is difficult to synthesize the polymer materials with refractive index higher than 1.7. In this regards, hybrid organic-inorganic materials have been attracting substantial attention as new materials, because of characteristic synergetic effects of organic and inorganic components.[4, 5] In general, inorganic metal oxides exhibit higher refractive index as compared with organic compounds. Therefore, incorporation of colorless and high refractive inorganic compound, such as titanium oxide, zirconium oxide, or zinc oxide, into polymeric compound could lead to fabrication of high refractive and transparent organic-inorganic materials. In most cases of the challenging works, however, homogeneous dispersion of inorganic particles or powder into polymeric materials is usually confronted with difficulties, because of extremely low compatibility

between organic and inorganic compounds.

On the other hand, since electroluminescence (EL) in conjugated polymers has been first reported about poly(*p*-phenylene vinylene) (PPV)[6] in 1990, considerable efforts have been devoted to developing conjugated materials as the active units in organic light emitting diodes (OLEDs) for use in display applications. Dialkyl polyfluorene (PF) have acquired much interest as prospective blue light emitting layer. Photo and thermal stability of PFs are also found to be higher than those of PPV. Also, PFs contain a rigid biphenyl unit, leading to large band gap with efficient blue emission, and the remote C-9 position which allows the facile substitution to improve the solubility without significantly increasing the steric interaction between polymer backbones. Nevertheless, there is still need for improvement of the electronic and optical properties to enhance their performances.

Herein, studies on strategies for synthesis of TiO_2 nanoparticles and incorporation into polymer matrix for fabrication of high refractive and transparent organic-inorganic hybrid materials, and syntheses and characterizations of novel conjugated polymers for organic light emitting diode are described.

In Chapter 1, hydrothermal synthesis of TiO_2 particles from peroxotitanic acid solution in the presence of polymer additives is reported. It was found out that addition of hydrophilic or amphiphilic polymer controlled well crystal polymorphs, size, and shape of TiO_2 particles in the crystallization from peroxotitanic acid in aqueous solution.[7, 8]

In Chapter 2, dispersion of TiO_2 particles into low polar organic solvents, using amphiphilic polymers and then incorporation of TiO_2 into PMMA matrix to obtain high refractive and transparent thin film is described. Well-dispersed TiO_2 particles in organic solvents were achieved by addition of amphiphilic polymer, poly(vinyl pyrrolidone) (PVP), PVP-*co*-PMMA, or PVP-*b*-PMMA block copolymer as effective dispersants. PVP_{154}-*b*-$PMMA_{156}$ dispersant addition led to high dispersion stability of TiO_2 particles of 20 nm in chloroform and effective incorporation into PMMA matrix to give hybrid films with increased refractive index and high transparency.[9]

In Chapter 3, a novel strategy for incorporation of TiO_2 particles into PMMA matrix aiming at high refractive and transparent materials is reported. It is very difficult to incorporate TiO_2 nanoparticles less than 20 nm in size into polymer matrixes by surface modification or by using polymer dispersants, because of relatively low surface charge. Synthesis of nanosized-TiO_2 particles of around 20 nm within core in polymer micelles of PMMA-*b*-PAA in toluene solution via sol–gel process from metal alkoxide, and then

incorporation of their nanoparticle into polymer film are described. It was found out that the refractive index of the films proportionally elevated with TiO_2 content to attain 1.579, at 30 wt% of TiO_2 content, which was 0.1 higher than that of PMMA films. The refractive index of hybrid films well agreed with calculated values by the Lorentz–Lorenz equation, using the index of anatase-type TiO_2.[10]

In Chapter 4, syntheses and properties of new series of the fluorene-based polymers with carbazole and oxadiazole pendants for application of OLEDs are described. In the case of copolymers incorporating alternately carbazole units into polyfluorene backbone, the EL spectra of their polymers showed two distinct peaks comprising the maximum peak at 427 nm and additional one at around 540 and 530 nm, respectively. The CIE coordinates of the devices was (0.28, 0.33), approaching the value of the standard white of National Television System Committee (NTSC) (0.33, 0.33). Additionally, it was confirmed that incorporating carbazole or phenothiazine units successfully tuned EL spectra of OLEDs.[11, 12]

References

1. (a) Alexandre, M.; Dubois, P. *Mater. Sci. Eng. R.-Rep.* **2000**, 28, 1. (b) Yaghi, O. M.; O'Keeffe, M.; Ockwiq, N. W.; Chae, H. K.; Eddaoudi, M.; Kim, J. *Nature* **2003**, 423, 705. (c) Caruso, F.; Caruso, R. A.; Mohwald, H. *Science* **1998**, 282, 1111. (d) Ray, S. S.; Okamoto, M. *Prog. Polym. Sci.***2003**, 28, 1539. (e) Forrest, S. R. *Nature* **2004**, 428, 911.
2. (a) Nazeeruddin, M. K.; Kay, A.; Rodicio, I.; Humphrybaker, R.; Muller, E.; Liskap, P.; Vlachpoulos, N.; Gratzel, M. *J. Am. Chem. Soc.* **1993**, 115, 6382. (b) Yu, G.; Gao, J.; Hummelen, J. C.; Wudl, F.; Heeger, A. J. *Science* **1995**, 270, 1789. (c) Brabec, C. J.; Sariciftci, N. S.; Hummelen, J. C. *Adv. Funct. Mater.* **2001**, 11, 15. (d) Huynh, W. U.; Dittmer, J. J.; Alivisatos, A. P. *Science* **2002**, 295, 2425.
3. (a) Cui, Z. C.; Lu, C. L.; Yang, B.; Shen, J. C.; Su, X. P.; Yang, H. *Polymer* **2001**, 42, 10095. (b) Okutsu, R.; Ando, S.; Ueda, M. *Chem. Mater*. **2008**, 20, 4017. (c) Hart, S. D.; Maskaly, G. R.; Temelkuran, B.; Prideaux, P. H.; Joannopoulos, J. D.; Fink, Y.

Science **2002**, 296, 510.

4. (a) Gomez-Romero, P. *Adv. Mater* **2001**, 13, 163. (b) Sanchez, C.; Julián, P.; Belleville, M.; Popall, M. *J. Mater. Chem*. **2005**, 15, 3559. (c) Mammeri, F.; Le Bourhis, E.; Rozes, L.; Sanchez, C. *J. Mater. Chem*. **2005**, 15, 3787. (d) Mlynarcíkova, Z.; Kaempfer, D.; Thomann, R.; Mühlhaupt, R.; Borsig, E.; Marcincin, A. *Polym. Adv. Technol*. **2005**, 16, 362.
5. Vu-Khanh, T.; Sanschagrin, B.; Fisa, B. *Polym. Compos*. **1985**, 6, 249.
6. Burroughes, J. H.; Bradley, D. D. C.; Brown, A. R.; Marks, R. N.; Mackay, K.; Friend, R. H.; Burn, P. L.; Holmes, A. B. *Nature* **1990**, 347, 539.
7. Yoshinaga K.; Yamauchi M.; Maruyama D.; Mouri E.; Koyanagi T. *Chem. Lett.* **2005**, 34, 1094.
8. Wang, Z. F.; Yamada, S.; Zhang, M.; Kanzaki, H.; Yoshinaga, K. *Colloid Polym. Sci.* **2010**, 288, 433.
9. Yamada, S.; Wang, Z. F.; Mouri, E.; Yoshinaga, K. *Colloid Polym. Sci*. **2009**, 287, 139.
10. (a) Yamada, S.; Mouri, E.; Yoshinaga, K. *J. Polym. Sci. Part A Polym. Chem*. **2011**, 49, 712. (b) Yamada, S.; Wang, Z.; Yoshinaga, K. *Chem. Lett.* **2009**, 38, 828.
11. Jin, Y.; Song, S.; Kim, J. Y.; Kim, H.; Lee, K.; Suh, H. *Thin Solid Films* **2008**, 516, 7373.
12. Yamada, S.; Park, S.; Song, S.; Heo, M.; Shim, J. Y.; Jin, Y.; Kim, I.; Lee, H.; Lee, K.; Yoshinaga, K.; Kim, J. Y.; Suh, H. *Polymer* **2010**, 51, 6174.

CHAPTER 1

Controlled Crystallization of Titanium Dioxide Nanoparticles in the Presence of Hydrophilic Polymer from Peroxotitanic Acid

1-1. Introduction

Titanium dioxide (TiO_2) has been widely used as a pigment[1] and sunscreen,[2, 3] paints,[4] ointment, toothpaste,[5] and so on,[6] since its commercial production in the early twentieth century. In 1972, Fujishima and Honda discovered photocatalytic properties of TiO_2 electrode under ultraviolet (UV) light.[7-9] Since then, enormous efforts have been devoted to the research of TiO_2 materials, which has led to many promising applications in areas ranging from photovoltaics and photocatalysis to photo-/electrochromics and sensors.[10-12] These applications can be divided into "energy" and "environmental" categories, many of which depend on only the properties of TiO_2 materials itself, but also on modifications of TiO_2 materials host with inorganic and organic dyes.

An exponential growth has been demonstrated in nanoscience and nanotechnology in the past decades.[13-17] When the size of the materials become smaller and smaller, and down to the nanometer scale, novel physical and chemical properties emerge.[18, 19] These properties of nanosized-TiO_2 depend on the crystal polymorphic phase, size, and shape. Therefore, completely controlled preparation of TiO_2 is an essential subject in this field. To date, uniform TiO_2 spherical particles were synthesized by hydrolysis of Ti^{4+} and sol-gel process.[20, 21] Especially, it has been receiving great attention that well-controlled preparation of TiO_2 nanometer-sized particles of spindle, cubic or fiber type in the reaction systems containing amines or amino acids, via sol-gel process was developed by Sugimoto et al.[22]

On the other hand, deoxygenation and/or dehydration of peroxotitanic acid, $Ti(OH)_3(OOH)$, which was produced by oxidation of hydrated TiO_2 sol with H_2O_2, afforded crystalline or noncrystalline TiO_2 particles.[23, 24] In these processes, TiO_2 particles should be produced via dehydration of dihydroxytitanium oxide, $TiO(OH)_2$. Thus, the presence of organic compound, being able to coordinate to the oxotitanium species, during dehydration or deoxygenation can be expected to control crystal phase, particle size and shape of TiO_2. Herein, we describe controlled preparation of rutile or anatase uniform

ultrafine TiO_2 particles from peroxotitanic acid in the present of hydrophilic or amphiphilic polymer. Also, effects of hydrophilic or amphiphilic polymer on the size and shape of TiO_2 particles were investigated.

1-2. Experimental Section

Materials

Titanium ethoxide was purchased from Merck, Germany. All polymers, poly(acrylic acid) (PAAc), poly(vinyl alcohol) (PVA), poly(sodium acrylate) ($PAAc^-Na^+$), poly(ethylene glycol) (PEG), poly(ethyleneimine) (PEI), and other reagents, hydrogen peroxide, ammonium peroxodisulfate (APS), methacrylic acid (MA) were purchased from Wako Pure Chemical Industries, Ltd., Japan. All the chemicals and solvents were used without further purification.

Measurement

Particles size and distribution were determined by a dynamic light scattering (DLS) method on DLS-7000DL, Otsuka Electronics Co., Ltd., Japan, with a He–Ne laser, at a reflection angle of 90 °C. Number-average molecular weight (M_n) and polydispersity index (M_w/M_n) of polymers were determined by a gel permeation chromatography on straightly connected-columns, PL-gel MIXED-C and PLgel MIXED-D, Polymer Lab. Co. Ltd., at 60 ℃ using DMF containing 10 mM LiBr as an eluent, at flow rate 0.8 mL/min, calibrated with poly(ethylene glycol) standard. Transmission electron microscope (TEM) observation was carried out on Hitachi H-800, Japan, with acceleration voltage of 100 kV. The samples for TEM observation were prepared by evaporating the suspension on a carbon-coated cupper grid. X-ray reflection analyses were carried out on JEOL JDX-3500K, Japan. The weight fraction of anatase in TiO_2 particles was determined by following equation,[25]

$$\text{Fraction of anatase (wt\%)} = 100\times I_A(I_A+1.265\ I_R)$$

where I_A and I_R represented strongest reflection for anatase (101) and rutile (110) at Bragg angles 12.68 º and 13.73 º for CuKα radiation, respectively.

Synthesis of Poly(methacrylic acid) (PMA) by Radical Polymerization

A mixture of MA (5 mL, 11.7 mmol) and APS (15 mg, 0.056 mmol) was added into 50 mL distilled water, and then the aqueous solution was refluxed at 100 °C under nitrogen atmosphere for 24 h. The resulting polymers were precipitated from the reaction mixture, by addition of 1 N hydrochloride (HCl). After collection by filtration, the obtained polymers were dried under reduced pressure.

Synthesis of TiO_2 Particles in the Presence of Polymer

A typical run was shown in Scheme 1. To 3 mL titanium ethoxide and 100 mL ethanol was gradually added 3 mL distilled water, and then the mixture was stirred for 30 min at room temperature. Resulting precipitates were centrifugally separated from the solution and then dried under reduced pressure. One hundred twenty milligrams of the obtained TiO_2 sol was added to a mixture of 10 mL distilled water and 15 mL 30% hydrogen peroxide and then the solution was irradiated by ultrasonic wave for 1 h to give peroxotitanic acid solution. Fifty milligrams PAAc was added to the peroxotitanic acid solution and then stirred at 70 °C for 48 h. Eventually, 2 mL of peroxotitanic acid were diluted with 38 mL of distilled water, and then its solution was heated in an autoclave at 220 °C for 5 h.

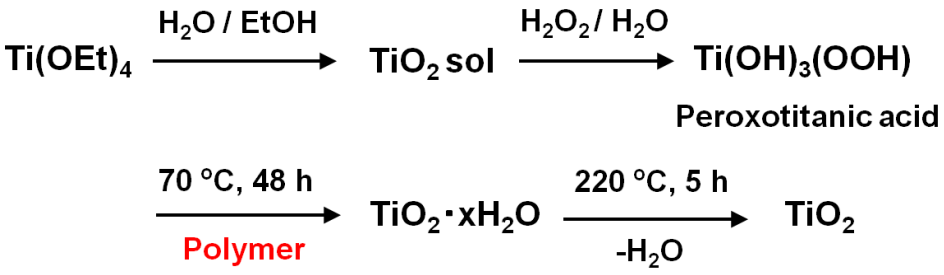

Scheme 1. Preparation of TiO_2 particles in the presence of polymer from peroxotitanic acid.

1-3. Results and Discussion

1-3-1. Effect of Polymer Addition on Crystal Structure and Size of TiO_2 Particles

In Table 1, the results of TiO_2 crystallization in the presence of hydrophilic or amphiphilic polymer are shown. Although synthesis of TiO_2 particles from peroxotitanic acid without any polymer addition showed the rutile-rich particles, the crystallization in the presence of poly(acrylic acid) (PAAc), poly(sodium acrylate) ($PAAc^-Na^+$), poly(vinyl alcohol) (PVA) and poly(methacrylic acid) (PMA) gave rise to anatase-rich TiO_2 particles in the range from 20 to 50 nm, which stably dispersed for long period over 1 week in aqueous solution. Also, it was confirmed that the crystallization with hydrophilic polymer containing carboxyl or hydroxyl groups on the side chain such as PAAc and PMA led to the formation of nanometer-sized particles. It is noteworthy that these polymers afforded anatase-rich TiO_2 particles, while amphiphilic polymers of poly(ethylene glycol) (PEG) and poly(ethylene imine) (PEI) gave rutile-rich TiO_2 particles in the range of particle size from 20 to 800 nm. In most cases, the fraction of anatase or rutile of TiO_2 particles increased with increasing amount of added polymer. At any rate, addition of large amount of hydrophilic polymer resulted in perfect controlling of crystallization (Figure 1). These results, therefore, suggested that coordination of carboxyl or hydroxyl groups on the polymer to peroxotitanic acid or dihydroxytitanium oxide plays an important role in terms of controlling crystal morphs and particles size during crystallization. In this respect, weak coordination of PEG or PEI to oxotitanium species, due to hydrophobic nature presumably gives large TiO_2 particles and stable crystal phase of rutile. Regarding molecular weight of polymer additive, an increase of number average molecular weight of PAAc from 5,000 to 25,000 scarcely affects particle size and crystal polymorphs of TiO_2. From XRD results, it was also confirmed that crystallization undergoes in heating at 150 °C, while lowering heating temperature led to increasing the amount of amorphous TiO_2. In order to synthesize highly crystallized TiO_2 particles, the hydrothermal treatment over 200 °C was required.

Table 1. Crystal structure and size of TiO_2 particles prepared with water soluble polymer.

Polymer	M_n / 10^3	Dosed polymer / mg	Fraction / wt% (Anatase / Rutile)	Size / nm
None	—	—	19 / 81	>200
PAAc	5	25	100 / 0	22 ± 2[a]
		100	100 / 0	18 ± 2[a]
$PAAc^-Na^+$	15	25	100 / 0	140 ± 50[b]
PMA	88	25	67 / 33	19 ± 2[a]
		50	100 / 0	17 ± 2[a]
PVA	22	25	90 / 10	35 ± 4[a]
		100	100 / 0	50 ± 7[a]
PEG	4	25	3 / 97	20 – 700[b]
		100	0 / 100	20 – 300[b]
PEI	10	25	17 / 83	20 – 800[b]
		100	31 / 69	20 – 250[b]

a) Determined by dynamic light scattering (DLS).

b) Estimated by TEM images.

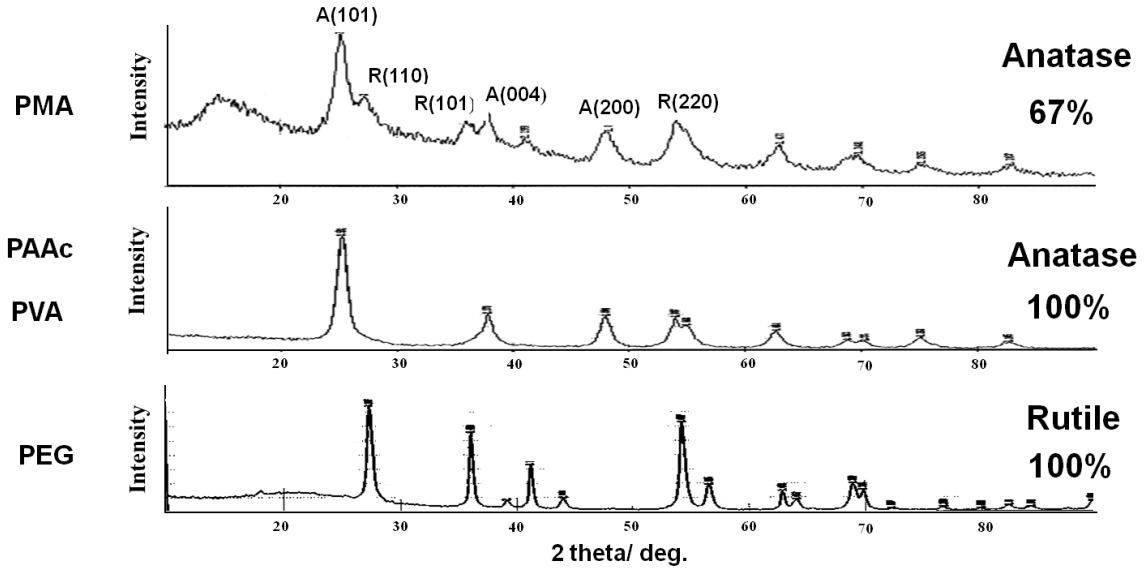

Figure 1. X-ray diffraction spectra of TiO_2 particles prepared in the presence of polymer.

1-3-2. Effect of Polymer Addition on Shape of TiO_2 Particles

In Figure 2, TEM images of TiO_2 particles prepared in the presence of PMA (50 mg) and PAAc (100 mg) were shown. It was observed that fiber-like crystals of 80–100 nm in length and fine particles of 10–20 nm size formed from PMA and PAAc aqueous solution, respectively. These results indicated that chemical structure of added polymer dramatically affects shape of TiO_2 crystal. Sugimoto et al. reported the shape of TiO_2 particles formed changed with pH value in the crystallization via sol-gel process, i.e., from uniform particles, around 50 nm size at pH 9.5 to fiber-like crystals at pH11.6.[22 (a)] In present cases, peroxotitanic acid aqueous solution containing PAAc or PMA exhibited pH 3.7, and then the crystallization of TiO_2 proceeded under acidic condition. It is therefore suggested that present crystallization was possibly controlled by quite different process from those in the sol–gel method proposed by Sugimoto et al.[22 (b), (c)] In this respect, the reaction system with poly(sodium acrylate) ($PAAc^-Na^+$), of average molecular weight 1200, also gave oval-shape particles in the range of size from 50 to 200 nm, as shown in Figure 2b, being similar to TiO_2 particles reported by Sugimoto et al.[22 (d)] Peroxotitanic acid aqueous solution containing 25 mg $PAAc^-Na^+$ exhibited pH 5.8. Thus, these results suggested that

shape of TiO_2 particles was controllable by additive polymer and pH of the solution. The PEG solution gave rise to a mixture of small particles and rod-like TiO_2 crystals of around 200 nm (Figure 3). Probably, weak coordination of PEG to the titanium species induced the formation of thermodynamically stable rutile. In Figure 4, 5, TEM images of TiO_2 particles prepared from $PAAc^-Na^+$ and PVA solution at pH 7.0 are shown. $PAAc^-Na^+$

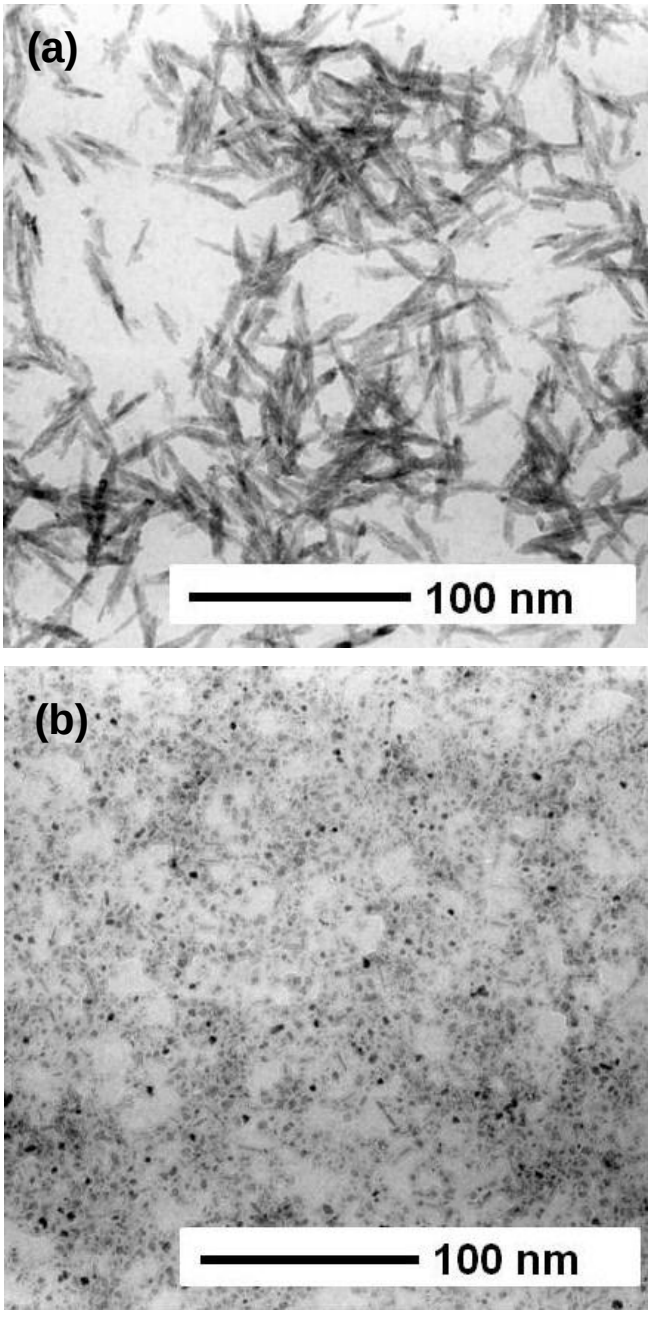

Figure 2. TEM images of TiO_2 particles prepared with PMA (a) and PAAc (b).

solution gave oval-shape crystals mostly the same as those formed at pH 5.8. Interestingly, we could observe relatively homogeneous anatase crystals in hamburger-box shape of 50–80 nm size in PVA solution of pH 7.0.

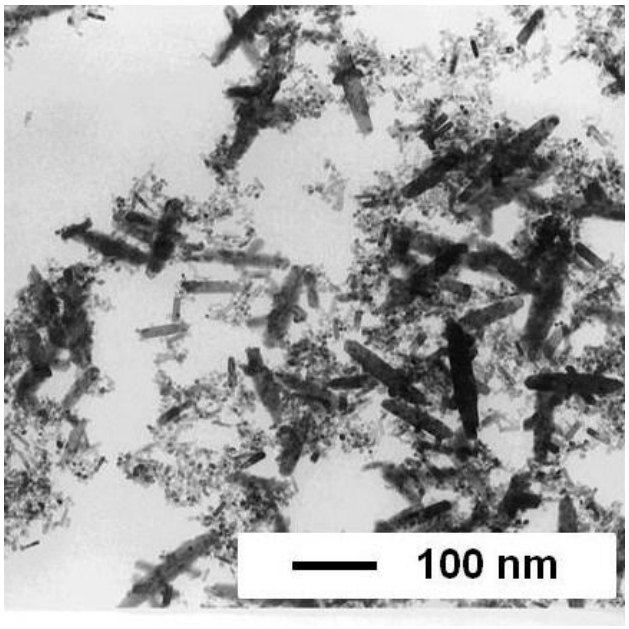

Figure 3. TEM image of TiO_2 particles prepared with PEG.

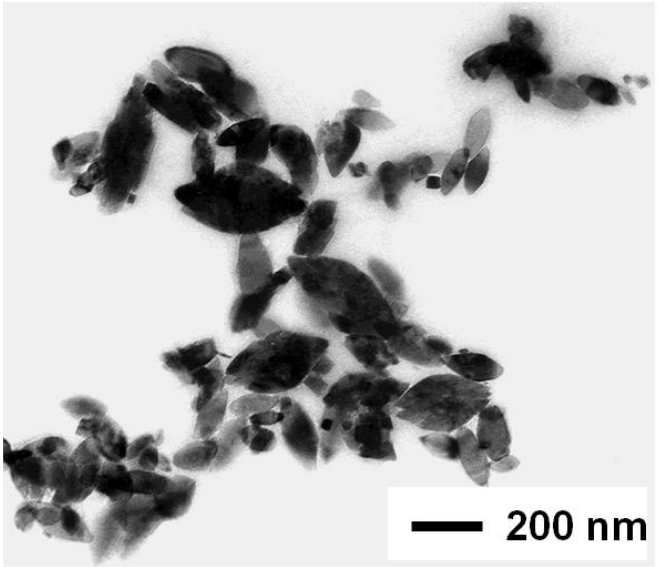

Figure 4. TEM image of TiO_2 particles prepared with $PAAc^-Na^+$.

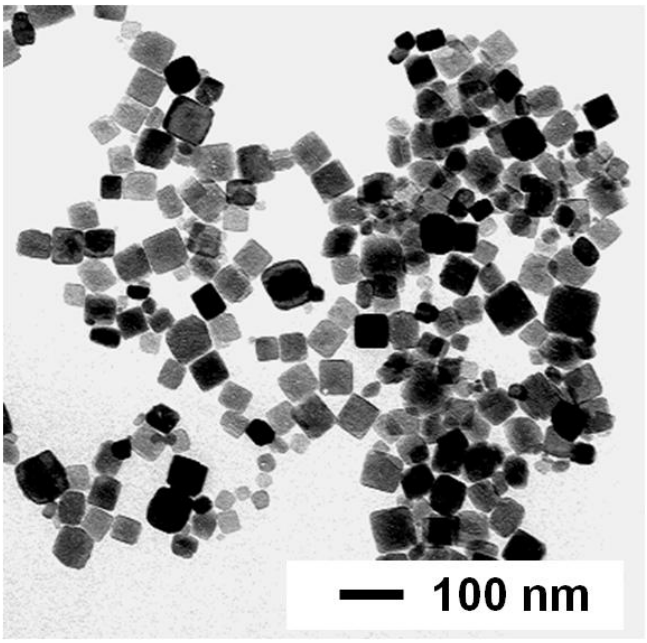

Figure 5. TEM image of TiO_2 particles prepared with PVA at pH 7.0.

Since hydroxyl group of alcohol generally shows a week acidity of pKa~18, the coordination to the oxotitanium species should be much weaker than H_2O molecules (pKa~16). Therefore, complexation of PVA with the titanium oxide species at early stage of crystallization presumably controls their growing to give fine crystalline particles. The reason for the formation of fine crystals in the presence of PVA is yet unclear.

1-3-3. Effect of pH on Dispersibility of TiO_2 Particles

TiO_2 particles produced using PMA, PAAc, and PVA stably kept dispersing in aqueous solution over 1 week. Thus, high dispersion of TiO_2 particles was probably due to protective colloidal effects of polymer molecules adsorbed on the particles. Especially, addition of polymer containing hydroxyl or carboxyl groups showed higher dispersion stability in aqueous solutions. Indeed, the addition of a poor solvent for coexisting polymer, such as acetonitrile, to TiO_2 suspension with PAAc brought about irreversible aggregation of the particles, due to precipitation of PAAc to make the polymer on the particle desorbed.

In this case, average particle size of TiO_2 particle in the PAAc solution increased to 280 nm from 22 nm after the addition of 6 mL of acetonitrile to the suspension (10 mL). Furthermore, successive removal of acetonitrile from the suspension under reduced pressure never returned to the same TiO_2 suspension in terms of particle size distribution as the original one. In order to obtain stable dispersion of TiO_2 particles at high concentration in aqueous solution and/or organic solvents, we investigated effect of pH value. The pH of peroxotitanic acid solution with PAAc additives was adjusted with NH_4OH aqueous solution in the range of pH from 3.7 to 10.5. The resulting TiO_2 particles formed in this pH range were mainly anatase type and then it was observed that fraction of small size particles around 20 nm increased with elevating pH of starting solution (Figure 6). Eventually, TiO_2 particles prepared at pH 10.5 were stably suspended for a long time. Also, TiO_2 particles at higher concentration were prepared in the following process. To a mixture of 10 mL distilled water and 15 mL 30% hydrogen peroxide was added 120 mg of obtained TiO_2 sol, and then the solution was irradiated by ultrasonic wave for 1h to give yellow peroxotitanic acid solution. Fifty milligrams of PAAc additives and NH_4OH aqueous solution was added to peroxotitanic acid solution and then stirred at 60 ºC for 48 h. Finally, the solution was directly heated in an autoclave at 220 ºC for 5h, without dilution by distilled water. The obtained anatase-type TiO_2 particles around 20 nm were stable suspended for a long period. TEM image and particles size distribution (DLS) were shown in Figure 7a and b, respectively. Moreover, the TiO_2 particles were successive dispersed by solvent exchange process, into organic solvents, in which coexisting polymer could be soluble well, such as methanol, ethanol, and dimethylformamide (DMF). We concluded these nanoparticles were expected to be widely applied for fabrication of organic-inorganic hybrid materials.

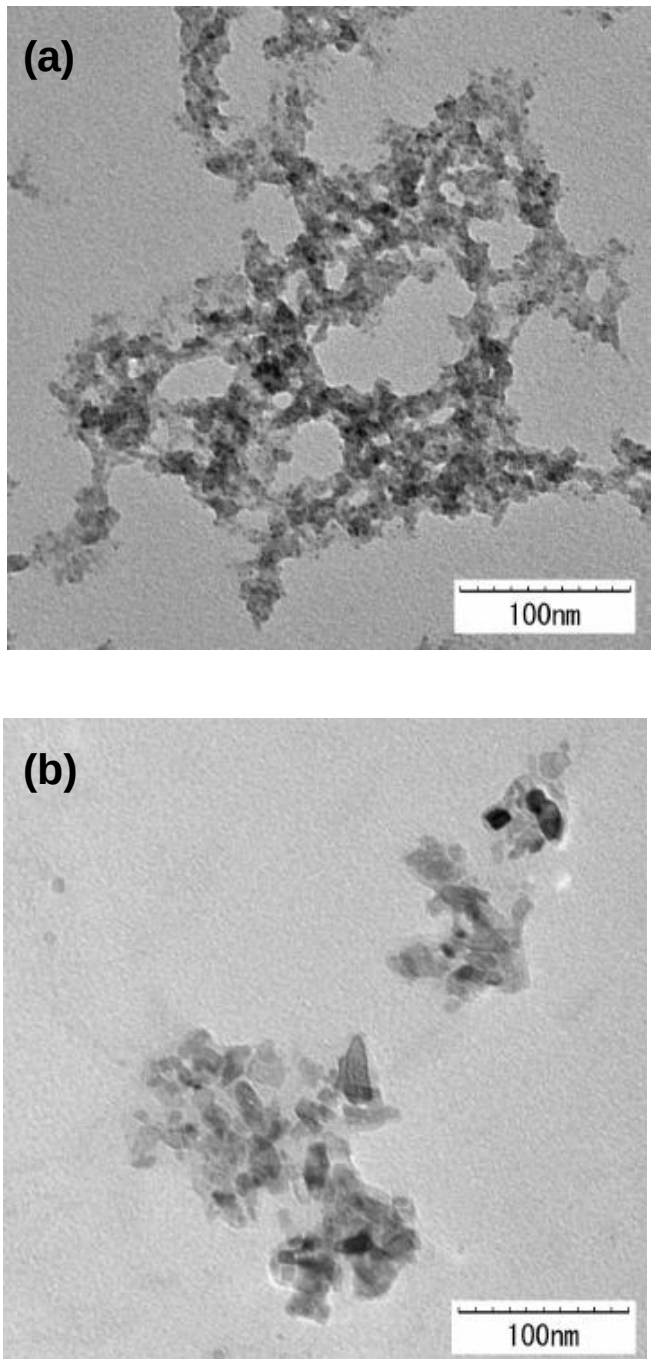

Figure 6. TEM images of TiO_2 particle synthesized with PAAc at pH 4.0 (a) and pH 8.2 (b).

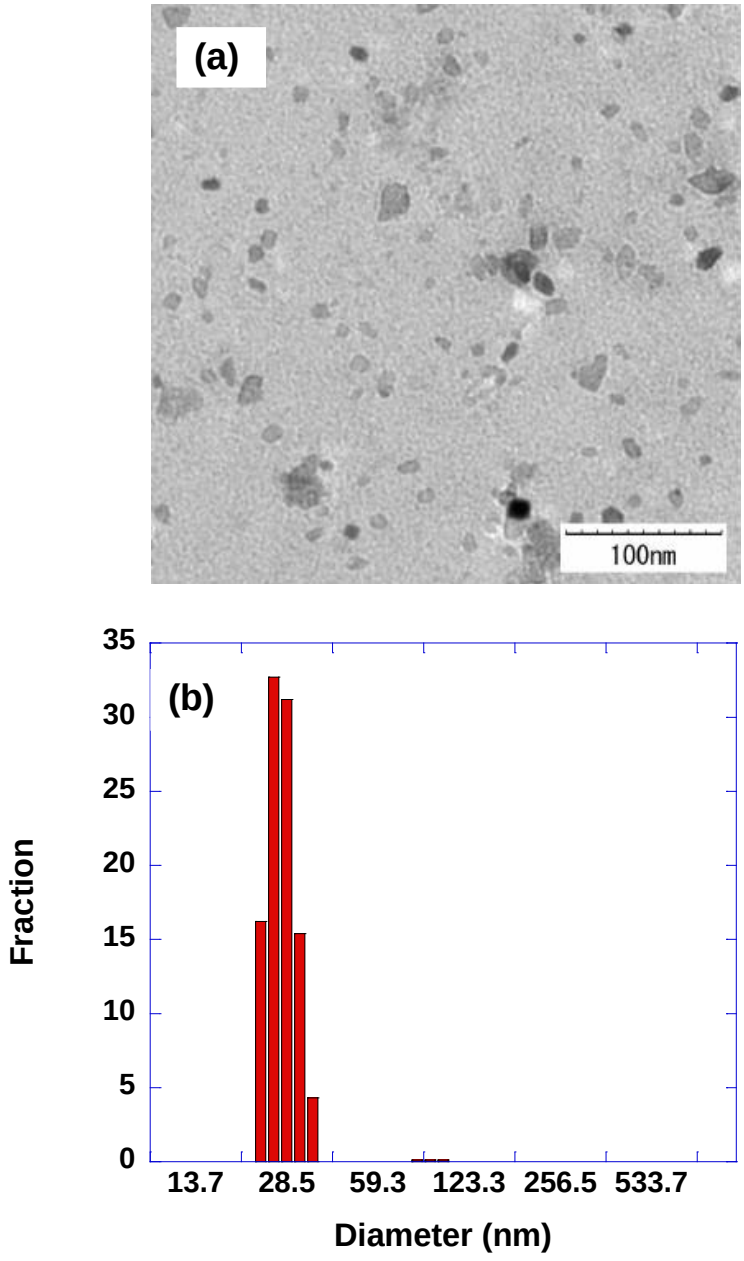

Figure 7. TEM image (a) and particle size distribution of TiO_2 particle synthesized with PAAc at pH 10.5 in the aqueous solution (b).

1-4. Conclusion

In this Chapter 1, we concluded that addition of hydrophilic or amphiphilic polymer controlled well crystal polymorphs, size, and shape of TiO_2 particles in the crystallization from peroxotitanic acid in aqueous solution. Rutile type of particles were prepared in the presence of poly(ethylene glycol) (PEG) or poly(ethylene imine) (PEI). On the other hand, addition of poly(methacrylic acid) (PMA) or poly(acrylic acid) (PAAc) gives rise to anatase type of TiO_2 nanoparticles around 20 nm. Moreover, in the case of poly(vinyl alcohol) (PVA) addition, homogeneous anatase TiO_2 particles of hamburger-box or fiber shape in nanometer size could be successively produced. Preparation of TiO_2 particles in the presence of PAAc addition at high pH value gave rise to stable aqueous suspension for a long time.

1-5. References

1. Salvador, A.; Pasual-Marti, M. C.; Adell, J. R.; Requemi, A.; March, J. G. *J Pharm. Biomed. Anal*. **2000**, 22, 301.
2. Zallen, R.; Moret, M. P. *Solid State Commun.* **2006**, 137, 154.
3. Braun, J. H.; Baidins, A.; Marganski, R. E. *Prog. Org. Coat.* **1992**, 20, 105.
4. Yuan, S. A.; Chen, W. H.; Hu, S. S. *Mater. Sci. Eng. C* **2005**, *25*, 479.
5. Lisebigler, L.; Lu, Q.; Yates, J. T. *Chem. Rev*. **1995**, 95, 735.
6. Fujishima, A.; Honda, K. *Nature* **1972**, 37, 238.
7. Fujishima, A.; Rao, T. N.; Tryk, D. A. *J. Photochem. Photobiol. C* **2000**, 1, 1.
8. Tryk, D. A.; Fujishima, A.; Honda, K. *Electrochim. Acta* **2000**, 45, 2363.
9. Grätzel, M. *Nature* **2001**, 414, 338.
10. Hagfeldt, A.; Grtäzel, M. *Chem. Rev.* **1995**, 95, 49.
11. Millis, A.; Le Hunte, S. *J. Photochem. Photobiol. A* **1997**, 108, 1.
12. Alivisatos, A. P. *J. Phys. Chem.* **1996**, 100, 13226.
13. Alivisatos, A. P. *Science* **1996**, 271, 933.

14. Burda, C.; Chen, X.; Narayanan, R.; El-Sayed, M. A. *Chem. Rev.* **2005**, 105, 1025.
15. Murray, C. B.; Kagan, C. R.; Bawendi, M. G. *Annu. Rev. Mater.Sci.* **2000**, 30, 545.
16. Yin, Y.; Alivisatos, A. P. *Nature* **2005**, 437, 664.
17. Chen, X.; Lou, Y.; Dayal, S.; Qiu, X.; Krolicki, R.; Burda, C.; Zhao, C.; Becker, *J. Nanosci. Nanotechnol.* **2005**, 5, 1408.
18. (a) Chemseddine. A.; Moritz, A. *Eur.J. Inorg. Chem.* **1999**, 235, (b) Moritz, T.; Reiss, J.; Diesner, K.; Su, D.; Chemseddine, A. *J Phys Chem B* **1997**, 101, 8052.
19. (a) Matijevic E.; Budnik M.; Meites L. *J. Colloid Interface Sci.* **1977**, 61, 302, (b) Barringer, E. A.; Browen, J. *J. Am. Ceram. Soc.* **1982**, 65, 199, (c) Jeans, J. H.; Ring T. A. *Langmuir* **1986**, 2, 251.
20. (a) Pierre, A. C.; Pajonk, G. M. *Chem. Rev.* **2002**, 102, 4243, (b) Lu, Z. L.; Lindner, E.; Mayer, H. A. *Chem. Rev*. **2002**, 102, 3543, (c) Wight, A. P.; Davis, M. E. *Chem. Rev*. **2002**, 102, 3589, (d) Schwarz, J. A.; Contescu, C.; Contescu, A. *Chem. Rev*. **1995**, 95, 477.
21. (a) Sugimoto, T.; Okada, T.; Itoh, H. *J. Colloid Interface Sci*. **1977**, 193, 140, (b) Sugimoto, T.; Zhou, X.; Muramatsu, A. *J. Colloid Interface Sci*. **2000**, 259, 53, (c) Kanie, K.; Sugimoto, T. *Chem. Commun*, **2004**, 14, 1584, (d) Kanie, K.; Sugimoto, T. *J. Am. Chem. Soc*. **2003**, 125, 10518.
22. Ichinose, H.; Katsuki, H. *J. Ceram. Soc. Jpn*. **1996**, 104, 914.
23. Wang, Z.; Chen, J.; Hu, X. *Mater. Lett.* **2000**, 43, 87.
24. Spurr, R. A.; Myers, H. *Anal. Chem*. **1957**, 29, 760.

CHAPTER 2

Dispersion of Titanium Dioxide Nanoparticles into Low Polar Organic Solvent Using Polymer Dispersant and Incorporation into Poly(methyl methacrylate)

2-1. Introduction

Recently, organic–inorganic hybrid material, which are composed of polymer matrix dispersed inorganic particles of the size less than one-tenth of visible light wavelength, has attracted attention as new functional materials in various areas, because of exhibiting improvement of mechanical and physical properties.[1] One of the concerned applications of hybrids materials, composed of fine inorganic particles, is fabrication of high refractive optical materials, because it is difficult to prepare materials with the index value higher than 1.7 from polymer materials. In this sense, so far, there are some reports in aims of fabrication of high refractive and transparence organic–inorganic hybrid material, such as an optical waveguide, optical filter, and lens.[2-4] On the other hand, titanium dioxide, TiO_2, is a stable and nontoxic inorganic compound with relatively high refractive index, 2.74 and 2.54 of respective rutile and anatase. Thus, some approaches of TiO_2/polymer hybrid material syntheses to fabricate high refractive polymeric materials were reported.[5, 6] However, impending problems encountered in the field of polymer-inorganic hybrid materials are the agglomeration of inorganic nanoparticles and their incompatibility with organic matrices due to their mineral nature. In this respect, surface modification by grafting organic polymers onto inorganic fine particles is an effective way to improve their dispersibility in organic solvents and the compatibility with polymer matrices. To date, there are some reports for dispersion of TiO_2 particles into organic solvent using organic surfactant, dodecylbenzenesulfonic acid,[7] dodecylamine,[8] oleic acid,[9] and stearic acid.[10] Nakayama et al. reported dispersion of TiO_2 particles into several organic solvents by two-step chemical modification using a mixture of propionic acid and *n*-hexylamine.[11] Regarding synthesis of TiO_2 particles in aqueous solution, Chemseddine et al. reported highly crystalline anatase TiO_2 particles with different size and shape could be obtained via hydrothermal treatment of titanium alkoxide in the presence of triethylammonium hydroxide.[12, 13] Sugimoto et al. reported synthesis of shape-controlled TiO_2 particles from

$Ti(OH)_4$ solution which was prepared by mixing titanium isopropoxide with triethanolamine, in the presence of ammonia as shape controller by hydrothermal treatment.[14-17] In these cases, shape control was proposed by taking place due to coordination of shape controller onto specific plane of TiO_2 crystal.

As described in Chapter 1, we have developed selective crystallization of TiO_2 particles from peroxotitanic acid in the presence of hydrophilic polymer by hydrothermal treatment in aqueous solution.[18] In this case, TiO_2 particles stably dispersed in aqueous solution due to protective effects of hydrophilic polymer adsorbed on the particle surface. In this paper, we report a strategy for dispersion of TiO_2 particles which were prepared by hydrothermal process in the presence of hydrophilic polymer, into organic solvents in aid of amphiphilic polymer dispersant; poly(*N*-vinyl pyrrolidone) (PVP), poly(*N*-vinyl pyrrolidone-*co*-methyl methacylate) (PVP-*co*-MMA) or poly(*N*-vinyl pyrrolidone-*block*-methyl methacrylate) (PVP-*b*-PMMA), and for preparation of homogeneously TiO_2-dispersed PMMA film. Our final goal is the fabrication of transparence and high refractive materials by hybridization of inorganic fine particles and polymer.

2-2. Experimental Section

Materials

Titanium ethoxide was purchased from Merck, Germany. Polymers, poly(acrylic acid) (PAAc) of number average molecular weight (M_n) 5,000, methyl methacrylate (MMA), *N*-vinyl pyrrolidone (VP), benzyl chloride, sodium *N*,*N*-diethyl dithiocarbamate trihydrate and 2,2-azobis (butyronitrile) (AIBN), were obtained from Wako Pure Chemical Industries, Ltd., Japan. Vinyl monomers were purified by distillation under reduced presser before use. Poly(methyl methacrylate) (PMMA) was synthesized by radical polymerization using AIBN in THF; M_n=2,000, M_w/M_n=1.89.

Measurement

Particles size and distribution were determined by a dynamic light scattering (DLS) method on DLS-7000DL, Otsuka Electronics Co., Ltd., Japan, with a He–Ne laser, at a

reflection angle of 90 °C. Number average molecular weight (M_n) and polydispersity index (M_w/M_n) of polymer were determined by a gel permeation chromatography (GPC) on straightly connected-columns, PL-gel MIXED-C and PLgel MIXED-D, Polymer Lab. Co. Ltd., at 60 °C using DMF containing 10 mM LiBr as an eluent at flow rate 0.8 mL/min, calibrated with poly(ethylene glycol) standard. ^{1}H NMR spectra were obtained on Bruker AVANCE 400, Germany. FT-IR spectra were recorded with KBr disk on JEOL JIR-5500, Japan. Thermogravimetric analysis was performed on Shimadzu TG-50, Japan, under nitrogen atmosphere in the range from room temperature to 800 °C at rate 10 °C/min. Absorption spectra were recorded on JASCO V-520, Japan. Scanning electron microscope (SEM) observation was performed on JEOL JSM 6320F, Japan. Transmission electron microscope (TEM) observation was carried out on Hitachi H-800, Japan, with acceleration voltage of 100 kV. The samples for TEM observation were prepared by evaporating the suspension on a carbon-coated cupper grid. In the case of PMMA/TiO_2 hybrid films, the sample was prepared by sliced the a film embedded with epoxy resin by a microtome. The refractive index of PMMA/TiO_2 hybrid film was determined at 589 nm on NAR-2T, ATAGO Co., Ltd., Japan. X-ray reflection analyses were carried out on JEOL JDX-3500K, Japan.

Synthesis of TiO_2 Particles in the Presence of Polymer

Titanium dioxide (TiO_2) particles were synthesized according to the method described in Chapter 1. A typical run was as follows. To 3 mL titanium ethoxide and 100 mL ethanol was gradually added 3 mL distilled water, and then the mixture was stirred for 30 min at room temperature. Resulting precipitate was centrifugally separated from the solution and dried under reduced pressure. One hundred twenty milligrams of the obtained TiO_2 solution was added to a mixture of 10 mL distilled water and 15 mL 30% hydrogen peroxide and then the solution was sonicated by ultrasonic wave for 1 h to give peroxotitanic acid solution. Fifty milligrams PAAc was added to the peroxotitanic acid solution and then stirred at 60 °C for 48 h; eventually, the solution was heated in an autoclave at 200 °C for 5 h.

Synthesis of Poly(*N*-vinyl pyrrolidone) (PVP)

Fifteen milligrams (91.3 μmol) AIBN, 3 mL (28.2 mmol) VP and 3 mL ethanol were put into a 50 mL flask, and then the mixture heated at 70 °C under nitrogen atmosphere for 24 h. The resulting mixture was dissolved in 5 mL of tetrahydrofuran. The polymer formed was precipitated with 200 mL diethyl ether and then dried under vacuum at 60 °C for 24 h; yield: 2.75 g, M_n=4,000, M_w/M_n=1.93.

^{1}H NMR ($CDCl_3$, 400 MHz) δ: 1.4-1.6 (m, -**CH_2**-CH-), 2.0-2.2 (m, -**CH_2**-), 2.4 (m, -**CH_2**(CO)-), 3.25 (m, -N-**CH_2**), 3.6-3.8 (m, -CH_2-**CH**-) ppm.

Synthesis of Poly(*N*-vinyl pyrrolidone-*co*-methyl methacylate) (PVP-*co*-PMMA)

Copolymerization of VP with MMA was carried out by the same procedure described above. A typical run was as follow: the mixture of 15 mg (91.3 μmol) AIBN, 3 mL (28.2 mmol) VP, and 3 mL (28.2 mmol) MMA were put into 50 mL flask containing 3 mL THF, and then refluxed at 70 °C under nitrogen atmosphere for 24 h. The copolymer formed after polymerization was precipitated with 200 mL diethyl ether and then dried under vacuum at 60 °C for 24 h.

^{1}H NMR ($CDCl_3$, 400 MHz) δ: 0.8-1.0 (m, -**CH_3**), 1.4-1.6 (m, -**CH_2**-CH-), 2.0-2.2 (m, -**CH_2**-), 2.4 (m, -**CH_2**(CO)-), 3.25 (m, -N-**CH_2**), 3.6-3.8 (m, -CH_2-**CH**-), 3.67 (m, -O**CH_3**) ppm. Molar fractions of MMA block and VP block in the copolymer were determined by ^{1}H NMR spectroscopy.

Synthesis of Benzyl *N*,*N*-Diethyl Dithiocarbamate (BDDC)

To 30 mL ethanol solution, in which 5.21 g (23.1 mmol) sodium *N*,*N*-diethyl dithiocarbamate trihydrate was dissolved, 2 mL (17.4 mmol) benzyl chloride was slowly added at 0 °C, and then the mixture was stirred for 12 h at room temperature. The resulting mixture was filtrated to remove the inorganic precipitate. After evaporation of ethanol and addition of 40 mL distilled water, yellow product was extracted with 20 mL diethyl ether three times. The organic phase was dried on anhydrous sodium sulfate and evaporation of

diethyl ether afforded the product. Yield: 3.75 g (90%),
^{1}H NMR ($CDCl_3$, 400 MHz); δ: 1.28 (q, 6H, -N(CH_2**CH_3**)$_2$), 3.72 (q, 2H, -N(**CH_2**CH_3)$_2$), 4.05 (q, 2H, -N(**CH_2**CH_3)$_2$), 4.53 (s, 2H, -**CH_2**Ph), 7.2–7.5 (m, 5H, -**Ph**) ppm.

Synthesis of Poly(*N*-vinyl pyrrolidone-*block*-methyl methacrylate) (PVP-*b*-PMMA) via Photo Iniferter

(1) First Step for Polymerization of PVP Homopolymer

A typical run was as follows: to a test tube was added 30 mg (0.125 mmol) BDDC, 3 mL (28.2 mmol) VP, and 3 mL ethanol. The reaction mixture was purged with high grade nitrogen for 1 h to remove traces of oxygen and then was carefully degassed by three freeze–pump–thaw cycles. Finally, the test tube was sealed off under reduced pressure and irradiated for 5 h, employing a high pressure mercury lamp. Resulting polymer was precipitated with diethyl ether and dried at 50 °C under vacuum; yield: 1.92 g (68%), M_n= 16,700, M_w/M_n=1.16.
^{1}H NMR (D_2O) for PVP; δ: 1.28 (m, -N(CH_2**CH_3**)$_2$), 1.4-1.6 (m, -**CH_2**-CH-), 2.0-2.2 (m, -**CH_2**), 2.4 (m, -**CH_2**(CO)-), 3.25 (m, -N-**CH_2**), 3.6-3.8 (m, -CH_2-**CH**-), 3.9 (m, -N(**CH_2**CH_3)$_2$), 4.55 (m, -**CH_2**Ph), 7.2–7.5 (m, -**Ph**) ppm.

(2) Second Step for Polymerization of PVP-*b*-PMMA

Two grams of PVP iniferter, 3 mL (28.2 mmol) MMA and 5 mL 1,4-dioxane were added to a test tube and then the polymerization was carried out as described above. Resulting polymer was precipitated with diethyl ether and then dried at 50 °C under vacuum for 24 h; yield: 4.32 g, M_n=32,000, M_w/M_n=1.58.
^{1}H NMR ($CDCl_3$, 400 MHz) for PVP-*b*-PMMA; δ: 0.8-1.0 (m, -**CH_3**), 1.28 (m, -N(CH_2**CH_3**)$_2$), 1.4-1.6 (m, -**CH_2**-CH-), 2.0-2.2 (m, -**CH_2**-), 2.4 (m, -**CH_2**(CO)-), 3.25 (m, -N-**CH_2**), 3.6-3.8 (m, -CH_2-**CH**-), 3.67 (m, -O**CH_3**), 3.9 (m, -N(**CH_2**CH_3)$_2$), 4.55 (m, -**CH_2**Ph), 7.2–7.5 (m, -**Ph**) ppm. Molar fractions of MMA block and VP block in the block copolymer were determined by ^{1}H NMR spectroscopy (Scheme 1).

Solvent Exchange of Aqueous TiO_2 Suspension with Chloroform

A typical run was as follows. Ten milliliters of TiO_2 particles suspension was slowly added to the 100 mL of the mixture of ethanol and acetonitrile (1:1 vol.) containing 100 mg PVP. Resulting solution was stirred at room temperature for 1 h, and then sonicated for 1 h. The solution was concentrated by evaporation of ethanol and water as azeotrope to give 20 mL suspension, and then TiO_2 particles were collected by centrifugation. Resulting wet TiO_2 particles was put into 40 mL chloroform and the solution was irradiated by ultrasonic wave to be well dispersed.

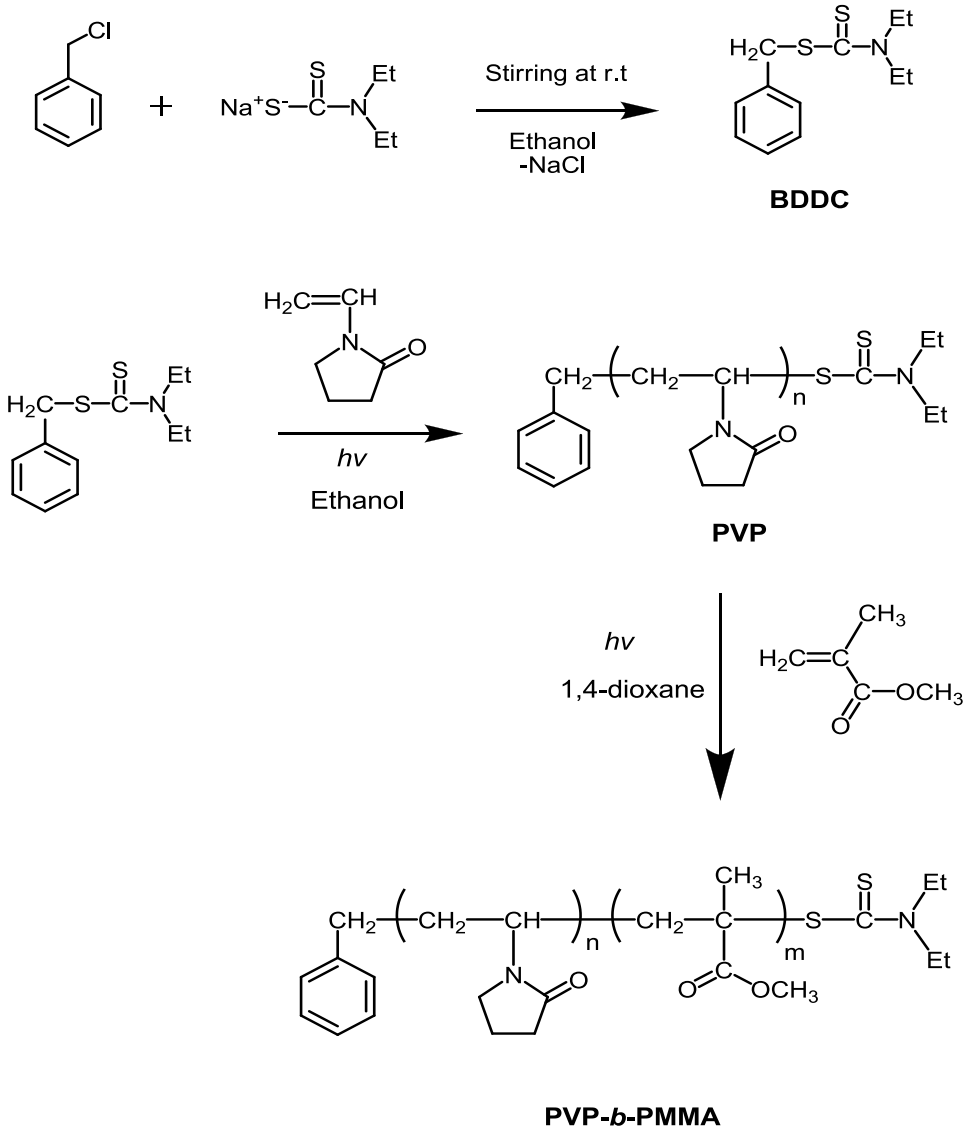

Scheme 1. The procedure for the synthesis of block copolymer via photo iniferter.

Preparation of PMMA/TiO_2 Hybrid Film

The required amount of chloroform suspension of TiO_2 particle were put into 2 ml of PMMA chloroform solution containing 30 mg PMMA (1.0 wt%). After sonication for 1 h, the mixture was put into a glass petri dish of 5 cm in diameter. Drying up at room temperature and followed by heating at 100 °C for 30 min gave the hybrid films. The weight fraction of TiO_2 in the hybrid film was evaluated by weight reduction during elevating temperature from 200 °C to 800 °C by thermogravimetric analysis.

2-3. Results and Discussion

2-3-1. Dispersion of TiO_2 Particles into Chloroform Using Polymer Dispersant

In the present crystallization described in Chapter 1, TiO_2 particles are formed in aqueous solution, so that it is so difficult to supply them directly to fabrication of functional materials. Thus, we examined dispersion of TiO_2 particles into chloroform using amphiphilic polymer, PVP, as a polymer dispersant via solvent exchange. Solvent exchange process of anatase-type TiO_2 particles formed in the presence of PAAc at pH of 10.5 using the dispersant is shown in Scheme 2. A key point of the exchange process is removal of water from the TiO_2 aqueous suspension through azeotropical evaporation, and outline of the procedure is as follows. After addition of PVP ethanol/acetonitrile solution to aqueous TiO_2 suspension, the mixture was heated to evaporate water as an azeotropic mixture with ethanol. Following addition of chloroform to the solution made the TiO_2 particles dispersed in chloroform. An FT-IR spectrum of dried particles obtained by evaporation of chloroform from the suspension showed the absorption peak around 1650 cm^{-1}, which is assignable to amide carbonyl group of PVP. These results suggested that PVPs were absorbed on the surface by the strong interaction between the amide carbonyl and hydroxyl groups of TiO_2. Therefore, the strong adsorption and consequent protecting colloidal effects of adsorbed PVP possibly prevented from aggregation or precipitation of the particles in chloroform.

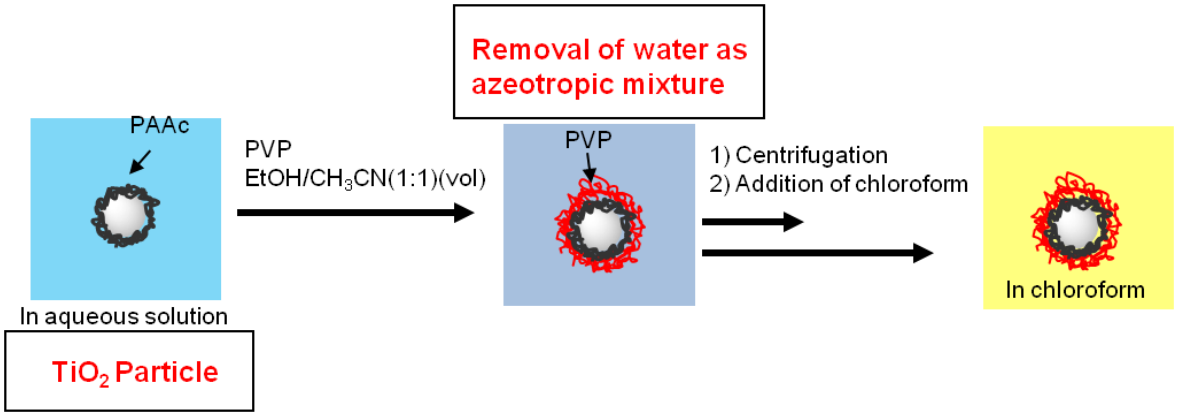

Scheme 2. The procedure for the dispersion of TiO_2 particles into chloroform.

2-3-2. Incorporation of TiO_2 Particles into PMMA Film

PMMA films containing TiO_2 particles were prepared by a spin coating of mixture of PVP-adsorbed TiO_2 chloroform suspension and PMMA on glass substrate. A typical SEM image of PMMA film composed of 1.0 wt% TiO_2 are shown in Figure 1a, b. In the film, TiO_2 particles of more than 100 nm size were observed. This result indicated that the particles were aggregated during the drying process due to low affinity between PVP and PMMA. In this case, therefore, an affinity between PVP adsorbed on TiO_2 surface and

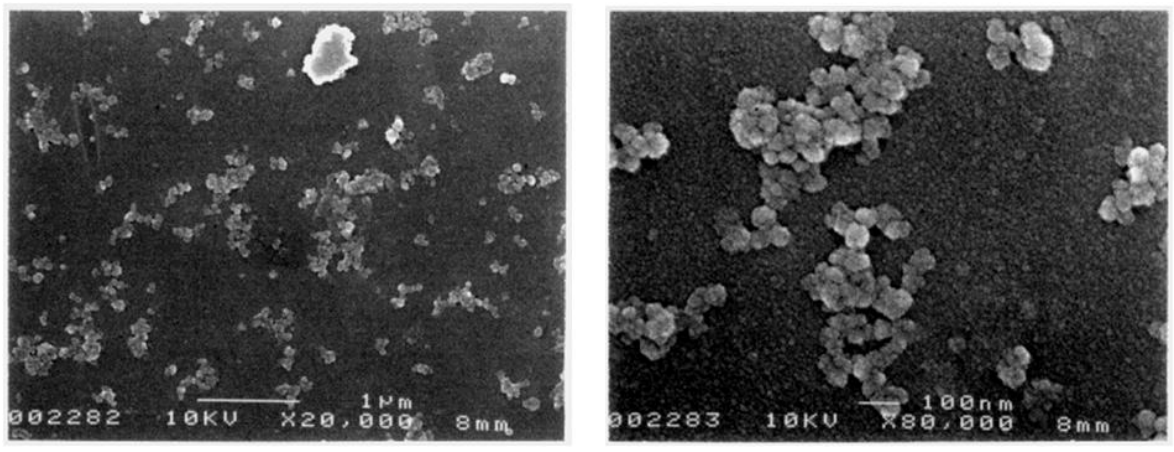

(a) **(b)**

Figure 1. SEM images of PMMA film containing PVP-modified TiO_2 with 1.0 wt% TiO_2 on the glass substrate, (a) ×20,000, (b) 80,000.

PMMA matrix was an important factor to prevent from aggregation of TiO_2 particles. In order to enhance the affinity between dispersant polymer and PMMA, preparation of TiO_2-dispersed PMMA films was examined by using dispersant copolymer of VP and MMA, VP/MMA mole ratio of which was in the range from the 1/18 to 1/1. In this copolymer synthesis, unfortunately, it was impossible to synthesize copolymers of high VP fraction more than 50 mol% by radical polymerization, because of low copolymerization reactivity between VP and MMA. Particles size of TiO_2 particles dispersed in chloroform using PVP-*co*-PMMA dispersant decreased with increasing of PVP fraction in copolymer and attained 20 nm when the copolymer of VP/MMA mole ratio 1/1 was employed (Table 1).

Table 1. Effect of copolymer addition on particle size in chloroform solution.

	Fraction of copolymer (VP / MMA)	M_n	M_w/M_n	Particle size [a)] (nm)
PVP		4,000	1.93	20 ± 5
PVP-*co*-PMMA	1/18	5,500	2.10	300 ± 10
	1/11	7,000	1.87	130 ± 15
	1/ 5	4,600	1.95	80 ± 10
	1/ 3	4,000	1.78	40 ± 10
	1/ 1	5,000	1.89	20 ± 5

a) Determined by DLS.

These results suggested that adsorption of VP moiety on TiO_2 particles plays an important role for dispersion of the particles in low polar solvent without any aggregations. However, incorporation of TiO_2 into PMMA using the chloroform suspension, prepared by employing PVP-*co*-PMMA, of VP/MMA mole ratio 1/1, gave the film composed of TiO_2 particles of around 80 nm size (Figure 2a, b).

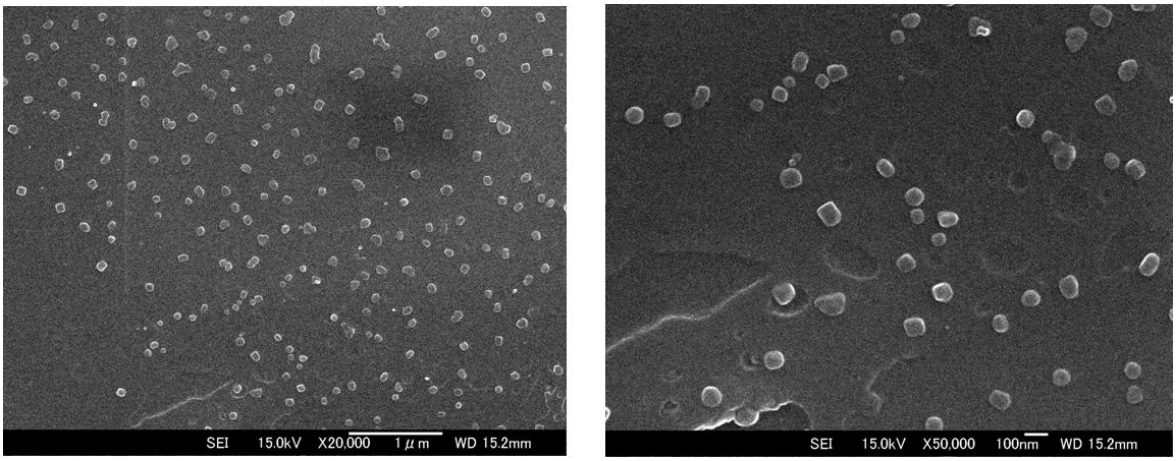

(a) **(b)**

Figure 2. SEM images of PMMA film containing PVP-*co*-PMMA, of VP/MMA ratio 1/1, -modified TiO_2 with 1.0 wt% TiO_2 on the glass substrate, (a) ×20,000, (b) 80,000.

Probably, the aggregation of TiO_2 particles during PMMA film processing comes from low MMA mole faction in copolymer dispersant. Therefore, the chemical composition, which is mole ratio of VP to MMA in the present case, is significant to keep dispersion of TiO_2 particles in chloroform and PMMA films. In these copolymers, the PVP moiety played a role as an adsorption unit on TiO_2 particles, while the PMMA layer brought about affinity with PMMA matrices. Therefore, it was expected that employing block polymer dispersant of VP and MMA gave rise to effective dispersion of TiO_2 not only in chloroform, but also in PMMA film. In the present study, block copolymers of VP/MMA mole ratio 1/1, as shown in Table 2, were examined for dispersion of TiO_2 in chloroform and incorporation into PMMA matrix.

Table 2. Characterization of block copolymer and effect of polymer addition on particle size in chloroform solution.

	PVP /g mol^{-1}	M_w/M_n of PVP	PMMA /g mol^{-1}	M_w/M_n of block copolymer	Particle size [a] / nm
PVP_{24}-*b*-$PMMA_{28}$	2,700	1.32	2,800	1.48	80 ± 15
PVP_{52}-*b*-$PMMA_{56}$	5,800	1.26	5,600	1.45	20 ± 5
PVP_{102}-*b*-$PMMA_{107}$	11,700	1.23	10,700	1.67	20 ± 5
PVP_{154}-*b*-$PMMA_{156}$	17,200	1.16	15,600	1.58	20 ± 5

a) Determined by DLS.

In the case of PVP_{24}-*b*-$PMMA_{28}$ addition, it was observed that addition of the polymer dispersant gave rise to aggregation of TiO_2 particles due to shorting of PMMA moiety. In addition of block copolymer of higher molecular weight than PVP_{24}-*b*-$PMMA_{28}$, TiO_2 particles were dispersed into chloroform without any aggregation or precipitations, after solvent exchanging. Adsorption of the block polymer on TiO_2 particles after solvent exchanging was confirmed by appearance adsorption bands at 1650 cm^{-1} assigned to amide carbonyl group of PVP moiety on IR spectra (Figure. 3). Incorporation of TiO_2 particle into PMMA film, around 60 μm in thickness, was carried out using TiO_2 particles dispersed in chloroform employing PVP_{154}-*b*-$PMMA_{156}$. The resulting PMMA thin film exhibited a high transparency up to 10 wt% of TiO_2 content in PMMA films. As shown in Figure. 4, however, UV–vis spectra indicated that absorbance in the visible light region increased with TiO_2 content in the range of 2.0 to 10 wt%, probably being due to strong light scattering on aggregated TiO_2 particles in the polymer matrices. In Figure 5,

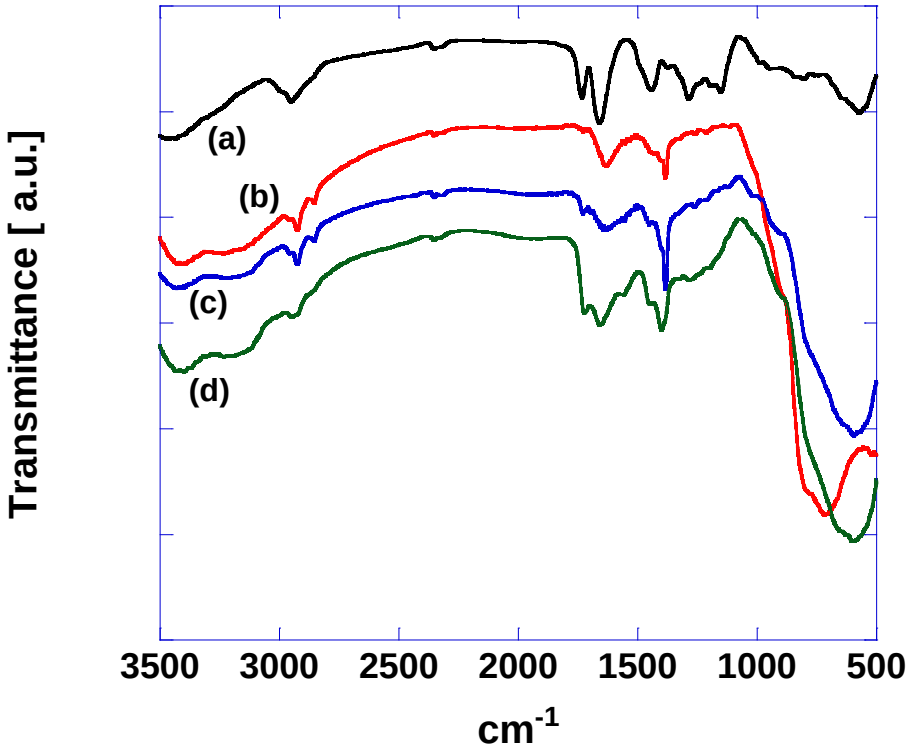

Figure 3. FT-IR spectra of PVP_{154}-*b*-$PMMA_{156}$ block copolymer (a), TiO_2 particle synthesized without polymer (b), TiO_2 particles synthesized in the presence of PAAc (c), TiO_2 particles dispersed in chloroform using block copolymer (d). All spectra were taken after drying under reduced pressure.

photographs of obtained PMMA film with TiO_2 particles content were shown. The relatively clear films of 60 μm in thickness were successfully prepared.

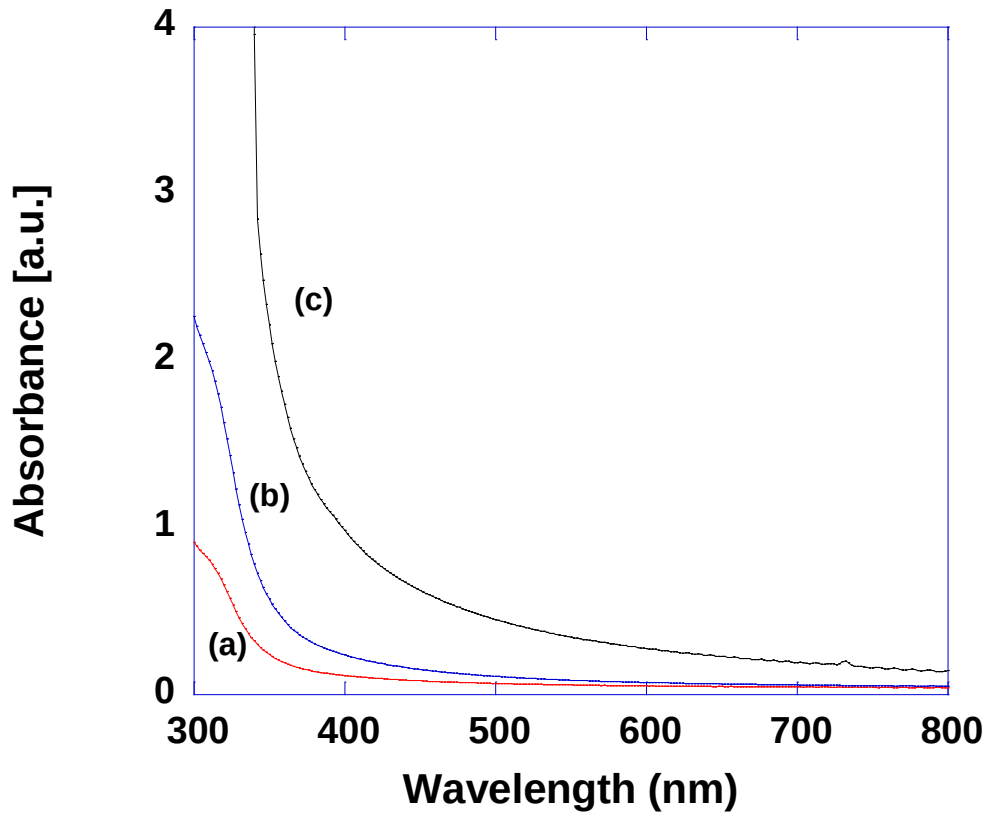

	Transmittance (%)				
	400 nm	500 nm	600 nm	700 nm	800 nm
PMMA	99.94 %	99.97 %	99.98 %	99.99 %	99 .99%
PMMA/TiO_2 (2.5 wt%)	76.80 %	85.54 %	88.61 %	89.72 %	90.97 %
PMMA/TiO_2 (5 wt%)	57.88 %	77.66 %	84.54 %	87.45 %	89.14 %
PMMA/TiO_2 (10 wt%)	10.34 %	35.55 %	52.57 %	64.10 %	71.83 %

Figure 4. UV-vis spectra and transmittance of PMMA/TiO_2 film (a) 2.0 wt %, (b) 5.0 wt %, (c) 10.0 wt %.

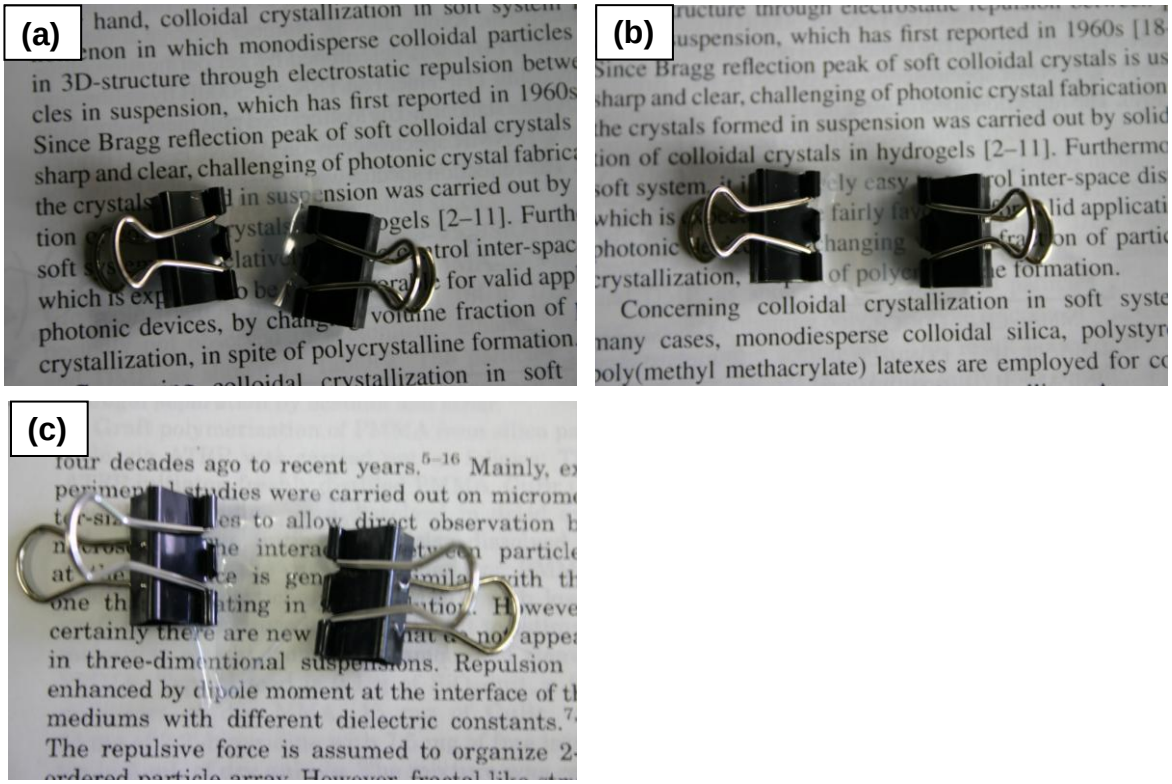

Figure 5. Photographs of PMMA thin films with TiO_2 particles, 60 μm in thickness, (a) 2.5 wt%, (b) 5 wt%, (c) 10 wt%.

In the TEM images of cross section of the PMMA films (Figure. 6, 7, 8), it was observed that TiO_2 particles were homogeneously dispersed in PMMA matrix, but some clusters around 100 nm were also formed. The formation of the cluster probably led to increasing absorbance in visible light region. However, the refractive index of PMMA hybrid film proportionally increased with TiO_2 content. The refractive index at 2.5, 5, and 10 wt% was 1.505, 1.510, and 1.511, respectively, and agreed with calculated values, as shown in Figure 9. The values were calculated by following Lorentz–Lorenz equation;[19, 20]

$$\frac{(n^2-1)}{(n^2+2)} = \sum v_i \frac{(n_i^2-1)}{(n_i^2+2)}$$

where n is refractive index of hybrid film, v_i and n_i are volume fraction and refractive index of component i, respectively. In this case, refractive indexes of anatase TiO_2 and PMMA

were employed following values of n=2.52 and n=1.49, respectively. Therefore, it was shown that the refractive indexes of the hybrid film were independent upon formation of TiO_2 cluster less than around 100 nm. Consequently, in order to achieve higher refractive index and transparency of the hybrid film at visible light region, extremely higher dispersion of TiO_2 nanoparticles of less than 20 nm in PMMA films should be attained.

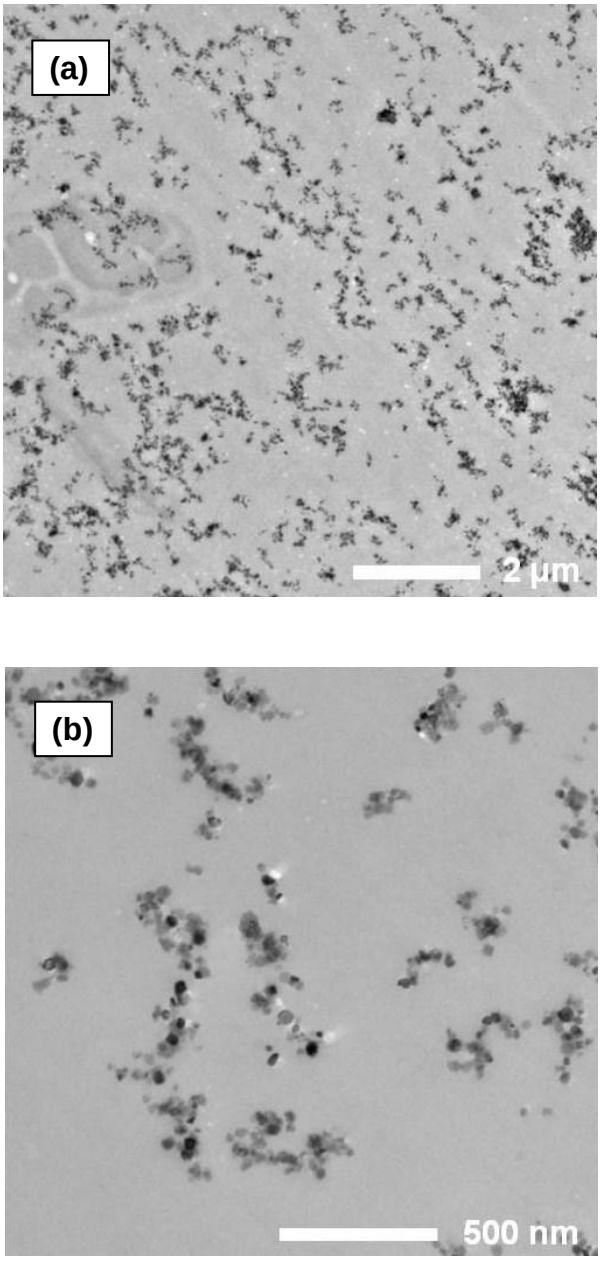

Figure 6. Cross-sectional TEM images of PMMA film (60 μm in thickness) containing PVP_{154}-*b*-$PMMA_{156}$ block copolymer-modified TiO_2 with 2.5 wt%, (a) ×2,000, (b) ×10,000.

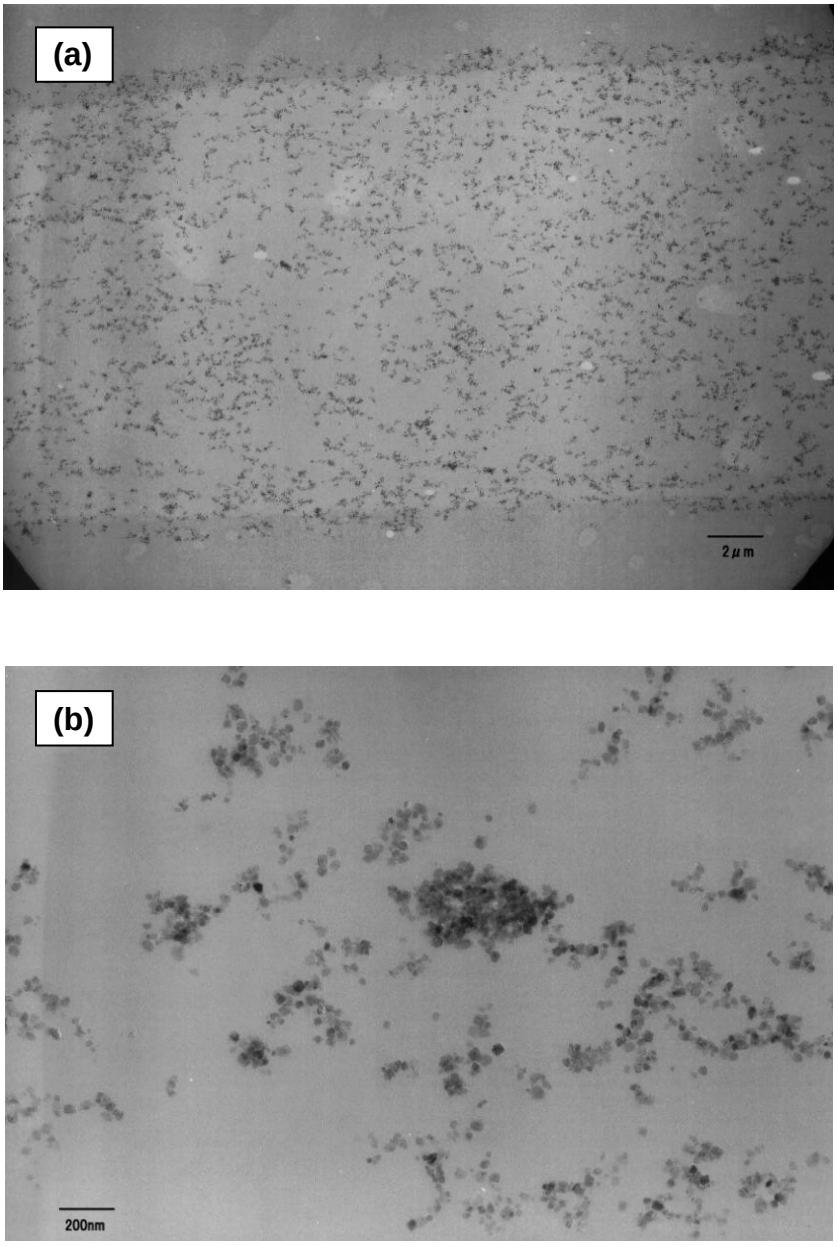

Figure 7. Cross-sectional TEM images of PMMA film (60 μm in thickness) containing PVP_{154}-*b*-$PMMA_{156}$ block copolymer-modified TiO_2 with 5 wt%, (a) ×10,000, (b) ×100,000.

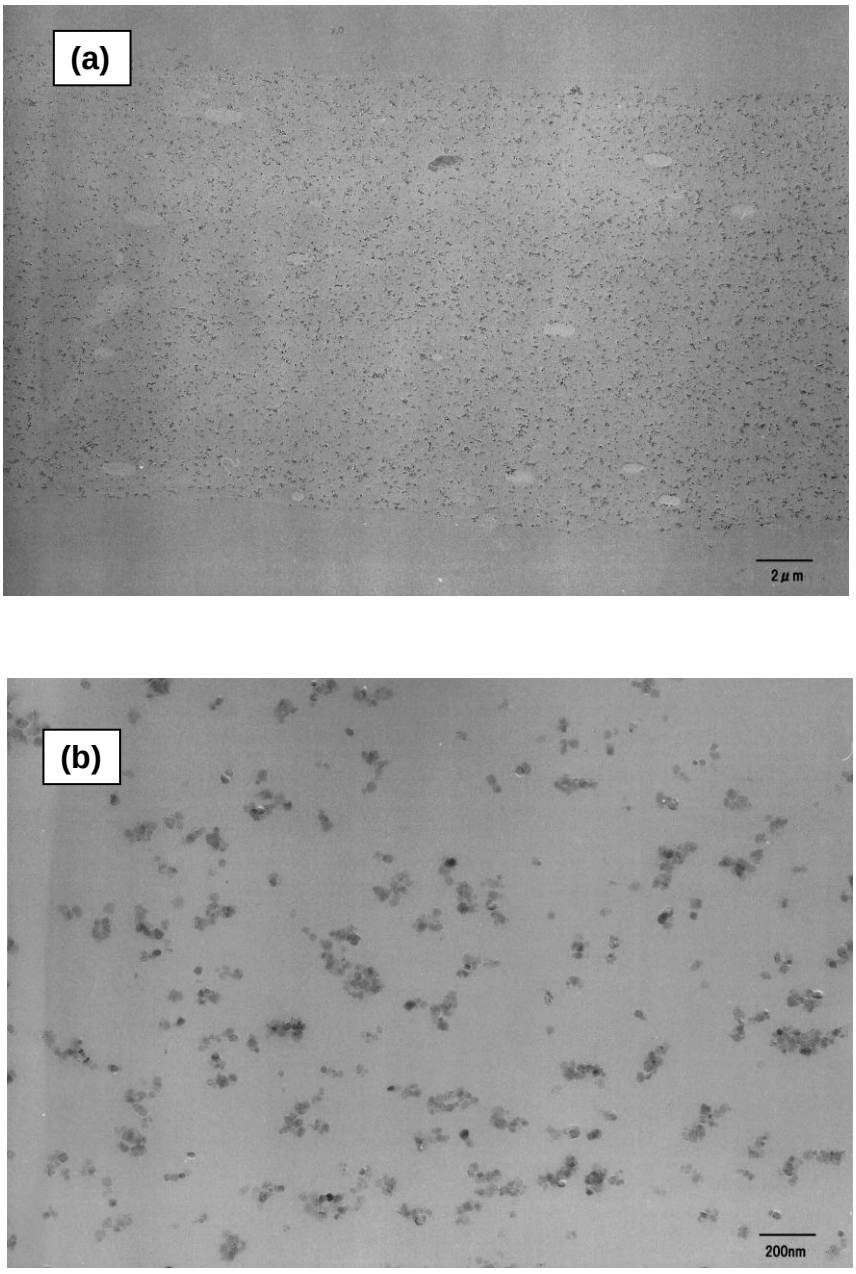

Figure 8. Cross-sectional TEM images of PMMA film (60 μm in thickness) containing PVP_{154}-*b*-$PMMA_{156}$ block copolymer-modified TiO_2 with 10 wt%, (a) ×10,000, (b) ×100,000.

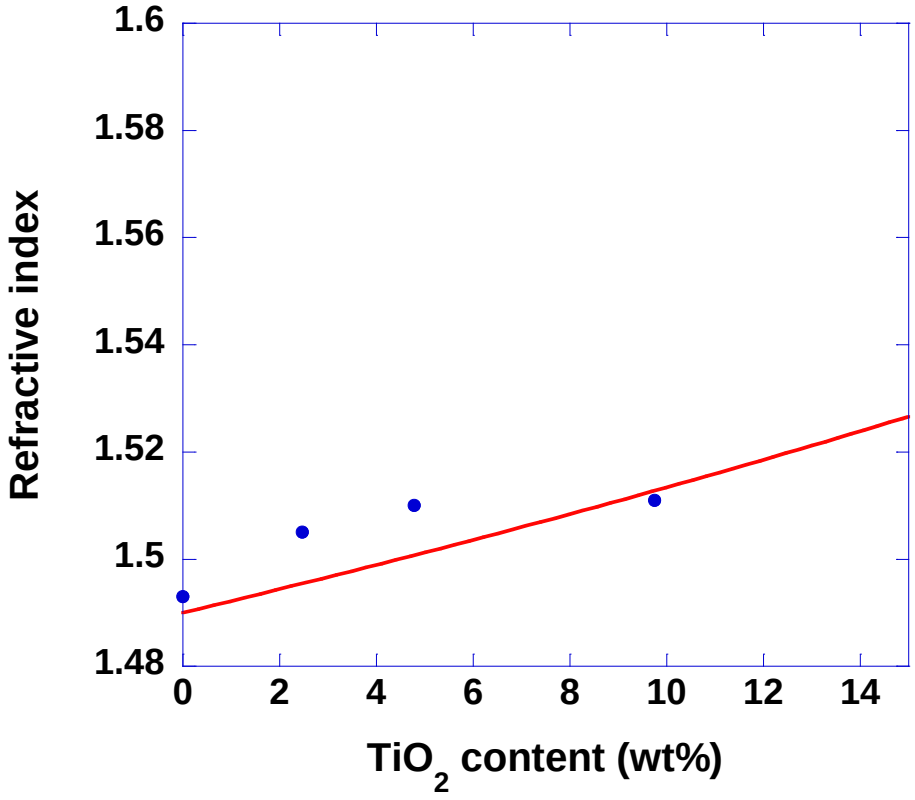

Figure 9. Plots of TiO_2 content vs. refractive index of hybrid film prepared using PVP_{154}-*b*-$PMMA_{156}$: solid line represents calculated values.

2-4. Conclusion

TiO_2 particles with diameter of 20 nm were synthesized from peroxotitanic acid in the presence of hydrophilic acid. Synthesis of TiO_2 particles in the presence of PAAc addition at high pH value gave stable aqueous suspension. The presence of hydrophilic polymer during crystallization of TiO_2 from peroxotitanic acid resulted in complete control of TiO_2 crystal morphs. Well-dispersed TiO_2 particles in chloroform were obtained by addition of amphiphilic polymer, PVP, PVP-*co*-PMMA, or PVP-*b*-PMMA block copolymer as a dispersant. PVP_{154}-*b*-$PMMA_{156}$ dispersant addition led to high dispersion of TiO_2 particles of 20 nm in chloroform and effective incorporation into PMMA matrix to give highly transparent PMMA films. The refractive index of the hybrid films proportionally increased with TiO_2 content in PMMA matrix.

2-5. References

1. Kojima Y.; Usuki A.; Kawasumi M.; Okada A.; Fukushima Y.; Kurauchi T.; Kamigaito O. *J. Mater. Res.* **1993**, 8, 185.
2. Yoshida M.; Prasad P. N. *Chem. Mater*. **1996**, 8, 235.
3. Wang J.; Montville D.; Gonsalves K. E. *J. Appl. Polym. Sci.* **1999**, 72, 1851.
4. Lu C. L.; Cui Z. C.; Li Z.; Yang B.; Shen J. C. *J. Mater. Chem.* **2003**, 13, 526.
5. Lu C. L.; Cui Z. C.; Guan C.; Guan J. Q.; Yang B.; Shen J. C. *Macromol. Mater. Eng.* **2003**, 288, 717.
6. Nakayama N.; Hayashi T. *J. Appl. Polym. Sci*. **2007**, 105, 3662.
7. Nussbaumer R. J.; Caseri W.; Tervoort T.; Smith P. *J. Nanopart. Res*. **2002**, 4, 319.
8. Wang Y.; Zhang S.; Wu X. H. *Nanotechnology* **2004**, 15, 1162.
9. Cozzoli P. D.; Kornowski A.; Weller H. *J. Am. Chem. Soc*. **2003**, 125, 14539.
10. Wu X. D.; Wang D. P.; Yang S. R. *J. Colloid Interface Sci.* **2000**, 222, 37.
11. Nakayama N.; Hayashi T. *Colloid Surface A* **2008**, 317, 543.
12. Chemseddine A.; Moritz A. *Eur. J. Inorg. Chem*. **1999**, 1999, 235.
13. Moritz T.; Reiss J.; Diesner K.; Su D. Chemseddine A. *J. Phys. Chem. B* **1997**,101,

8052.

14. Sugimoto T.; Okada K.; Itoh H. *J. Colloid Interface Sci.* **1997**, 193, 140.
15. Sugimoto T.; Okada K.; Itoh H. *J. Disper. Soc. Technol*. **1998**, 19, 143.
16. Kanie K.; Sugimoto T. *Chem. Commun.* **2004**, 14, 1584.
17. Sugimoto T.; Zhou X. P.; Muramatsu A. *J. Colloid. Interface Sci*. **2003**, 259, 53.
18. Yoshinaga K.; Yamauchi M.; Maruyama D.; Mouri E.; Koyanagi T. *Chem. Lett.* **2005**, 34, 1094.
19. Chen H.; Kou H.; Yang Z.; Ni W.; Wang J. *Langmuir* **2008**, 24, 5233.
20. Aspnes D. E. *Am. J. Phys*. **1982**, 50, 704.

CHAPTER 3

Incorporation of Titanium Dioxide Particles into Polymer Matrix Using Block Copolymer Micelles for Fabrication of High Refractive and Transparent Organic-Inorganic Hybrid Materials

3-1. Introduction

Recently, high refractive and transparent polymer materials have received great attentions to be used in a wide range of optical designs and applications,[1–9] such as ophthalmic lenses, filters, optical adhesives, and highly refractive and antireflection coating. Inorganic materials generally have high refractive index between 2.0 and 5.0, but they have shortcomings for fabrication of devices, such as high density and low flexibility. On the other hand, organic polymer materials possess excellent advantages of processability, low density, flexibility, and transparency, compared with inorganic materials. Most of high refractive polymer materials are synthesized by incorporation of sulfur atoms, aromatic rings, metallic elements, and halogen atoms, excluding for fluorine, into backbones or side chains of polymers, and these polymers have achieved increasing refractive index up to 1.7.[10–15] However, to date, it is difficult to obtain polymers exhibiting higher refractive index than 1.8.

The development of organic–inorganic hybrid materials, which were constructed by incorporating high refractive inorganic materials, such as titanium dioxide (TiO_2), ZrO_2, ZnO, ZnS, CdS, and PbS, into polymer materials, is also one of promising and effective ways to fabricate high refractive materials.[16–20] In these hybrid materials, homogeneous dispersion of inorganic materials with the diameter less than one-tenth the wavelength of visible light range is necessary for high transparency, because large aggregates usually caused significant light scattering, hampering optical applications.[21,22] Thus, control over interaction between inorganic material and polymer matrix is essential to give highly homogeneous dispersion. To prevent from aggregations of particles and improve the compatibility between inorganic material and polymer matrix, the chemical modification of inorganic surface is an available and conventional technique. In many cases, the surface modifications are widely conducted by adsorption or covalent bonding of modifiers, such as surfactants and silane coupling agents, on the surface.

As described in Chapters 1 and 2, we have previously reported incorporation of highly crystallized nanometer TiO_2 particles,[23,24] synthesized by a hydrothermal process from peroxotitanic acid in the presence of hydrophilic polymer, into poly(methyl methacrylate) (PMMA) matrix by using poly(*N*-vinylpyrrolidone-*block*-methyl methacrylate) block copolymer as a dispersant.[25] However, in this case, it was impossible to obtain the hybrid films containing TiO_2 particles over 10 wt%, because of irreversible and undesirable aggregations during solvent exchange process from water to chloroform. In general, it is very difficult to incorporate TiO_2 nanoparticles less than 20 nm in size into polymer matrixes by surface modification or by using polymer dispersants, because of relatively low surface charge.

On the other hand, amphiphilic block copolymers are known to assemble into spherical reverse micelles composed of hydrophilic core and hydrophobic corona in some organic solvents. Therefore, the formation of TiO_2 particles in hydrophilic core in the micelles through hydrolysis and condensation of metal alkoxides via sol-gel process is expected to give highly dispersed nanoscale particles, and then successive incorporation of particles into polymer matrix makes possible fabrication of TiO_2/polymer hybrid materials, homogeneously dispersed the particles. In this article, we report formation of TiO_2 particles in the copolymer micelles of poly(methyl methacrylate-*block*-acrylic acid) (PMMA-*b*-PAA), which is synthesized by an anionic polymerization technique, and fabrication of TiO_2/PMMA hybrid materials with highly refractive index and transparency in visible light range (Scheme 1). This present technique enables to prepare various types of metal oxide/polymer hybrid nanoparticles, which exhibit high compatibility with organic solvent and polymer materials, and is expected to be used to fabricate advanced functional hybrid materials.

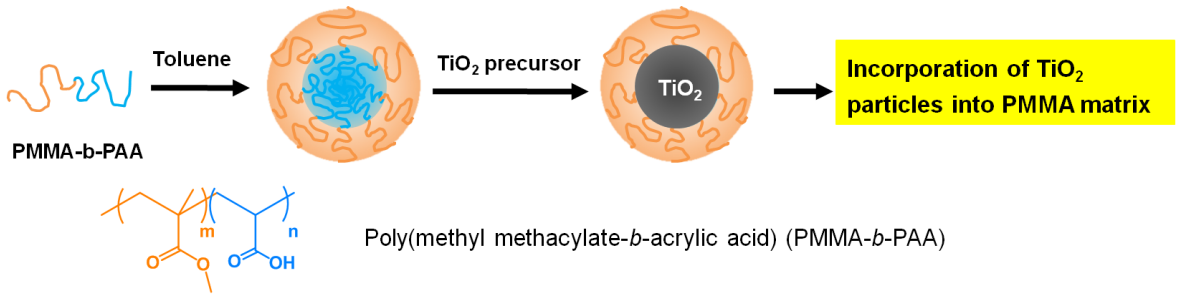

Scheme 1. Fabrication for PMMA hybrid films containing TiO_2 particles.

3-2. Experimental Section

Materials

1,1-Diphenylethylene, triethylaluminum (1.0 M in hexane), lithium chloride (LiCl), *n*-butyllithium (1.6 M in hexane), titanium isopropoxide (TTIP), dehydrated tetrahydrofuran (THF), 2-propanol, toluene, calcium hydride (CaH_2), and hydrochloric acid (12 N HCl) were purchased from Kanto Chemical, Japan and used as received without further purification. Methyl methacrylate (MMA), *tert*-butyl acrylate (tBA), and 2,2'-azobis(isobutyronitrile) (AIBN) were obtained from Wako Pure Chemical Industries, Japan.

Measurement

Number-average molecular weight (M_n) and polydispersity index (M_w/M_n) of the synthesized polymers were determined by a GPC on the columns (PL-gel MIXED-C and MIXED-D, Polymer Lab.) at 35 ºC using THF as an eluent at the flow rate of 0.8 mL/min, calibrated with a polystyrene standard. ^{1}H NMR spectra were obtained on a Bruker AVANCE 400 (400 MHz), Germany. UV–vis spectra were recorded on a JASCO V-520, Japan. IR spectra were taken with KBr disks on a JEOL JIR-5500, Japan. TGA was performed on a Shimadzu TGA-50, Japan, under nitrogen atmosphere in the range from room temperature to 800 ºC at the heating rate of 10 ºC/min. The atomic force microscope (AFM) observations were carried out on a Digital Instruments Nanoscope by a tapping mode. The dynamic light scattering (DLS) was measured on an Otsuka Electronics DLS-7000 spectrophotometer equipped with a He-Ne laser (10 mW, 633 nm). X-ray diffraction (XRD) analysis was carried out by JEOL JDX-3500K, Japan. The transmission electron microscope (TEM) was operated on Hitachi H-9000NAR with an acceleration voltage of 100 kV. In the case of the observation for TiO_2 particles, the samples were prepared by dropping solution on a carbon-coated copper grid followed by evaporation of solvents. The cross-sectional TEM observations of TiO_2/PMMA hybrid films were conducted after slicing a film embedded with epoxy resin by a microtome. Refractive index of hybrid films at a wavelength of 633 nm using a He-Ne laser was recorded by a prism coupler on a Metricon Corp. model 2010.

Synthesis of Poly(methyl methacrylate-*block*-*tert*-butyl acrylate) (PMMA-*b*-PtBA)

The block copolymers used in this study were synthesized using an anionic polymerization technique, reported in the literature.[26, 27] A typical run was as follows. LiCl was dried under vacuum overnight at 120 ºC. All monomers were distilled under vacuum in the presence of CaH_2 after stirring at room temperature and then stored under nitrogen at –20 ºC. Before polymerization reaction, these monomers were further purified by distillation after addition of triethylaluminum (1.0 M in hexane). An initiator of 1,1-diphenylhexyllithium (0.1 M in THF) was synthesized by the reaction of 1.25 mL *n*-butyllithium with an equimolar amount of 0.35 mL 1,1-diphenylethylene in 20 mL THF solution at –40 ºC. After stirring for half an hour, the initiator was added to previously flamed flask containing LiCl (mole ratio LiCl/initiator = 10/1) dissolved in 100 mL THF under nitrogen atmosphere. The mixture was titrated with the initiator until red color persisted, followed by addition of the required amount of initiator. The reaction flask was cooled to –78 ºC using a dry ice/acetone bath followed by addition of 2.5 mL MMA. After polymerization of MMA for 1 h, an aliquot of the reaction mixture was taken out for analysis of polymerization degree by gel permeation chromatography (GPC). Subsequently, 1 mL tBA was added into the reaction mixture for polymerization of the second block, and then the polymerization reaction was terminated by the excessive addition of degassed methanol. The purification of the block copolymers was carried out by the precipitation with the mixture of methanol and water (8:2 vol), and then $PMMA_{350}$-*b*-$PtBA_{93}$ was dried under vacuum overnight: yield 2.5–3.0 g. The synthesis procedures were illustrated in Figure 1.

Hydrolysis of PMMA-*b*-PtBA

The block copolymers, PMMA-*b*-PtBA (2.5 g) were dissolved in 50 mL of 1,4-dioxane and then 1 mL of 12 N HCl corresponding to 5 mole times, and tBA moieties were added to the solution. The hydrolysis of block copolymers was carried out under refluxing for 10 h to get poly(methyl methacrylate-*block*-acrylic acid) (PMMA-*b*-PAA). After cooling, the block copolymers were precipitated with hexane, and the block copolymer was dried under vacuum overnight.

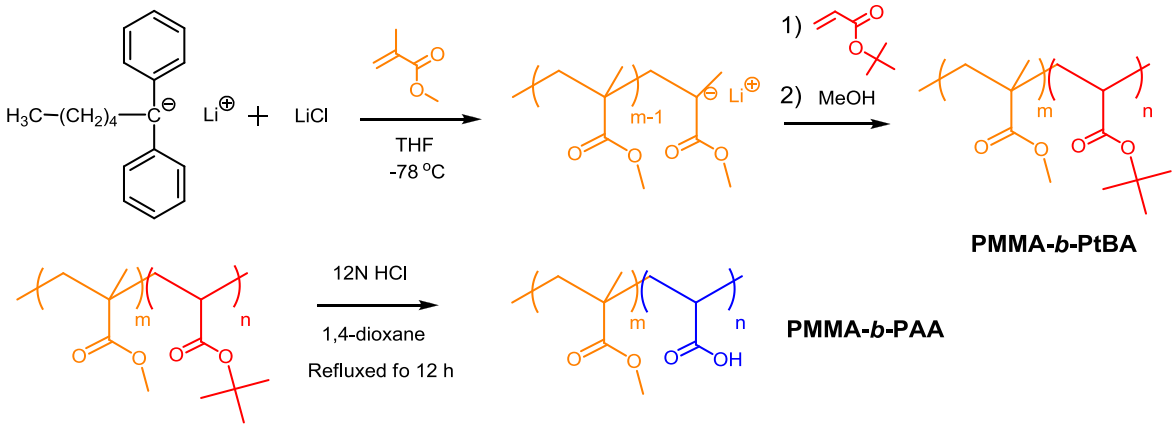

Figure 1. Synthesis procedure for PMMA-*b*-PtBA and PMMA-*b*-PAA block copolymers via anionic polymerization technique.

Synthesis of TiO_2 Particles Using PMMA-*b*-PAA Micelles

The resulting block copolymers, PMMA-*b*-PAA, were completely dissolved in toluene to adjust concentration of 12 mg/mL. TiO_2 precursor solution was prepared by addition of 12 N HCl (0.12 g) into a mixture of 2-propanol (2.5 mL) and TTIP (0.37 g) and then stirred for 1 h until the solution became clear. The precursor solution was added to the copolymer micelles solution to make molar ratio range of Ti^{4+} to carboxyl groups in the block copolymer from 1.0 to 4.0. The resulting mixtures were then stirred for 1 h at room temperature to completely react TiO_2 precursor via sol-gel process, as shown in Scheme 2.

Preparation of TiO_2/PMMA Hybrid Films

PMMA polymer (M_n=30,000, M_w/M_n=2.00) was synthesized by conventional radical polymerization of MMA, using AIBN as an initiator. The micelle solutions containing TiO_2 precursor were put into 2 wt% PMMA toluene solution. After stirring for 1 h at room temperature, the resulting toluene solution was poured into a petri dish and then dried at 60 °C for 12 h to evaporate the solvent completely. The content of TiO_2 component in hybrid films was determined by thermal gravimetric analysis (TGA).

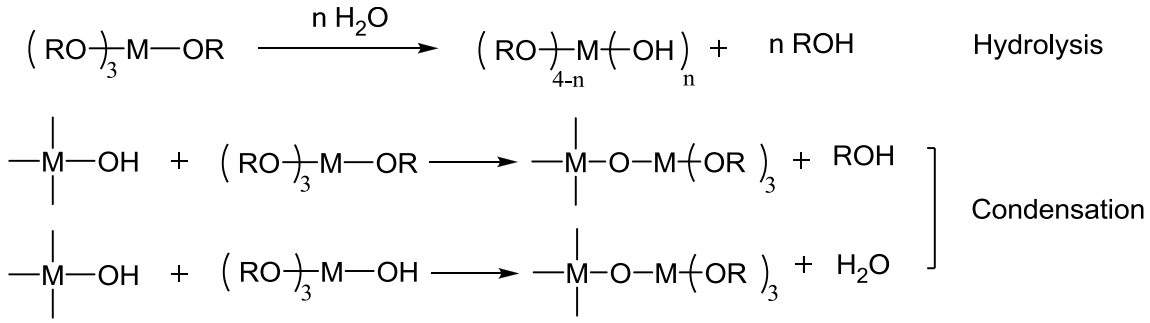

Scheme 2. Sol-gel process from metal alkoxides.

3-3. Results and Discussion

3-3-1. Synthesis and Characterization of Block Copolymers

Block copolymers, poly(methyl methacrylate-*block*-*tert*-butyl acrylates) (PMMA-*b*-PtBAs), were synthesized by anionic polymerization of MMA and tBA monomers in dehydrated THF solution with LiCl using 1,1-diphenylhexyllithium as an initiator. The molecular weight and polydispersity index of these block copolymer are summarized in Table 1. All of resulting block copolymers possessed well-defined molecular weight and a very narrow polydispersity index ($M_w/M_n < 1.10$). From ^{1}H NMR spectra, the component ratio of MMA and tBA moieties in the block copolymers was determined from the integrated intensity of peaks at $\delta = 3.59$ and 1.42 ppm, corresponding to methyl of MMA and *tert*-butyl protons of tBA, respectively. Hydrolysis of *tert*-butyl group in the PMMA-*b*-PtBA block copolymer was carried out under refluxing in the acidic condition (12 N HCl) to form PAA moieties. As shown in Figures 2 and 3, the hydrolysis reaction was confirmed by the disappearance of proton resonance peak at 1.42 ppm on ^{1}H NMR spectra assigned to *tert*-butyl group. Also, hydrolysis of *tert*-butyl group to form carboxylic acid was confirmed by FT-IR spectroscopy by noting the disappearance of characteristic absorbance of *tert*-butyl group at 1360 cm^{-1} (Figure 4)

Table 1. Characterization of block copolymers.

Samples	Before hydrolysis		After hydrolysis	M_w/M_n [a)]
	PMMA [a)] (g/mol)	PtBA [b)] (g/mol)	PAA [b)] (g/mol)	
$PMMA_{125}$-*b*-PAA_{40}	12,500	5,100	2,900	1.08
$PMMA_{228}$-*b*-PAA_{48}	22,800	6,100	3,500	1.06
$PMMA_{350}$-*b*-PAA_{93}	35,000	12,000	6,700	1.10
$PMMA_{800}$-*b*-PAA_{160}	80,000	20,400	11,600	1.05

a) Determined by GPC.

b) Estimated by ^{1}H NMR spectrum.

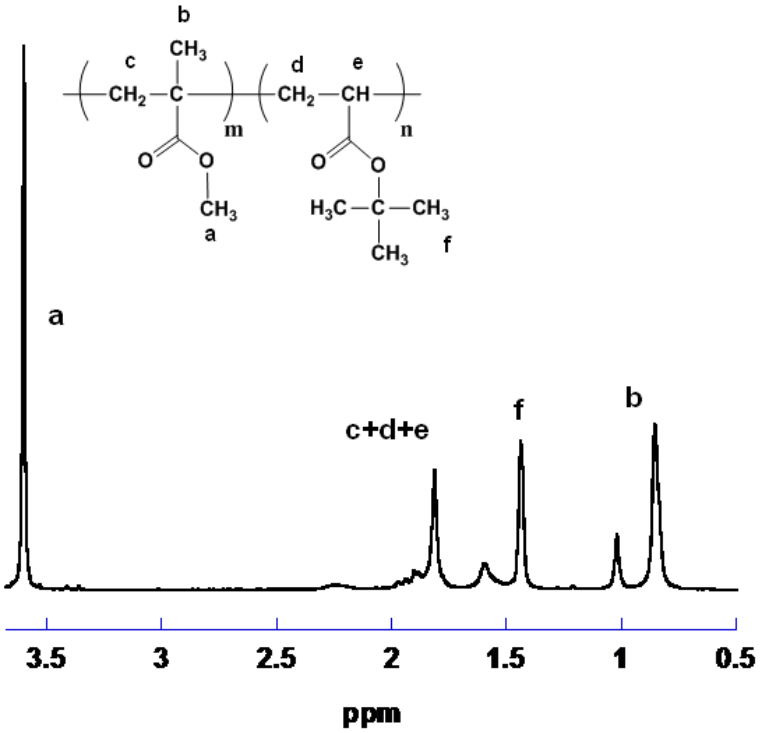

Figure 2. ^{1}H NMR spectrum of block copolymers, PMMA-*b*-PtBA before hydrolysis of *tert*-butyl group in chloroform-*d*.

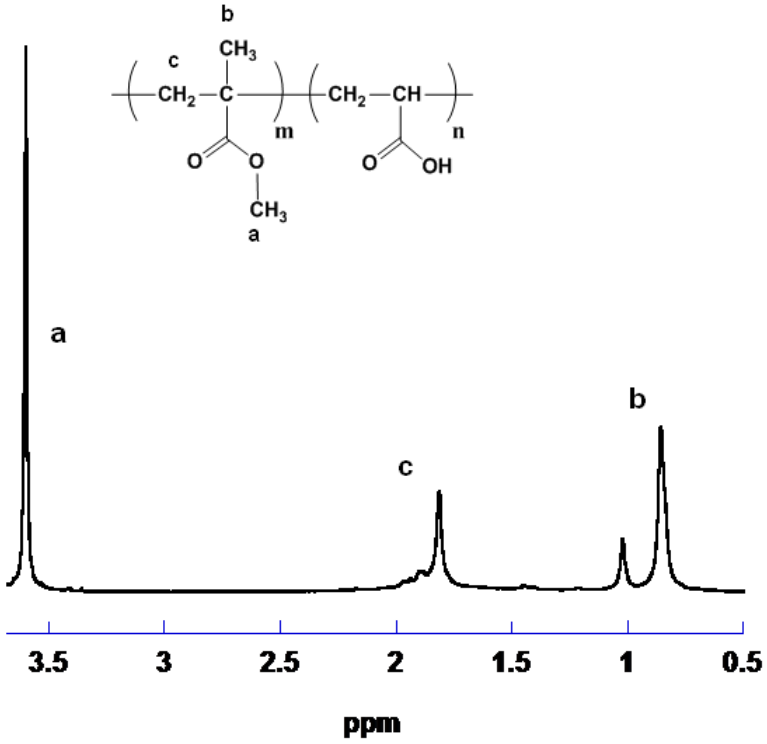

Figure 3. ^{1}H NMR spectrum of block copolymers, PMMA-*b*-PAA after hydrolysis of *tert*-butyl group in chloroform-*d*.

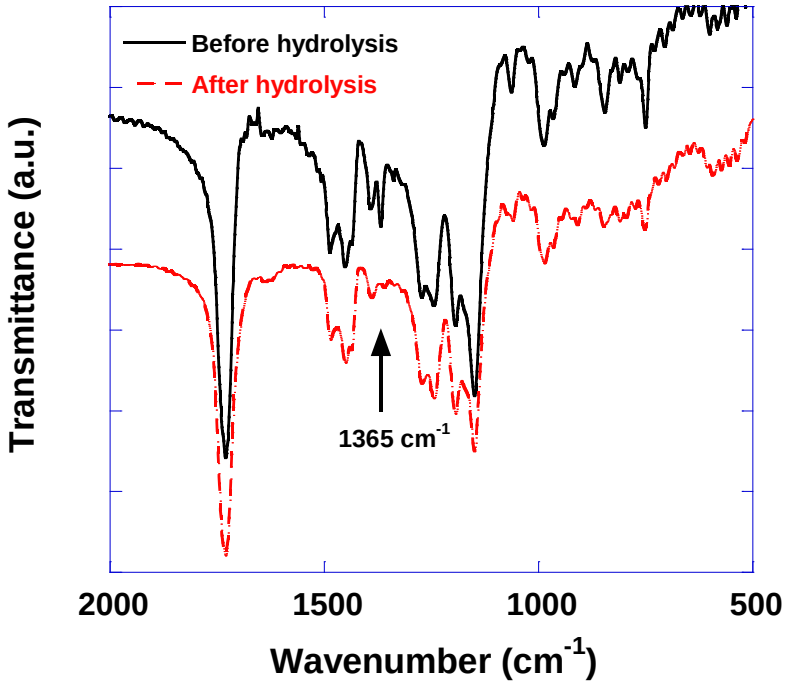

Figure 4. FT-IR spectra of PMMA-*b*-PtBA and PMMA-*b*-PAA.

3-3-2. Formation of Copolymer Micelles Loaded with TiO_2 precursor

Dissolving PMMA-*b*-PAA in toluene gave colorless and transparent solution. Formation of copolymer micelles in toluene was confirmed by appearance of light scattering in DLS measurement. The hydrodynamic diameter (D_h) was estimated by plots of square of scattering vector (q^2) and relaxation rates (Γ) by DLS, as described in Figure 5. The D_h values of copolymer micelles formed by $PMMA_{125}$-*b*-PAA_{40}, $PMMA_{228}$-*b*-PAA_{48}, $PMMA_{350}$-*b*-PAA_{93}, and $PMMA_{800}$-*b*-PAA_{160} in toluene were 30, 95, 80, and 198 nm, respectively. The values mostly depended on length of PMMA moiety, rather than the length of PAA moiety in block copolymers. In addition, AFM observations of copolymer micelles deposited on Si substrates were carried out to investigate morphology of

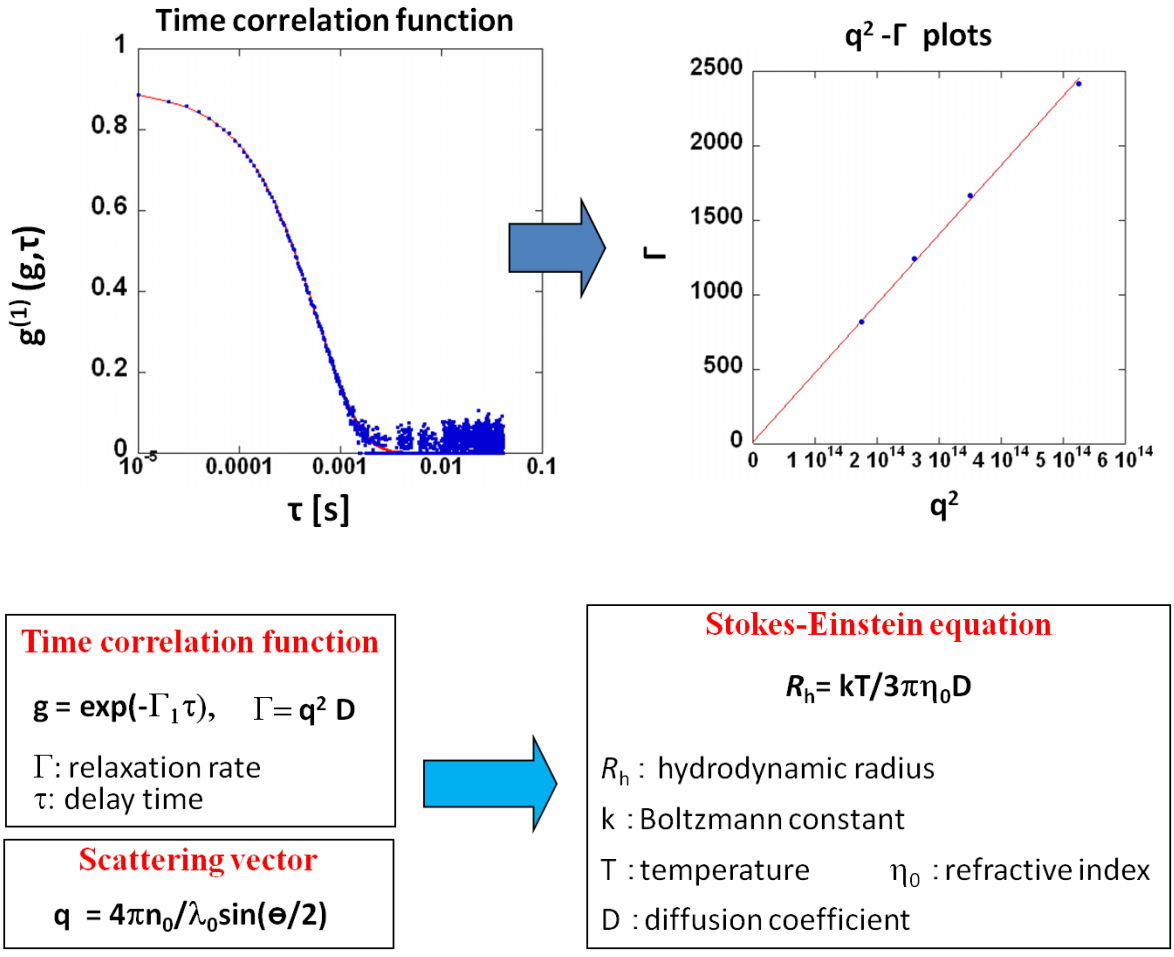

Figure 5. Estimation of hydrodynamic diameter (D_h) by plots of square of scattering vector (q^2) and relaxation rates (Γ).

copolymer micelles in dry state. As shown in Figure 6, an AFM image of $PMMA_{350}$-*b*-PAA_{93} copolymer micelles showed spherical particles of around 20 nm in the diameter, which is much smaller than D_h in solution.

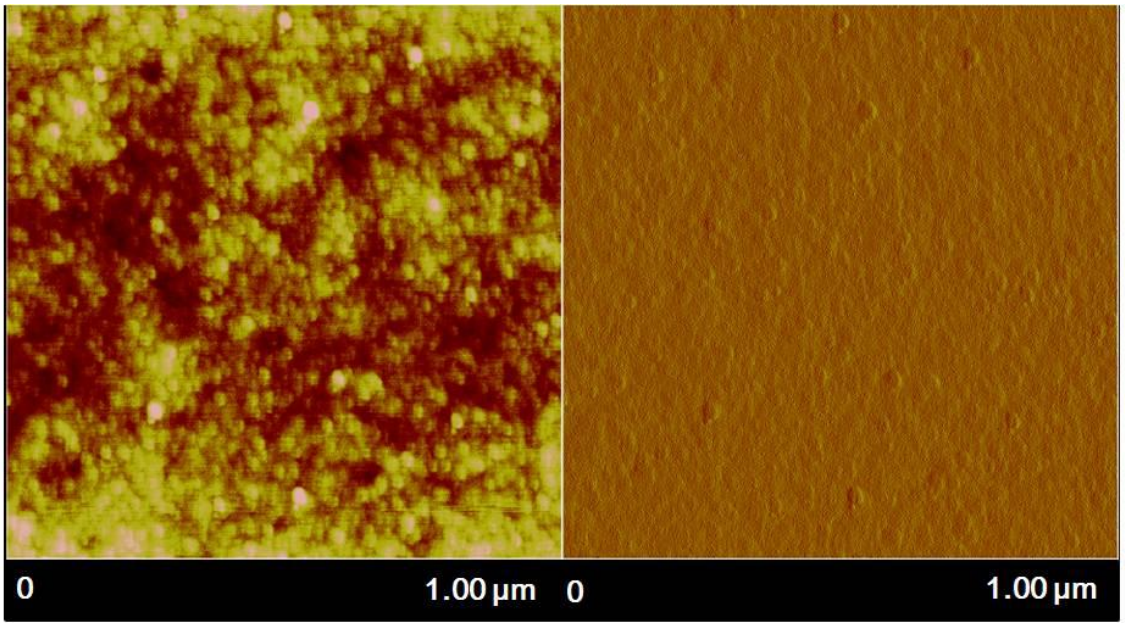

Figure 6. AFM images of polymer micelles of $PMMA_{350}$-*b*-PAA_{93} on Si substrate.

In present cases, D_h values probably correspond to whole size including both corona and core of copolymer micelles in solution, whereas particles size obtained from AFM images is possibly close to core size, composed of PAA block.

Effects of loading TiO_2 precursor on D_h of copolymer micelles were also investigated. Changes of D_h with molar ratio of Ti^{4+} in TiO_2 precursor to carboxyl group in block copolymers from 1.0 to 4.0 are shown in Figure 7. The addition of TiO_2 precursor to copolymer micelles solution gave rise to increasing D_h of copolymer micelles. The D_h values of copolymer micelles loaded by TiO_2 precursor at the mole ratio 4.0 were 67, 125, 135, and 320 nm for $PMMA_{125}$-*b*-PAA_{40}, $PMMA_{228}$-*b*-PAA_{48}, $PMMA_{350}$-*b*-PAA_{93}, and $PMMA_{800}$-*b*-PAA_{160}, respectively. These results obviously indicated that TiO_2 precursors less than the mole ratio 4.0 were selectively loaded within hydrophilic cores formed by PAA moiety without destruction of micelles, probably because of strong interaction

between titanium cation and carboxyl group. The copolymer micelles loaded with TiO_2 precursor were stably dispersed in toluene without any precipitations. Furthermore, morphologies of TiO_2 particles-loaded copolymer micelles were observed by TEM images. In the case of copolymer micelles obtained by $PMMA_{125}$-*b*-PAA_{40} loaded the precursor of Ti^{4+}/carboxyl mole ratio 1.0, inhomogeneous particles of around 10–15 nm in diameter were observed (Figure 8a). Addition of the precursor of high Ti^{4+}/carboxyl mole ratio resulted in formation of heterogeneous particles and in partial deformation of micelles (Figure 8b). On the other hand, when copolymer micelles of $PMMA_{228}$-*b*-PAA_{48} with higher PMMA length were used, spherical particles of around 15 nm in diameter, even at the mole ratio 4.0, were formed (Figure 8c, d). From these results, it was suggested that PMMA chain length played an important role in preservation of precursor-loaded particles, TiO_2 particles, during drying process, probably because of steric repulsion between PMMA chains. In the case of $PMMA_{350}$-*b*-PAA_{93}, morphologies of precursor-loaded micelles were relatively similar to those of $PMMA_{228}$-*b*-PAA_{48}. The particle size was mainly around 20 nm, which was larger than those of particles obtained from other copolymer micelles in Figure 9a. These results indicated that the size of TiO_2 particles depends on core size of copolymer micelles, which were formed by PAA chains. Moreover, the particles size of copolymer micelles was slightly increased with increasing of the mole ratio in precursor, and some aggregates of around 50 nm were partially observed at mole ratio 4, probably owing to saturation of loading capacity of the micelles (Figure 9b). In addition, we investigated copolymer micelles of $PMMA_{800}$-*b*-PAA_{160} with longer PMMA and PAA chains. From TEM images of the precursor-loaded micelles obtained from $PMMA_{800}$-*b*-PAA_{160}, formations of the particles around 15 nm along with aggregates larger than 50 nm were observed (Figure 9c, d). From these results, we concluded that control over component ratio and length in block polymers is important factor for formation of desired size nanoparticles and high stability of TiO_2 precursor-loaded copolymer micelles system. Consequently, we used block copolymer micelles of $PMMA_{350}$-*b*-PAA_{93} for fabrication of TiO_2/PMMA hybrid materials.

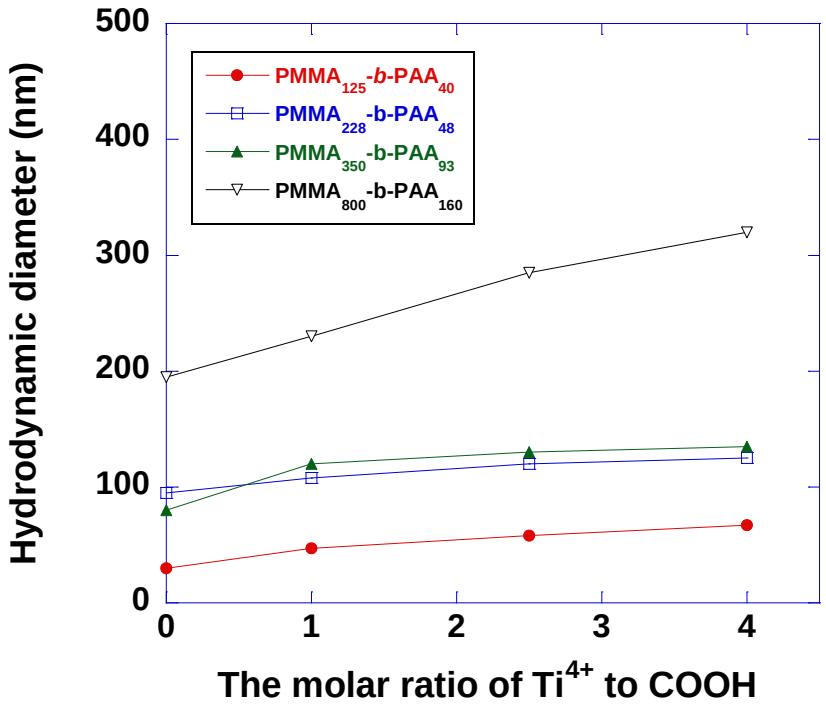

Figure 7. Effects of Ti^{4+}/COOH mole ratio in precursor on hydrodynamic diameter of copolymer micelles.

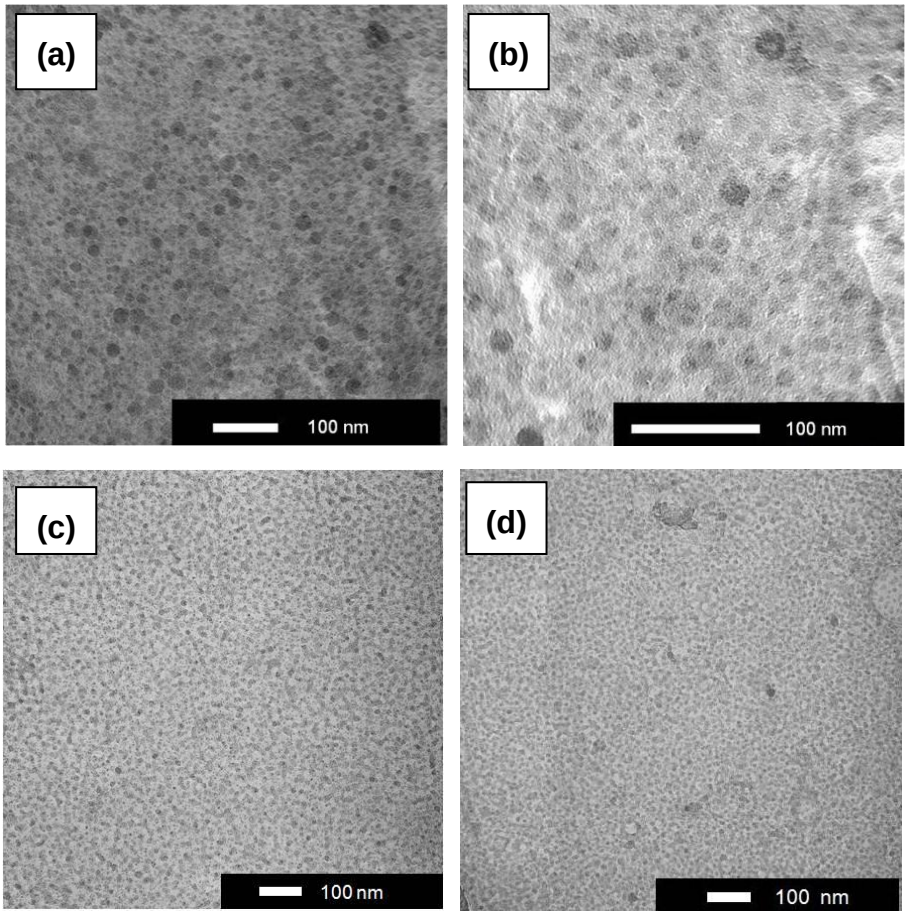

Figure 8. TEM images of copolymer micelles loaded with sol-gel precursor. Mole ratio of Ti^{4+}/COOH: (a) 1.0 and (b) 4.0 in $PMMA_{125}$-*b*-PAA_{40}; (c) 1.0 and (d) 4.0 in $PMMA_{228}$-*b*-PAA_{48}.

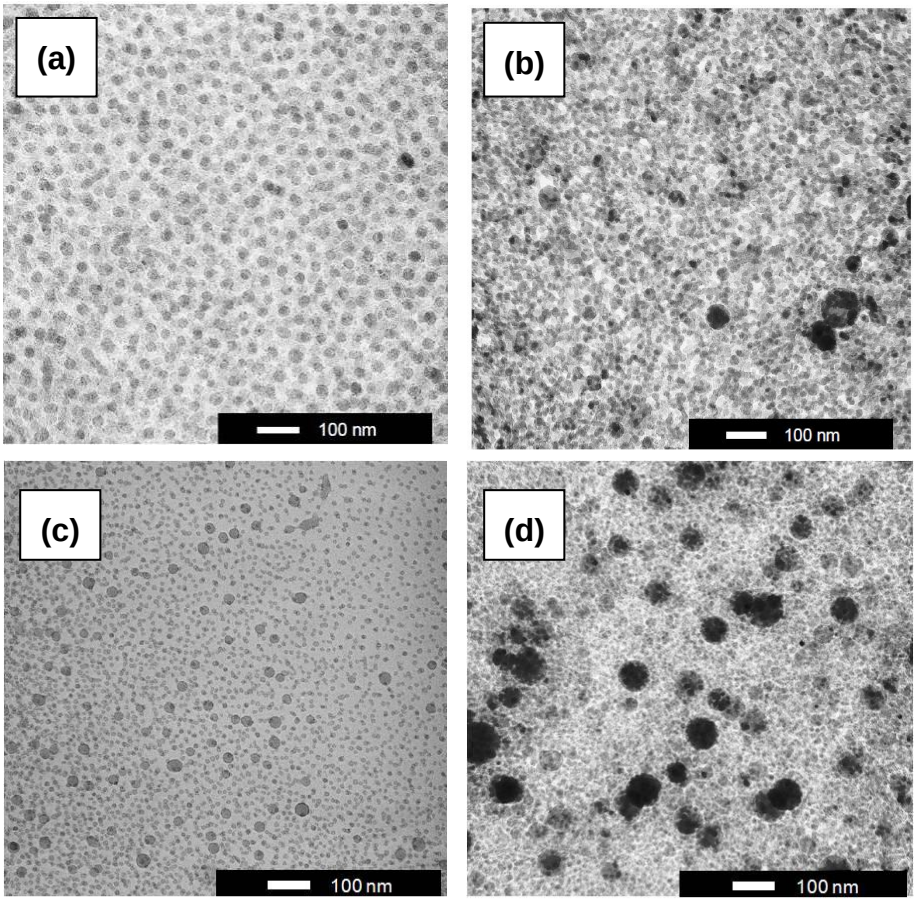

Figure 9. TEM images of polymer micelles loaded with sol-gel precursor. Mole ratio of Ti^{4+}/COOH; (a) 1.0 and (b) 4.0 in $PMMA_{350}$-*b*-PAA_{93}; (c) 1.0 and (d) 4.0 in $PMMA_{800}$-*b*-PAA_{160}.

3-3-3. Properties of TiO_2/PMMA Hybrid Films

Incorporation of resultant TiO_2 particles into PMMA matrix was carried out by casting toluene solution of precursor-loaded copolymer micelle, prepared from $PMMA_{350}$-*b*-PAA_{93}, and precursor of Ti^{4+}/carboxyl mole ratio 4.0 and PMMA of M_n = 30,000 to obtain TiO_2/PMMA hybrid films in 20-μm thickness. Effects of TiO_2 incorporation into PMMA matrix on thermal durability were examined by TGA. In Figure 10, thermodiagrams of the hybrid films are shown. Decomposition temperature, corresponding to 10% weight loss, of the films increased with TiO_2 content and elevated to 310 ºC, at 30 wt% TiO_2 content, which was 25 ºC higher than that of PMMA. Also, the char yield at 600 ºC increased with increasing TiO_2 content in the hybrid film, which indicated that the sol–gel precursor successfully incorporated into network of PMMA matrix.

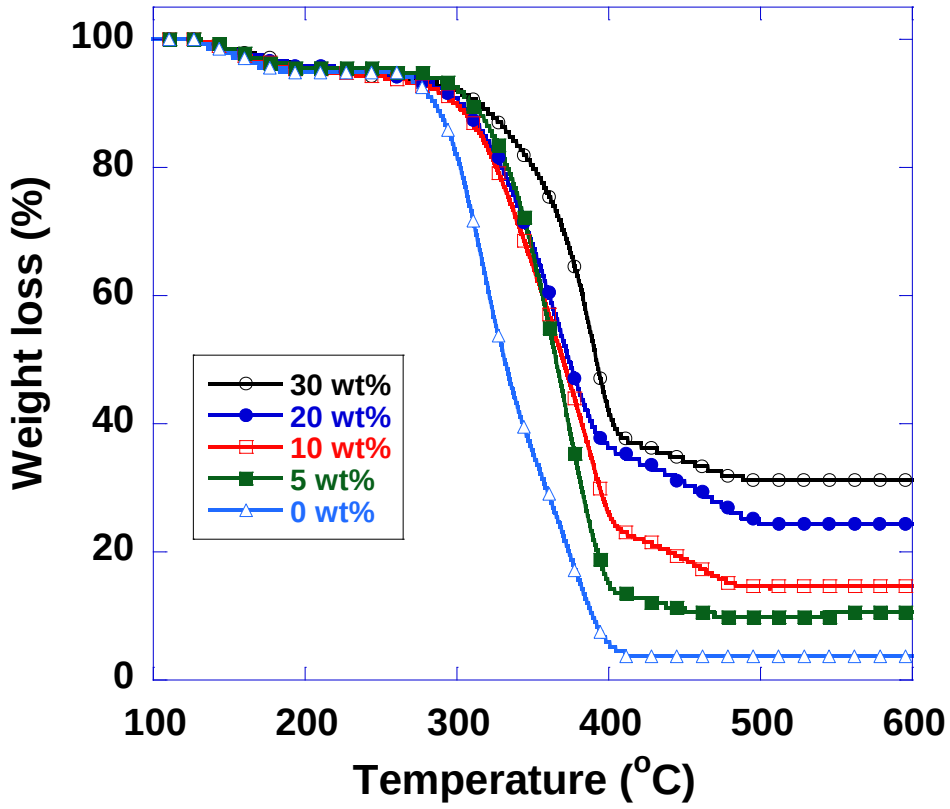

Figure 10. TGA curves of TiO_2/PMMA hybrid films containing 0-30 wt% TiO_2.

A photograph of TiO_2/PMMA hybrid film (20-μm thickness) with 30 wt% TiO_2 content is shown in Figure 11. The optical clear thin film was obtained. Transmission spectra of PMMA and 30 wt% TiO_2-contained PMMA hybrid film of 20-μm thickness are shown in Figure 12a. The hybrid film showed absorption bands below 350 nm, corresponding to band gap of TiO_2. Transmittances of the hybrid film at 400, 500, and 600 nm were, respectively, 83, 87, and 89%, being slightly 7, 4, and 2% lower than those of PMMA film of 20-μm thickness, respectively. Slight low transparency of the hybrid film is probably due to light scattering on aggregates of the particles. Actually, transmittance of the hybrid films at 500 nm gradually decreased with TiO_2 content in hybrid films (Figure 12b).

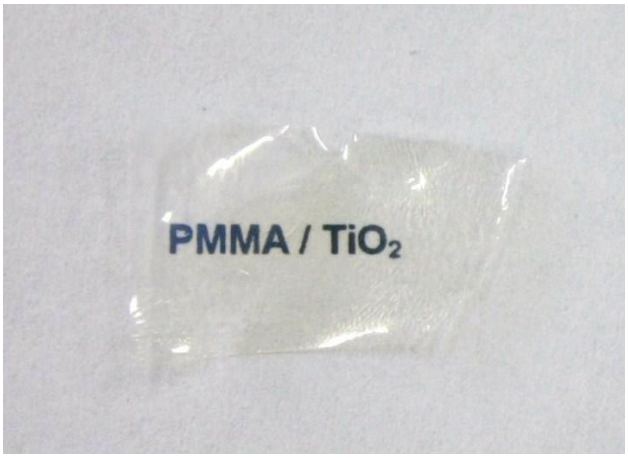

Figure 11. Photograph of TiO_2/PMMA hybrid films containing 30 wt% TiO_2 (20-μm thickness).

Refractive index of the hybrid films at 633 nm is also shown in Figure 12b. The indexes increased with TiO_2 content to attain 1.579 at 30 wt%, which is 0.1 higher than that of PMMA, and well agreed with the values calculated by the Lorentz–Lorenz equation:[28]

$$\frac{(n^2-1)}{(n^2+2)} = \sum v_i \frac{(n_i^2-1)}{(n_i^2+2)}$$

where n is the refractive index of hybrid film, and v_i and n_i are the volume fraction and refractive index of component i, respectively. In this case, refractive indexes of anatase TiO_2 and PMMA, 2.52 and 1.49, were used, respectively. In Figure 13, 14, 15

cross-sectional TEM images of the TiO_2/PMMA hybrid films are shown. In the film of low content of TiO_2 (10 wt%), both primary particles and domains of TiO_2 over 100 nm formed by aggregation were observed (Figure 13). Incorporation of more high content of TiO_2 of 20 or 30 wt% into PMMA led to formation of larger domain and/or aggregates of TiO_2 particles (Figure 14, 15). As TiO_2 precursor-loaded micelles of block copolymer were homogeneously dispersed in toluene, the domains or aggregates were possibly formed through mesostable phases consisted of micelles and PMMA in casting process. Furthermore, crystal structure of TiO_2 particles in PMMA matrix was investigated. From XRD analysis of TiO_2/PMMA hybrid films, any significant peaks attributable to anatase or rutile phase of TiO_2 were not observed, indicating that most of TiO_2 particles incorporated in PMMA matrix were amorphous or extremely small crystallized particles. From the fact that refractive index of the present films agreed with calculated values, estimated by using refractive index of anatase TiO_2, the particles incorporated into PMMA matrix were possibly composed of nanometer-size anatase TiO_2 particles. Application of the present technique to incorporation of other metal oxide particles such as ZrO_2, and ZnO into high refractive and transparent polymer when compared with PMMA is now in progress.

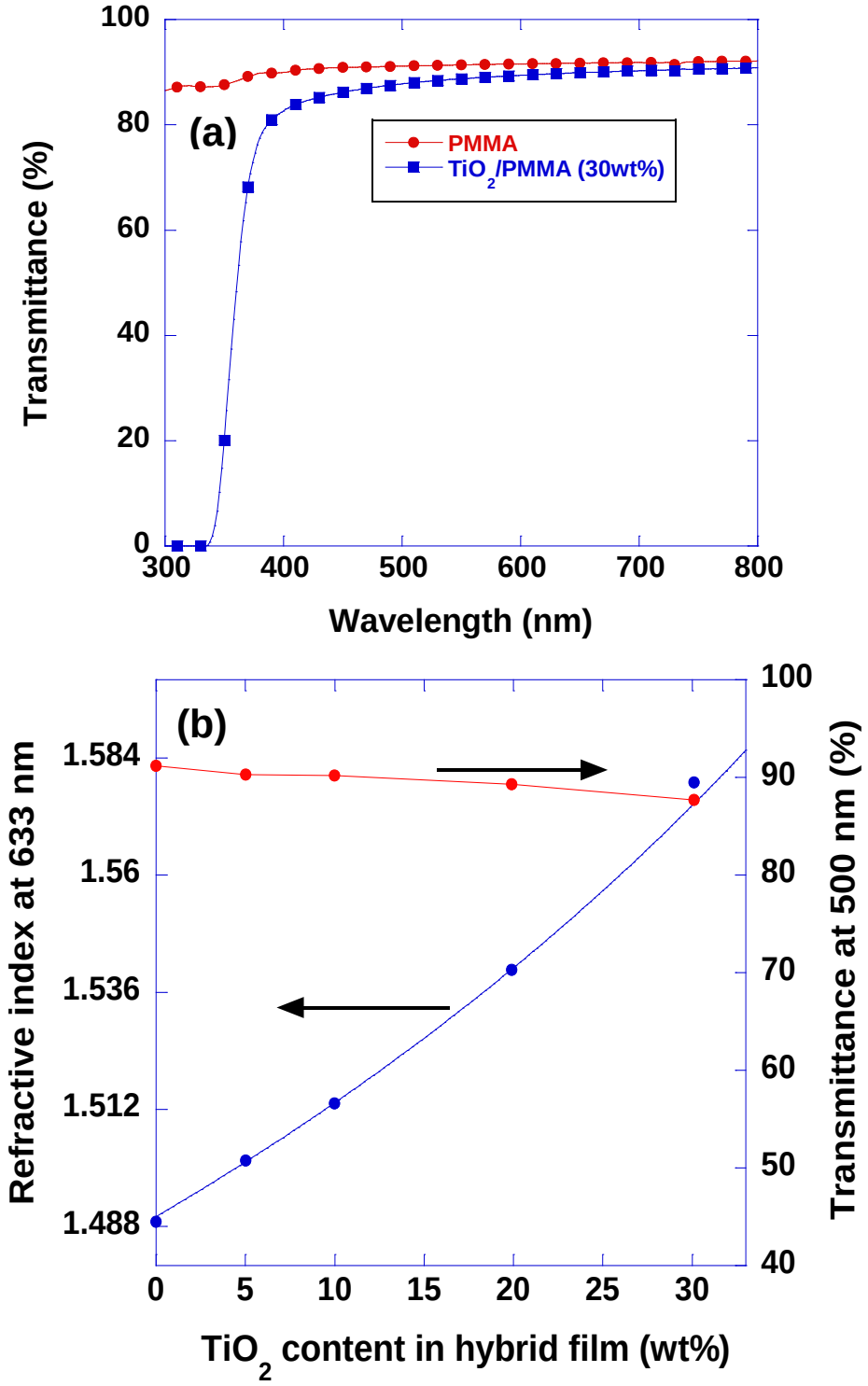

Figure 12. Transmission spectra of PMMA and TiO_2/PMMA (30 wt%) hybrid film with 20-μm thickness (a) and plots of TiO_2 content vs. refractive index and transmittance of TiO_2/PMMA hybrid films, for refractive index, solid line represents calculated values (b).

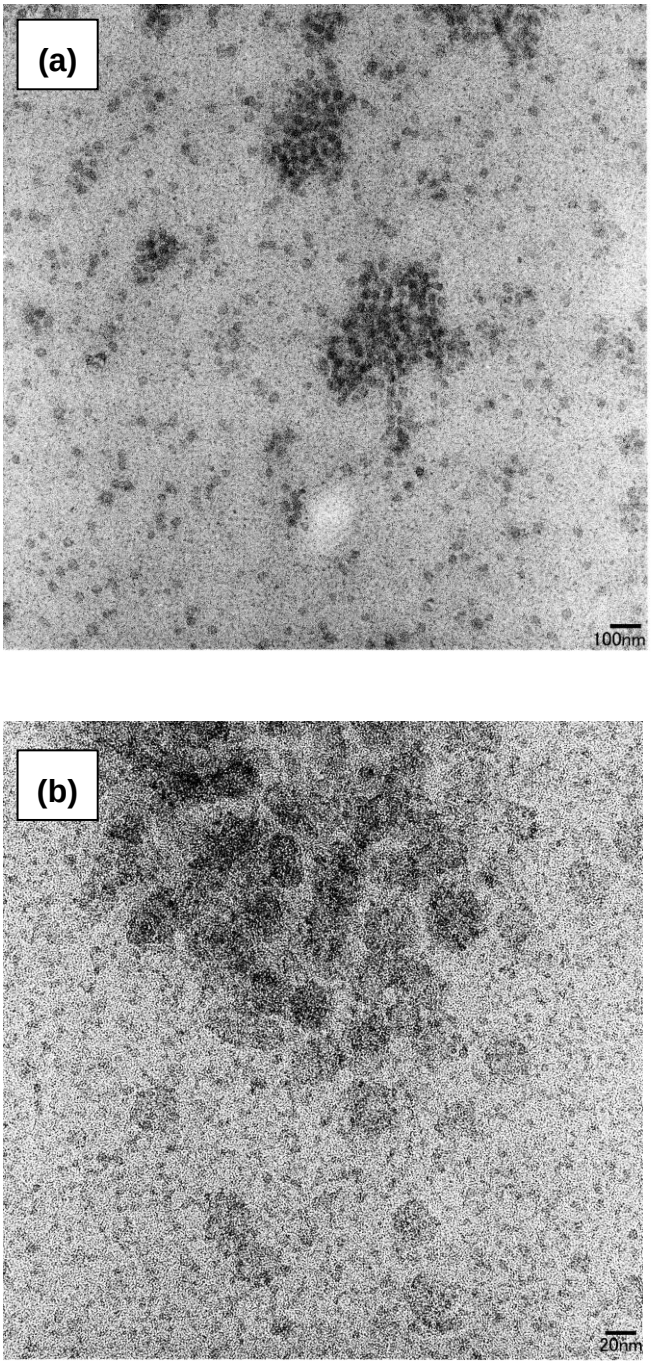

Figure 13. Cross-sectional TEM images of TiO_2/PMMA film (20 μm in thickness) with 10 wt%, (a) ×100,000, (b) ×500,000.

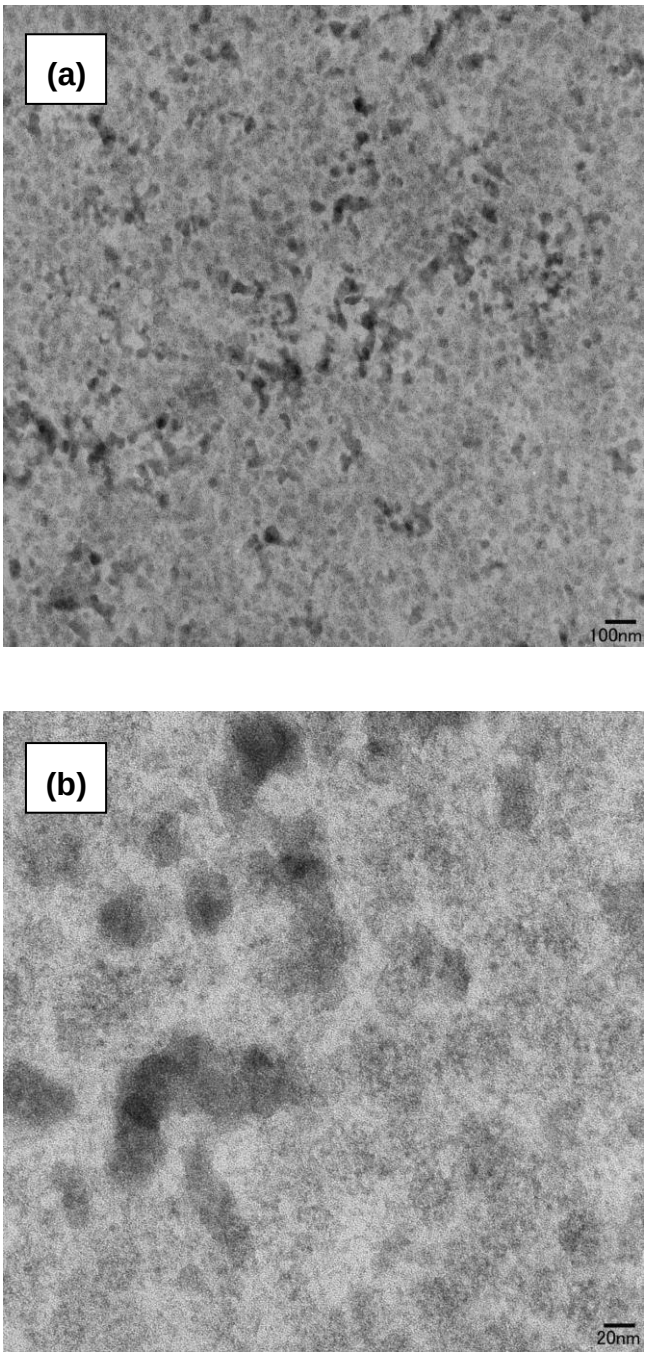

Figure 14. Cross-sectional TEM images of TiO_2/PMMA film (20 μm in thickness) with 20 wt%, (a) ×100,000, (b) ×500,000.

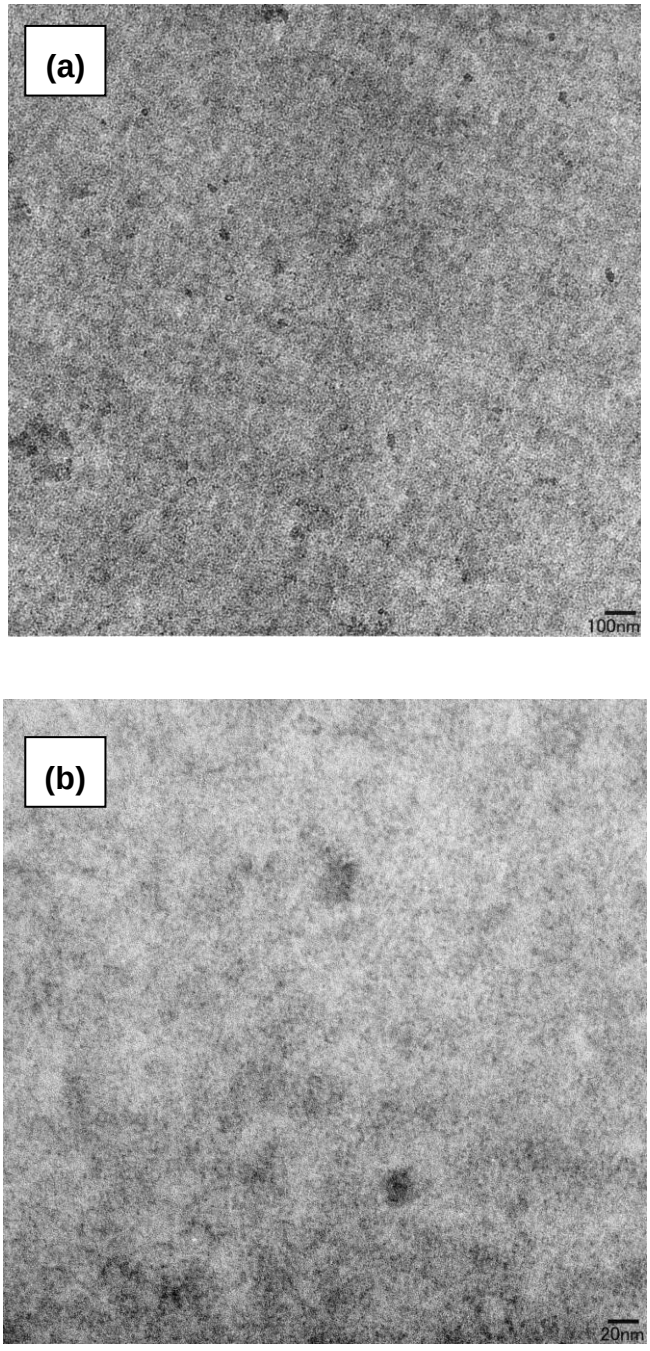

Figure 15. Cross-sectional TEM images of TiO_2/PMMA film (20 μm in thickness) with 30 wt%, (a) ×100,000, (b) ×500,000.

3-4. Conclusion

In this study, we successfully prepared nanosized TiO_2 particles of around 20 nm within polymer micelles of PMMA-*b*-PAA in toluene solution via sol–gel process from metal alkoxide. These particles were stably dispersed in toluene without any precipitations. Incorporation of TiO_2 particles into PMMA matrix was carried out by casting TiO_2 precursor-loaded micelle and PMMA in toluene to obtain hybrid films. The resultant TiO_2/PMMA hybrid films exhibited relatively high thermal stability than PMMA. Transmittance of TiO_2/PMMA hybrid films at 500 nm slightly decreased with increasing TiO_2 content, probably because of light scattering of aggregates of TiO_2 particles. The refractive index of the films proportionally elevated with TiO_2 content to attain 1.579 at 30 wt% TiO_2 content, which was 0.1 higher than that of PMMA. The refractive index of hybrid films agreed well with calculated values by the Lorentz–Lorenz equation, using the index of anatase TiO_2. From these results, TiO_2 particles incorporated into PMMA matrix were possibly composed of anatase TiO_2 particles in nanometer size. These TiO_2/PMMA hybrid materials could be used for highly refractive and antireflection coatings on the optical materials.

3-5. References

1. Hart, S. D.; Maskaly, G. R.; Temelkuran, B.; Prideaux, P. H.; Joannopoulos, J. D.; Fink, Y. *Science* **2002**, 296, 510.
2. Matsuda, T.; Funae, Y.; Yoshida, M.; Yamamoto, T.; Takaya, T. *J. Appl. Polym. Sci.* **2000**, 76, 50.
3. Gao, C.; Yang, B.; Shen, J. *J. Appl. Polym. Sci.* **2000**, 75, 1474.
4. Temelkuran, B.; Hart, S. D.; Benoit, G.; Joannopoulos, J. D.; Fink, Y. *Nature* **2002**, 420, 650.
5. Okutsu, R.; Ando, S.; Ueda, M. *Chem. Mater*. **2008**, 20, 4017.
6. Dobrowolski, J. A.; Ho, F. *Appl. Opt.* **1982**, 21, 288.
7. Cui, Z. C.; Lu, C. L.; Yang, B.; Shen, J. C.; Su, X. P.; Yang, H. *Polymer* **2001**, 42, 10095.
8. Yablonovitch, E. *Science* **2000**, 289, 557.

9. Yoshida, M.; Prasad, P. N. *Chem. Mater*. **1996**, 8, 235.
10. Matsuda, T.; Funae, Y.; Yamamoto, T.; Takaya, T. *J. Appl. Polym. Sci*. **2000**, 76, 45.
11. Okutsu, R.; Suzuki, Y.; Ando, S.; Ueda, M. *Macromolecules* **2008**, 41, 6165.
12. Matsuura, T.; Ishizawa, M.; Hasuda, Y.; Nishi, S. *Macromolecules* **1992**, 25, 3540.
13. Lee, K. S.; Lee, J. S. *Chem. Mater*. **2006**, 18, 4519.
14. Liu, J. G.; Nakamura, Y.; Ogura, T.; Shibasaki, Y.; Ando, S.; Ueda, M. *Chem. Mater*. **2008**, 20, 273.
15. You, N. H.; Higashihara, T.; Oishi, Y.; Ando, S.; Ueda, M. *Macromolecules* **2010**, 43, 4613.
16. Lee, L. H.; Chen, W. C. *Chem. Mater*. **2001**, 13, 1137.
17. Lee, S.; Shin, H. J.; Yoon, S. M.; Yi, D. K.; Choi, J. Y.; Paik, U. *J. Mater. Chem*. **2008**, 18, 1751.
18. Demir, M. M.; Memesa, M.; Castignolles, P.; Wegner, G. *Macromol. Rapid Commun*. **2006**, 27, 763.
19. Lu, C. L.; Cheng, Y. R.; Liu, Y. F.; Liu, F.; Yang, B. *Adv. Mater*. **2006**, 18, 1188.
20. Kyprianidou-Leodidou, T.; Caseri, W.; Suter, U. W. *J. Phys. Chem*. **1994**, 98, 8992.
21. Gehr, R. J.; Boyd, R. W. *Chem. Mater*. **1996**, 8, 1807.
22. Zhang, Q. Y.; Wang, J.; Shen, J.; Buddhude, S. *Mater. Chem. Phys*. **2001**, 72, 56.
23. Yoshinaga, K.; Yamauchi, M.; Maruyama, D.; Mouri, E.; Koyanagi, T. *Chem. Lett.* **2005**, 34, 1094.
24. Wang, Z. F.; Yamada, S.; Zhang, M.; Kanzaki, H.; Yoshinaga, K. *Colloid Polym. Sci*. **2010**, 288, 433.
25. Yamada, S.; Wang, Z. F.; Mouri, E.; Yoshinaga, K. *Colloid Polym. Sci*. **2009**, 287, 139.
26. Varshney, S. K.; Hautekeer, J. P.; Fayt, R.; Jerome, R.; Teyssie, P. *Macromolecules* **1990**, 23, 2618.
27. Varshney, S. K.; Jacobs, C.; Hautekeer, J. P.; Bayard, P.; Jerome, R.; Fayt, R.; Teyssie, P. *Macromolecules* **1991**, 24, 4997.
28. Aspnes, D. E. *Am. J. Phys*. **1982**, 50, 704.

CHAPTER 4

Synthesis and Characterization of Fluorene-Carbazole and Fluorene-Phenothiazine Copolymers with Carbazole and Oxadiazole Pendants for Organic Light Emitting Diode

4-1. Introduction

Conjugated polymers have been utilized as active materials in several kinds of electronic devices such as thin film transistor,[1] photovoltaic cell,[2, 3] and organic light emitting diodes (OLEDs),[4] including flexible displays.[5] OLEDs have attracted much attention with several advantages over conventional devices including low driving voltage, wide viewing angle, and a simple manufacturing process.[6-9] Much effort has been devoted to the fabrication of white-organic-light-emitting diodes (WOLEDs), because of possible applications for low-cost room illumination. One of the methods of the realization of WOLED is the multilayer device system with red, green and blue light emitting materials.[10-12] Although the multilayer devices show high efficiencies and long lifetimes, the fabrication of the multilayer using spin-coating process is unsuitable with polymeric light emitting materials which are soluble only in organic solvents. Another method is using a single light emitting layer with red, green, and blue light emitting polymer blends.[13, 14] Even though using polymer blends is a promising process for the generation of white light emission, phase separation, low efficiency, and voltage dependence of emitting color limit their utilization. Recently, several groups achieved the fabrication of WOLEDs from polyfluorene-based polymers containing red and green light emitting portions on the backbones.[15-18] In these cases, the color of the emission was easily tuned by adjusting the composition of the polymers to control the partial energy transfer to red, or green emissive units.

We previously reported the intriguing results of white light emission from poly(9-(6-(9*H*-carbazolyl)hexyl)-9-(6-(4-(5-phenyl-1,3,4-oxadiazolyl)-phenoxy)hexyl)-9*H*-fluorene) (PFCzOxd), containing carbazole and oxadiazole units as pendants, due to the peak at 426 nm and broad peak around 540 nm which is attributed to the aggregations caused by the carbazole and oxadiazole units.[19] The OLEDs fabricated with PFCzOxd generated electroluminescence (EL) with excellent Commission Internationale d' Enclairage (CIE) coordinate (x=0.31, y=0.33) for the white color. In this Chapter 4, we

describe the synthesis and characterization of new series of the fluorene-based polymers with carbazole and oxadiazole pendants for the generation of the white emission out of the EL device. In the fluorene backbone, hole transporting units such as carbazole or phenothiazine were incorporated to improve the EL properties since carbazole and phenothiazine units have good hole transporting behavior caused by the electron lone pair on nitrogen or sulfur atoms. The carbazole and phenothiazine were incorporated into the backbone to perform as hole transporter to improve hole injection and hole trapping site for efficient electron-hole recombination to yield emitting excitons.

4-2. Experimental Section

Materials

The materials used in this study, 2-(4-(6-bromohexyloxy)phenyl)-5-phenyl-1,3,4-oxadiazole (1), 2,7-dibromo-9-(6-(4-(5-phenyl-1,3,4-oxadiazolyl)phenoxy)hexyl)-9*H*-fluorene (3), 2,7-dibromo- 9,9-bis(6-(9*H*-carbazolyl)hexyl)-9*H*-fluorene (4), 9-(heptadecan-9-yl)-2,7-bis(4,4,5,5-tetramethyl-1,3,2-dioxaborolan-2-yl)-9*H*-carbazole (5), 2,7-dibromo-9-(heptadecan-9-yl)-9*H*-carbazole (6), and 3,7-dibromo-10-octyl-10*H*-phenothiazine (7) were synthesized according to the procedure outlined in the literatures.[19-24] The hole-injection-transport material, PEDOT:PSS, was purchased from H.C. Starck with Clevios PH grade. All used reagents for organic synthesis were purchased from Aldrich and used without further purification.

Measurement

^{1}H and ^{13}C NMR spectra were recorded with a Varian Gemini-300 (300 MHz) spectrometer and chemical shift were recorded in ppm units with TMS as the internal standard. Flash column chromatography was performed with Merck silica gel 60 (particle size 230–400 mesh ASTM). Analytical thin layer chromatography (TLC) was conducted using Merck 0.25 mm silica gel 60F pre-coated aluminum plates with fluorescent indicator UV254. Molecular weights and polydispersities of the polymer were determined by gel

permeation chromatography (GPC) with a polystyrene standard calibration. The differential scanning calorimetry analysis was performed under nitrogen atmosphere (50 mL/min) on a DSC 822 at a heating rate of 10 ºC/min. Thermogravimetric analysis was performed with a Dupont951 TGA instrument in nitrogen atmosphere at a heating rate of 10 ºC/min to 600 ºC. Fast atom bombardment (FAB) mass spectra were determined using at Korea Basic Science Institute Seoul Branch and Korea Basic Science Institute Daegu Branch. Cyclic voltammetric waves were produced by using an EG&G Parc model 273 potentiostat/galvanostat at a constant scan rate of 100 mV/s. UV spectra were recorded with Varian CARY-5EUV/vis spectrophotometer. The PL and EL spectra were measured using Oriel InstaSpec IV CCD detection systems. For PL spectrum measurement, a xenon lamp was used as the excitation source and incident beam took the maximum absorption peak of the polymers. For the determination of device characteristics, current-voltage (*I*-*V*) characteristics were measured using a Keithley 2400 source measure unit.

EL Device Fabrication and Measurements

For the EL device fabrication and measurements, poly(3,4-ethylenedioxythiophene) (PEDOT) doped with poly(styrenesulfonate) (PSS), as the hole-injection-transport layer, was introduced between emissive layer and ITO glass substrate cleaned by successive ultrasonic treatments. The solution of the PEDOT:PSS in aqueous isopropyl alcohol was spin-coated on the surface-treated ITO substrate and dried on a hot plate for 30 min at 110 ºC. On top of the PEDOT layer, the emissive polymer film was obtained by spin casting chlorobenzene solution of the polymer. The emissive polymer thin film prepared had a uniform surface with a thickness of around 110 nm. The emissive film was dried in vacuum, and calcium (20 nm) and aluminum (100 nm) electrodes were deposited on the top of the polymer films through a mask by vacuum evaporation at pressures below 10^{-7} Torr, yielding active areas of 4 mm^2. For the determination of device characteristics, current density-voltage (*J*-*V*) and luminance-voltage (*L*-*V*) characteristics of the devices were measured using a Keithley 2400 Source Measure Unit equipped with a calibrated photo-multiplier tube. EL device was totally fabricated and measured in glove box. The CIE coordinate's numbers were calculated automatically by the Keithley 2400 Source Measure Unit, for the EL measurement.

Synthesis of 2,7-Dibromo-9,9-bis(6-(4-(5-phenyl-1,3,4-oxadiazolyl) phenoxy)hexyl)-9*H*-fluorene (2)

A solution of 2,7-dibromo-9*H*-fluorene (5 g, 15.4 mmol), 2-(4-(6-bromohexyloxy)phenyl)-5-phenyl-1,3,4-oxadiazole (1) (12.4 g, 30.8 mmol), and catalytic amounts of triethylbenzyl ammonium chloride in 200 mL of DMSO was stirred at 60 ºC for 1 h under argon. The reaction mixture was treated with 4 mL of 50% NaOH aqueous solution at room temperature and then stirred for 5 h. An excess amount of ethyl acetate was added to the resulting mixture to generate a precipitation of NaOH. After collection of NaOH by filtration, the organic phase was washed with water, dried over $MgSO_4$ and then concentrated under reduced pressure. The crude product was purified by flash column chromatography (ethyl acetate/hexane = 1/2 as an eluent) to get 5.60 g (37%) of the target product as a white solid.

^{1}H NMR (300 MHz, $CDCl_3$) δ (ppm): 8.15-8.10 (m, 4H), 8.05 (d, 4H, J = 9.0 Hz), 7.56–7.44 (m, 12H), 6.99 (d, 4H, J = 9.0 Hz), 3.93 (t, 4H, J = 6.3 Hz), 2.00-1.93 (m, 4H), 1.67-1.62 (m, 4H), 1.29–1.16 (m, 8H), 0.90–0.62 (m, 4H). ^{13}C NMR (75 MHz, $CDCl_3$) δ (ppm): 164.82, 164.31, 162.08, 152.48, 139.32, 131.75, 130.55, 129.27, 128.88, 127.04, 126.33, 124.32, 121.80, 121.50, 116.36, 115.15, 68.28, 55.84, 40.37, 29.78, 29.19, 25.88, 23.84. HRMS (*m/z* FAB$^+$) Calcd for $C_{53}H_{48}Br_2N_2O_2$ 964.2022, found 965.2215.

Synthesis of Alternating Copolymers via Suzuki Coupling Reaction

Carefully purified monomer 3 (or 4 or (2 + 4)), monomer 5, and tetrakis(triphenylphosphine) palladium(0) ($Pd(PPh_3)_4$) as the catalyst were dissolved in a mixture of toluene (3 mL) and aqueous 2 M K_2CO_3 (2.5 mL). The mixture was refluxed with vigorous stirring for 3 days under argon atmosphere. After 72 h, phenylboronic acid was added to the mixture, and then 12 h later, bromobenzene was added and the reaction mixture refluxed overnight to complete the end capping reaction. After the mixture was cooled to room temperature, it was poured into methanol. The precipitated material was collected by filtration. The resulting solid material was reprecipitated using 100 mL of THF/1.0 L of methanol several times to remove catalyst residues and to generate PFCzOxd-*alt*-PCz

(with monomer 3), PFCzCz-*alt*-PCz (with monomer 4), and PFCzCzPCz-*co*-PFOxdOxdPCz (with monomer 2+4). The yields of the polymers ranged from 40 to 60%. The resulting polymers were soluble in THF, $CHCl_3$, ODCB and toluene.

^{1}H NMR (300 MHz, $CDCl_3$) δ (ppm): PFCzOxd-*alt*-PCz: 8.18 (s), 8.12-7.99 (m), 7.87 (s), 7.73 (s), 7.51-7.50 (m), 7.40-7.14 (m), 6.94 (d), 4.17 (s), 3.90 (s), 2.40 (s), 2.15(s), 1.99 (s), 1.67 (m), 1.27-1.15 (m), 0.89-0.78 (m). PFCzCz-*alt*-PCz: 8.02 (s), 8.06 (d), 7.87 (s), 7.71 (m), 7.55-7.41 (m), 7.38-7.15 (m), 4.68 (s), 4.17-4.15 (m), 2.38 (s), 2.19 (s), 2.11 (s), 1.96 (s), 1.82 (s), 1.72 (s), 1.27-1.14 (m), 0.83-0.78 (m). PFCzCzPCz-*co*-PFOxdOxdPCz: 8.16 (s), 8.11-8.03 (m), 7.99 (s), 7.87-7.69 (m), 7.60-7.39 (m), 7.36-7.13 (m), 6.97 (d), 4.69 (s), 4.15 (s), 3.89 (d), 2.38 (s), 1.98-1.59 (m), 1.25 (s), 1.14-0.77 (m).

Synthesis of Random Copolymers via Yamamoto Coupling Reaction

In a three neck flask was placed bis(1,5-cyclooctadiene)nickel(0) ($Ni(COD)_2$) (350 mg, 1.27 mmol), 2,2'-dipyridyl (200 mg, 1.27 mmol), 1,5-cyclooctadiene (0.16 mL, 1.27 mmol), and *N*,*N*-Dimethylformamide (DMF) (8mL). After three freezing-thaw cycles, the catalyst was heated to 80 ºC for 30 min to form the purple complex. The reaction mixture was treated with monomer 3 and monomer 6 (or monomer 7) in 5 mL of toluene and heated at 80 ºC for 4 days. After cooling to room temperature, the reaction mixture was poured into the mixture of 1 N HCl solution (100 mL), acetone (100 mL), and methanol (200 mL), and stirred for 6 h. The precipitate was filtered, redissolved in chloroform and precipitated again with a large amount of methanol. The yields of the polymers ranged from 40 to 50%. The resulting polymers were soluble in THF, $CHCl_3$, ODCB and toluene. The co-monomers feed ratios of 3 to 6 are 99:1, 97:3, 95:5 and 90:10, and the corresponding copolymers were named as PFCzOxd-*co*-PCz1, PFCzOxd-*co*-PCz3, PFCzOxd-*co*-PCz5, and PFCzOxd-*co*-PCz10, respectively. The co-monomers feed ratios of 3 to 7 are 99:1, 97:3, 95:5 and 90:10, and the corresponding copolymers were named as PFCzOxd-*co*-PPTZ1, PFCzOxd-*co*-PPTZ3, PFCzOxd-*co*-PPTZ5, and PFCzOxd-*co*-PPTZ 10, respectively.

^{1}H NMR (300 MHz, $CDCl_3$) δ (ppm): PFCzOxd-*co*-PCz1: 8.05-7.93 (m), 7.77-7.47 (m), 7.39-7.10 (m), 6.88 (d), 4.07 (s), 3.78 (s), 2.05 (s), 1.59-1.12 (m), 0.88-0.82 (m). PFCzOxd-*co*-PCz3: 8.062-7.949 (m), 7.671-7.491 (m), 7.338-7.138 (m), 6.861 (d), 4.084

(s), 3.793 (s), 2.012 (s), 1.691-1.135 (m), 0.974-0.888 (m). PFCzOxd-*co*-PCz5: 8.06-7.95 (m), 7.78 (s), 7.67 (s), 7.49 (s), 7.36-7.14 (m), 6.86 (d), 4.09 (s), 3.79 (s), 2.08 (s), 1.29-1.14 (m), 0.89-0.79 (m). PFCzOxd-*co*-PCz10: 8.05-7.94 (m), 7.66-7.47 (m), 7.39-7.12 (m), 6.85 (d), 4.07 (s), 3.78 (s), 2.02 (s), 1.25-1.13 (m), 0.88-0.78 (m). PFCzOxd-*co*-PPTZ1: 8.07-7.99 (m), 7.66-7.47 (m), 7.26-7.14 (m), 6.86 (s), 4.07 (s), 3.78 (s), 2.06 (s), 1.57-1.13(m), 0.87-0.81 (m). PFCzOxd-*co*-PPTZ3: 8.06-7.95 (m), 7.78-7.31 (m), 7.27-7.14 (m), 6.87 (d), 4.08 (s), 3.79 (s), 2.05 (s), 1.59-1.13 (m), 0.88-0.83 (m). PFCzOxd-*co*-PPTZ5: 8.05-7.94 (m), 7.78-7.40 (m), 7.33-7.11 (m), 6.86 (d), 4.08 (s), 3.79 (s), 2.06 (s), 1.65-1.13 (m), 0.88-0.75 (m). PFCzOxd-*co*-PPTZ10: 8.06-7.94 (m), 7.80-7.40 (m), 7.38-7.14 (m), 6.87 (d), 4.08 (s), 3.79 (s), 2.06 (s), 1.71-1.13 (m), 0.89-0.80 (m).

4-3. Results and Discussion

4-3-1. Synthesis and Characterization of Conjugated Polymers

The general synthetic routes toward the monomer and polymers are outlined in Scheme 1 and Scheme 2. The monomers (3, 4, 5, 6, and 7) used for the polymerization were synthesized and purified carefully according to the procedure outlined in the literatures.[19-23] The monomer 2 was synthesized by the alkylation of 2,7-dibromo-9*H*-fluorene with 2-(4-(6-bromohexyloxy)phenyl)-5- phenyl-1,3,4-oxadiazole (1) in the presence of catalytic amounts of triethylbenzyl ammonium chlo ride and 50% NaOH aqueous solution. The polymerization was conducted by the Pd(0)-catalyzed Suzuki coupling polymerization. In the case of poly(9-(6-(9*H*-carbazolyl)hexyl)-9-(6-(4-(5-phenyl-hexyl)-9-(6-(4-(5-phenyl-1, 3,4-oxadiazolyl)phenoxy)hexyl)-9*H*-fluorene-*alt*-9-(heptadecan-9-yl)-9*H*-carbazole)(PFCz Oxd-*alt*-PCz) (or poly(9,9-bis(6-(9*H*-carbazolyl)hexyl)-9*H*-fluorene-*alt*-9-(heptadecan-9-y l)-9*H*-carbazole) (PFCzCz-*alt*-PCz)), the molar feed ratio of monomer 3 (or 4) and diborommic ester monomer 5 was 1:1. In case of poly(2-(9-(heptadecan-9-yl)-9*H*-carbazo-l-2-yl)-9,9- bis(6-(9*H*-carbazolyl)hexyl)-9*H*-fluorene-*co*-2-(9-(heptadecan-9-yl)-9*H*-carba-zol-2-yl)-9,9-bis(6-(4-(5-phenyl-1,3,4-oxadiazloyl)phenoxy)-hexyl)-9*H*-fluorene) (PFCzCz PCz-*co*-PFOxdOxdPCz), the molar feed ratio of monomer 2, 4 and 5 was 1:1:2. Monomer 3 was copolymerized with monomer 6 or 7 by nickel-catalyzed Yamamoto coupling, using bis(1,5-cyclooctadiene)nickel(0) ($Ni(COD)_2$), 2,2'-dipyridyl, and 1,5-cyclooctadiene. To

generate the copolymers, poly(9-(6-(9*H*-carbazolyl)hexyl)-9-(6-(4-(5-phenyl-1,3,4-oxadiazolyl)-phenoxy)hexyl)-9*H*-fluorene-*co*-9-(heptadecan-9-yl)-9*H*-carbazole) (PFCzOxd-*co*-PCz), different ratios of monomer 3 and 6 were used. The feed ratios of fluorene unit with carbazole and oxadiazole pendants and carbazole unit fragments were 99:1, 97:3, 95:5, and 90:10 for the syntheses of PFCzOxd-*co*-PCz1, PFCzOxd-*co*-PCz3, PFCzOxd-*co*-PCz5, and PFCzOxd-*co*-PCz10, respectively. To generate the copolymers, poly(9-(6-(9*H*-carbazolyl)hexyl)-9-(6-(4-(5-phenyl-1,3,4-oxadiazolyl)phenoxy)hexyl)-9*H*-fluorene-*co*-10-octyl-10*H*-phenothiazine) (PFCzOxd-*co*-PPTZ), different ratios of monomer 3 and 7 were also used. The co-monomer feed ratios of monomer 3 to phenothiazine unit are 99:1, 97:3, 95:5, and 90:10 and the corresponding polymers were named as PFCzOxd-*co*-PPTZ1, PFCzOxd-*co*-PPTZ3, PFCzOxd-*co*-PPTZ5, and PFCzOxd-*co*-PPTZ10, respectively. The carbazole or phenothiazine unit in the polymer backbones was introduced to improve the device performance. All of the resulting polymers were soluble in organic solvents such as

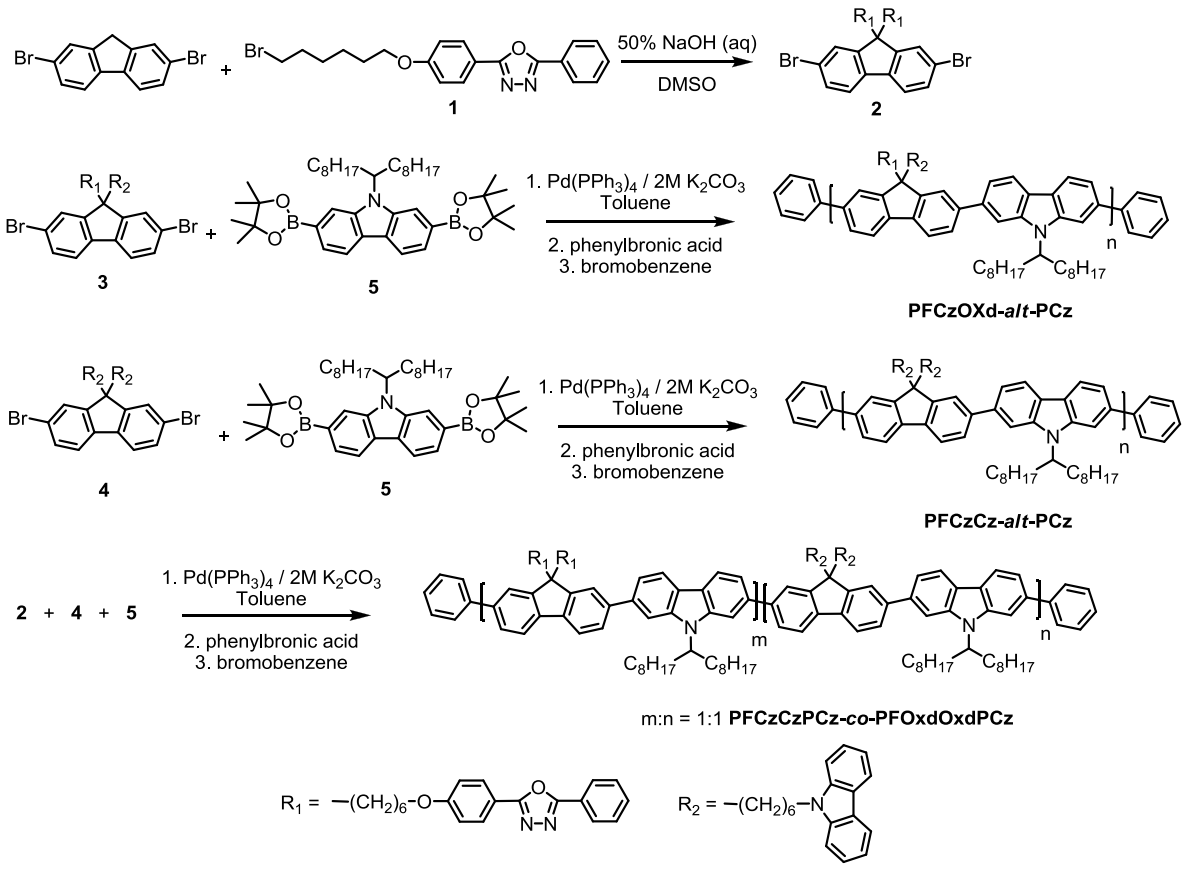

Scheme 1. Synthetic routes for the monomer and the polymers.

chloroform, chlorobenzene, THF, dichloromethane and ODCB. The polymerization results including molecular weight, polydispersity (PDI), and thermal stability of the polymers were summarized in Table 1. In the case of the copolymers via Suzuki coupling polymerization, the number-average molecular weights (M_n) and weight-average molecular weights (M_w) were 12,000-16,000 and 46,000-58,000, respectively. In the case of the random copolymers via Yamamoto polymerization, the number-average molecular weights (M_n) and weight-average molecular weights (M_w) were 30,000-52,000 and 100,000-165,000, respectively. The thermal properties of the polymers were characterized by both differential scanning calorimetry (DSC) and thermal gravimetric analysis (TGA) as shown in Table 1. DSC analysis was performed under nitrogen atmosphere (50 mL/min) on a DSC 822 at a heating rate of 10 ºC/min. TGA was performed with a DuPont951 TGA instrument in nitrogen atmosphere at a heating rate of 10 ºC/min to 600 ºC. TGA showed that copolymers are thermally stable with only about 5% weight loss at temperatures of 341-407 ºC, which could afford the advantages for the PLED device fabrication. The polymers showed good thermal stability with glass transition temperatures (T_g) of 74-109 ºC, using DSC performed at a temperature range of 30-250 ºC.

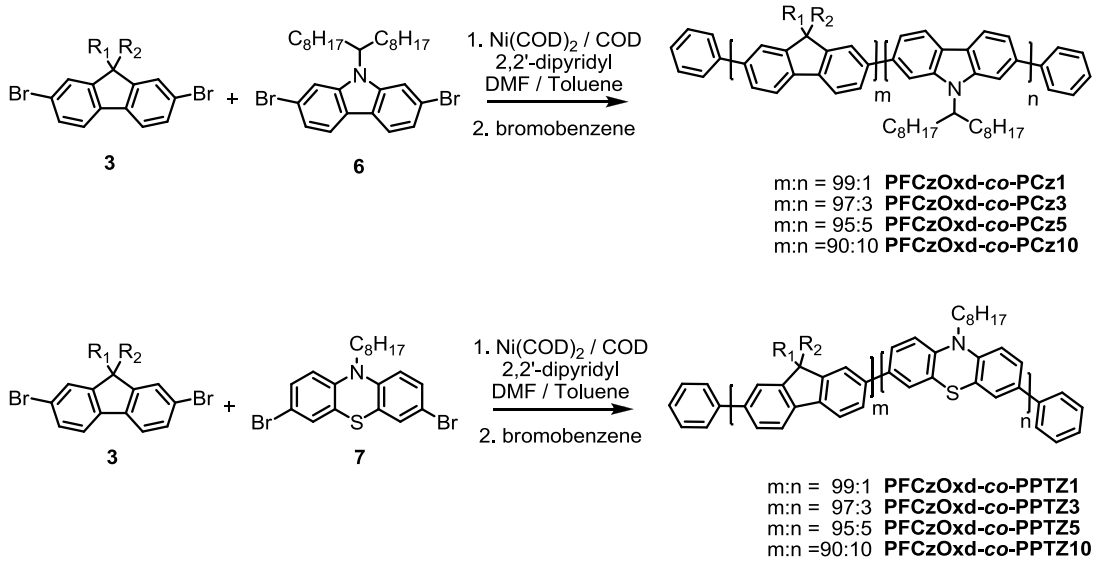

Scheme 2. Synthetic routes for copolymers by Yamamoto coupling reaction.

Table 1. Characterization of the synthesized polymers.

Polymers	M_n[a]	M_w[a]	PDI[a]	DSC(T_g)[b]	TGA(T_d)[c]
PFCzOxd-*alt*-PCz	12,000	47,000	3.92	74	375
PFCzCz-*alt*-PCz	16,000	58,000	3.63	84	407
PFCzCzPCz-*co*-POxdOxdPCz	12,000	46,000	3.83	83	394
PFCzOxd-*co*-PCz1	34,000	137,000	4.03	108	364
PFCzOxd-*co*-PCz3	36,000	131,000	3.64	101	367
PFCzOxd-*co*-PCz5	35,000	117,000	3.34	104	341
PFCzOxd-*co*-PCz10	43,000	143,000	3.32	100	361
PFCzOxd-*co*-PPTZ1	30,000	108,000	3.60	107	362
PFCzOxd-*co*-PPTZ3	38,000	116,000	3.05	106	371
PFCzOxd-*co*-PPTZ5	52,000	165,000	3.17	109	343
PFCzOxd-*co*-PPTZ10	32,000	100,000	3.13	108	371

[a]Molecular weight and Polydispersity (PDI) of the polymers were determined by gel permeation chromatography (GPC) in THF using polystyrene standards.
[b]Glass temperature was measured by DSC under N_2.
[c]Onset decomposition temperature (5 % weight loss) was measured by TGA under N_2.

4-3-2. Optical Properties

The absorption and photoluminescence (PL) properties of the synthesized polymers were investigated in chloroform solutions and the thin films by spin-coating on quartz plates from the solutions in ODCB, as summarized in Table 2. As shown in Figure 1, and 2, the adsorption peaks, corresponding to π–π transition of the conjugated backbones, appear at around 380–390 nm. The absorption spectra of the films are very similar to those of the solutions with all of the polymers. The absorption onset wavelengths of the polymers in the film states were around 430 nm, which corresponds to the band gap of 2.88 eV. The edge of the absorption spectra was red-shifted, caused by interactions between conjugated polymer chains in film, which results in a higher degree of exciton–exciton annihilation.[25]

Figure 3, and 4 shows the PL spectra of the polymers with the excitation of 380 nm in both chloroform solution and thin film. As shown in Figure 3, the solutions of the polymers (PFCzOxd-*alt*-PCz, PFCzCz-*alt*-PCz, PFCzCzPCz-*co*-PFOxdOxdPCz) showed PL emission peaks with a maximum at 418 nm, and a shoulder at 440 nm. The PL spectra of their thin films consist of typical vibronically structured bands comprising a maximum at 427 nm, a shoulder at 453 nm, and a broad tail at 490 nm. All of PL emission peaks in the film states were red-shifted about 10–20 nm as compared to those of the solutions, which can be attributed to increased interactions between conjugated polymer chains in the films, which results in a higher degree of exciton-exciton annihilation.[25] In case of the random copolymers containing carbazole units in the polymer backbone (Figure 4a), the PL spectra of the solutions were quite similar as compared to the case of polyfluorene. In contrast, the PL spectra of the thin films showed peaks at around 540 nm, caused by the aggregation due to the oxadiazole unit with electron withdrawing effect and carbazole unit with electron donating effect. As compared to the homopolymer, PFCzOxd, reported previously by us,[19]

Table 2. Characteristics of the UV-vis absorption and photoluminescence.

Polymers	Solution			Film			EL λ_{max} (nm)
	Abs λ_{max} (nm)	PL λ_{max} (nm)	Fwhm [a] of PL	Abs λ_{max} (nm)	PL λ_{max} (nm)	Fwhm [a] of PL	
PFCzOxd-*alt*-PCz	383	418	39	383	427	43	427, 541
PFCzCz-*alt*-PCz	386	418	39	383	428	45	425
PFCzCzPCz-*co*-POxd OxdPCz	383	418	39	383	428	47	425, 529
PFCzOxd-*co*-PCz1	388	419	40	384	430, 537	117	427, 543
PFCzOxd-*co*-PCz3	388	419	40	385	428, 534	100	428, 547
PFCzOxd-*co*-PCz5	387	419	40	383	429, 537	118	426, 541
PFCzOxd-*co*-PCz10	388	419	40	383	429, 539	144	428, 550
PFCzOxd-*co*-PPTZ1	384	418	41	383	430, 480	109	429, 488
PFCzOxd-*co*-PPTZ3	385	418	41	384	484	111	487
PFCzOxd-*co*-PPTZ5	386	418	42	383	487	111	492
PFCzOxd-*co*-PPTZ10	384	418	42	383	490	86	490

[a]Full width at half-maximum of PL spectra.

the intensity of the PL emission peak at long wavelength was enhanced by the incorporation of carbazole units in the backbone as low as 1% on the backbones. The PL emission of the random copolymers containing phenothiazine units was investigated as shown in Figure 4b. The PL emission peaks in the solutions were also quite similar to the case of fluorene. In the film state, all of the polymers showed two PL emission peaks at around 430 nm and 480 nm. With increasing amounts of phenothiazine contents, the PL spectra exhibit decreased peaks at 430 nm and increased peaks at 480 nm. Consequently, the PL emission peak at 430 nm was nearly quenched with phenothiazine contents of 10% in the copolymers.

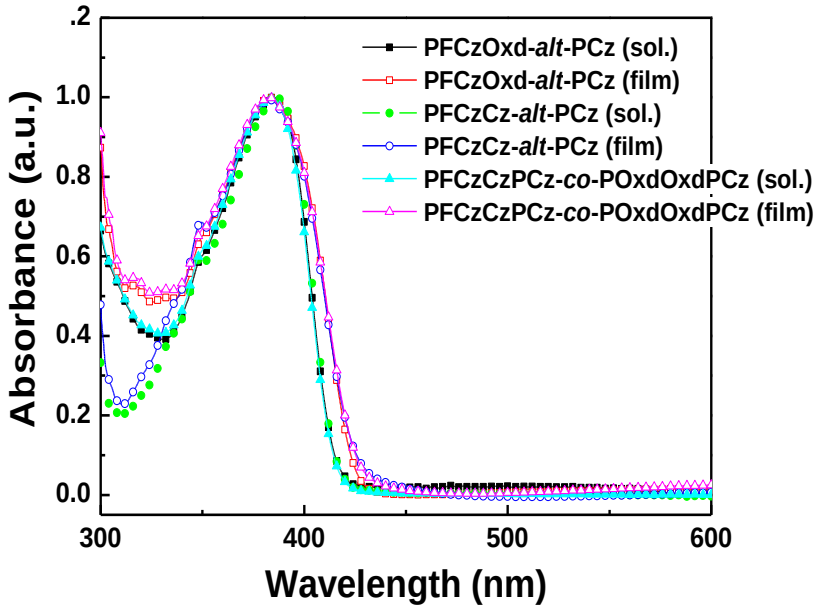

Figure 1. UV-vis absorption spectra of the alternating copolymers.

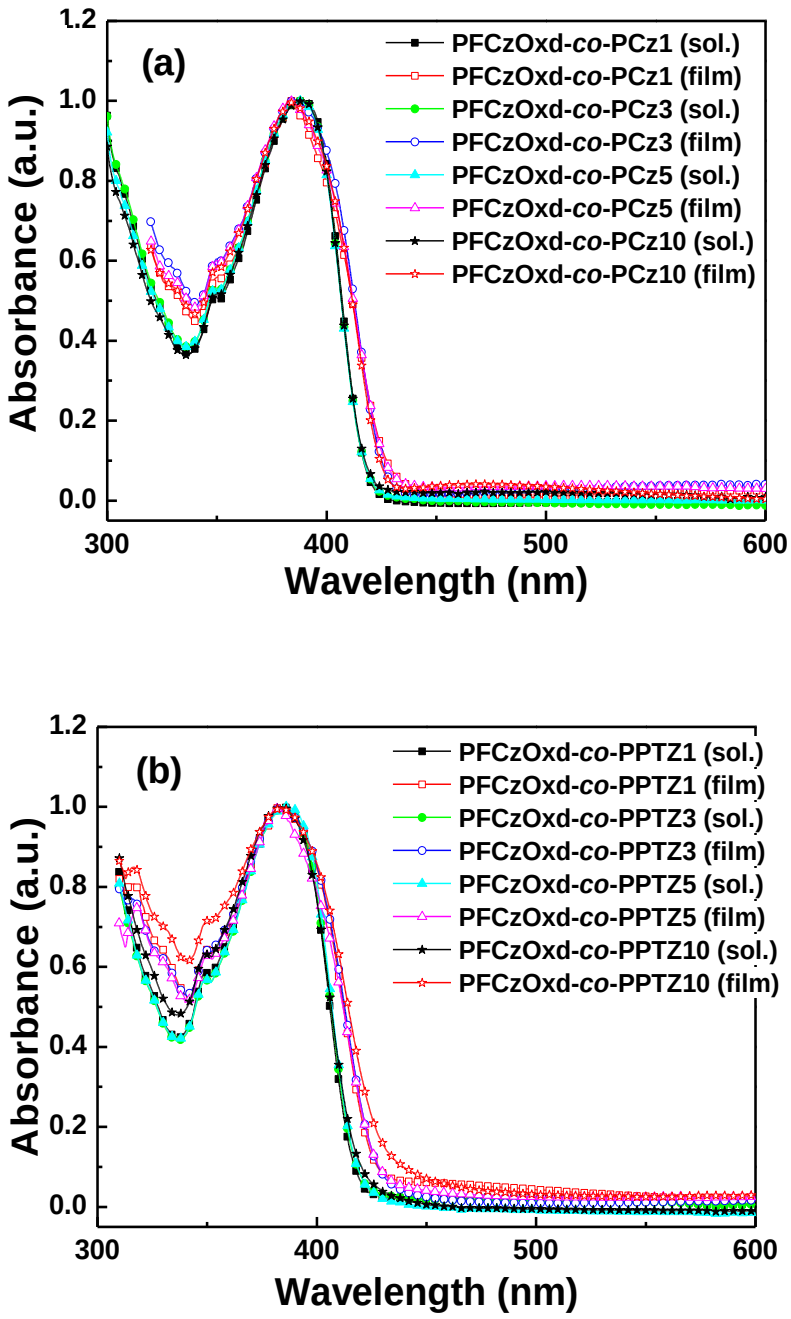

Figure 2. UV-vis absorption spectra of the polymers of random copolymers with PCz units (a), and random copolymers with PPTZ units (b).

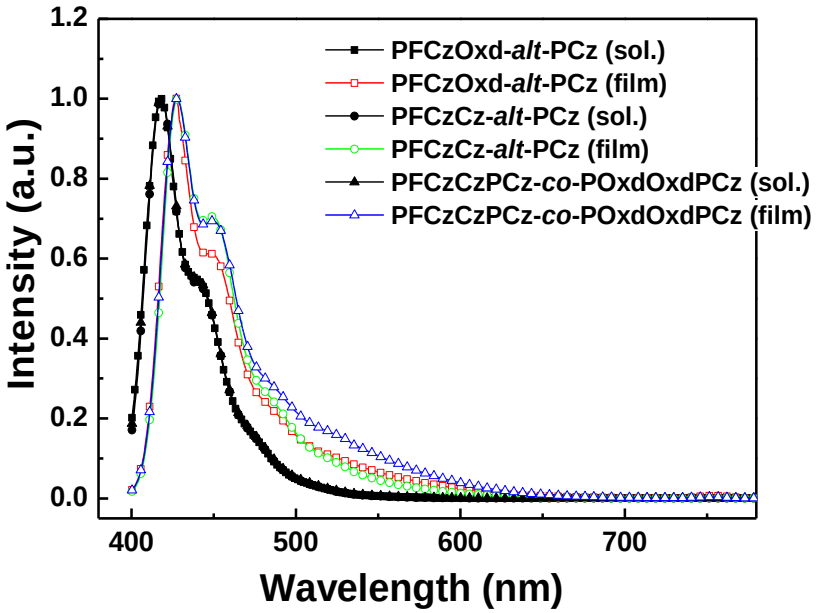

Figure 3. PL emission spectra of the alternating polymers.

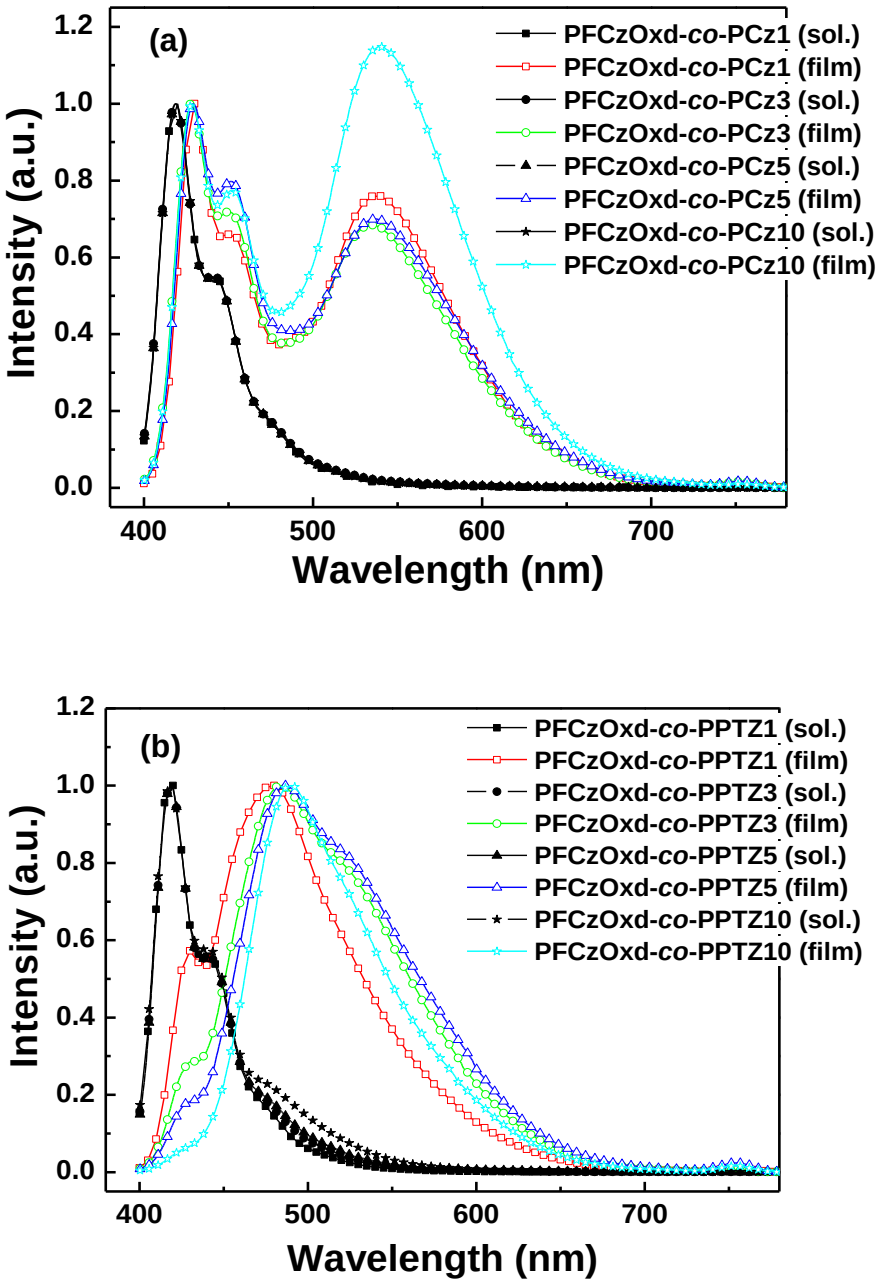

Figure 4. PL emission spectra of the random copolymers with PCz units (a), and random copolymers with PPTZ units (b).

4-3-3. Electrochemical Properties

The electrochemical properties of the polymer were determined from the band gap estimated from the absorption onset wavelength, and the HOMO energy level which was estimated from the cyclic voltammetry (CV). The CV was performed with a solution of tetrabutylammonium tetrafluoroborate (Bu_4NBF_4) (0.10 M) in acetonitrile at a scan rate of 100 mV/s at room temperature under argon atmosphere. A platinum electrode (~0.05 cm^2) coated with a thin polymer film was used as the working electrode. Pt wire and $Ag/AgNO_3$ electrode were used as the counter electrode and reference electrode, respectively. The energy level of the $Ag/AgNO_3$ reference electrode (calibrated by the Fc/Fc^+ redox system) was 4.8 eV below the vacuum level. The oxidation potentials derived from the onsets of electrochemical p-doping are summarized in Table 3. HOMO levels were calculated according to the empirical formula ($E_{HOMO} = -([E_{onset}]^{ox} + 4.8)$ eV). The polymers

Table 3. Electrochemical potentials and energy levels of the polymers.

Polymers	E_{onset}[a] (V)	HOMO[b] (eV)	LUMO[c] (eV)	E_g[d] (eV)
PFCzOxd-*alt*-PCz	0.87	-5.67	-2.78	2.89
PFCzCz-*alt*-PCz	0.86	-5.66	-2.76	2.90
PFCzCzPCz-*co*-POxdOxdPCz	0.88	-5.68	-2.80	2.88
PFCzOxd-*co*-PCz1	0.88	-5.68	-2.79	2.89
PFCzOxd-*co*-PCz3	0.88	-5.68	-2.78	2.90
PFCzOxd-*co*-PCz5	0.89	-5.69	-2.78	2.91
PFCzOxd-*co*-PCz10	0.89	-5.69	-2.79	2.90
PFCzOxd-*co*-PPTZ1	0.88	-5.68	-2.78	2.90
PFCzOxd-*co*-PPTZ3	0.88	-5.68	-2.78	2.90
PFCzOxd-*co*-PPTZ5	0.87	-5.67	-2.77	2.90
PFCzOxd-*co*-PPTZ10	0.87	-5.67	-2.79	2.88

[a]Onset oxidation and reduction potential measured by cyclic voltammetry.
[b]Calculated from the oxidation potentials.
[c]Calculated from the HOMO energy levels and optical band gap.
[d]Optical energy band gap was estimated from the onset wavelength of the optical absorption.

exhibited the absorption onset wavelengths of 426-430 nm in solid thin films, which correspond to the band gaps of 2.88–2.91 eV. The polymers exhibit irreversible processes in an oxidation scan. The oxidation onsets of the polymers were estimated to be 0.86–0.89 V, which corresponds to HOMO energy levels of –5.66 ~ –5.69 eV. The LUMO energy levels of the polymers can be calculated with the HOMO energy levels and optical band gaps. The LUMO energy levels of the polymers were thus determined to be –2.76 ~ –2.80 eV.

4-3-4. Electroluminescence Properties

The investigations of electroluminescence properties of the copolymers were conducted by fabricating the devices with the configuration of ITO/PEDOT:PSS (40 nm)/Polymer (80 nm)/Ca (10 nm)/Al (100 nm). The electroluminescence (EL) spectra of the devices are shown in Figure 5, and 6. In case of PFCzOxd-*alt*-PCz and PFCzCzPCz-*co*-PFOxdOxdPCz, the EL spectra of the polymers showed two distinct peaks comprising the maximum at 427 nm, which corresponds to the peak of the polyfluorene, and additional large one at around 540 and 530 nm, respectively. As compared to homopolymer, PFCzOxd,[19] the intensities of the long wavelength EL peaks at 540 and 530 nm were obviously enhanced

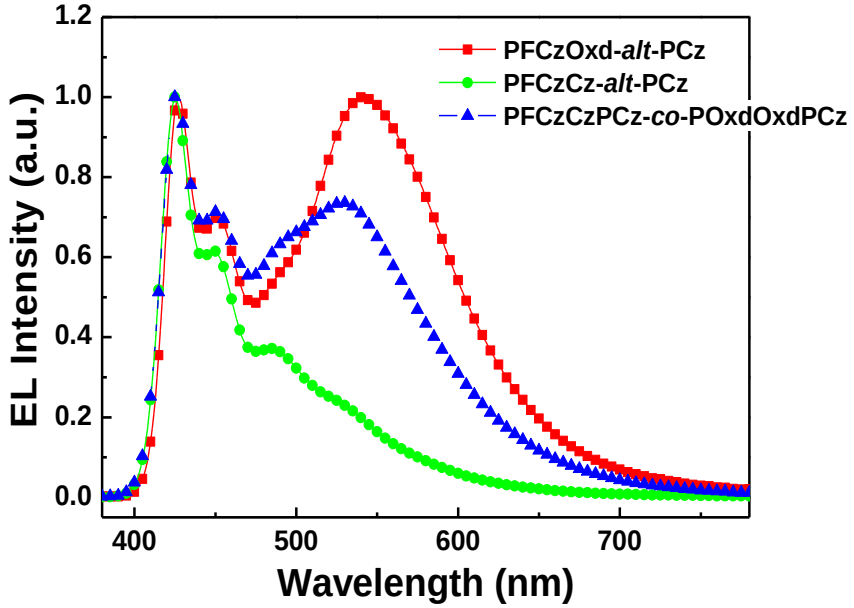

Figure 5. EL spectra of the alternating polymers.

by the incorporation of carbazole units at the polymer backbones. The CIE coordinates of the devices with PFCzOxd-*alt*-PCz and PFCzCzPCz-*co*-PFOxdOxdPCz were (0.28, 0.33) and (0.25, 0.32), respectively, which are close to that of the standard white of National Television System Committee (NTSC) (0.33, 0.33). On the other hand, the EL spectrum of PFCzCz-*alt*-PCz exhibited maximum peak at 427 nm and CIE coordinates of (0.18, 0.17),

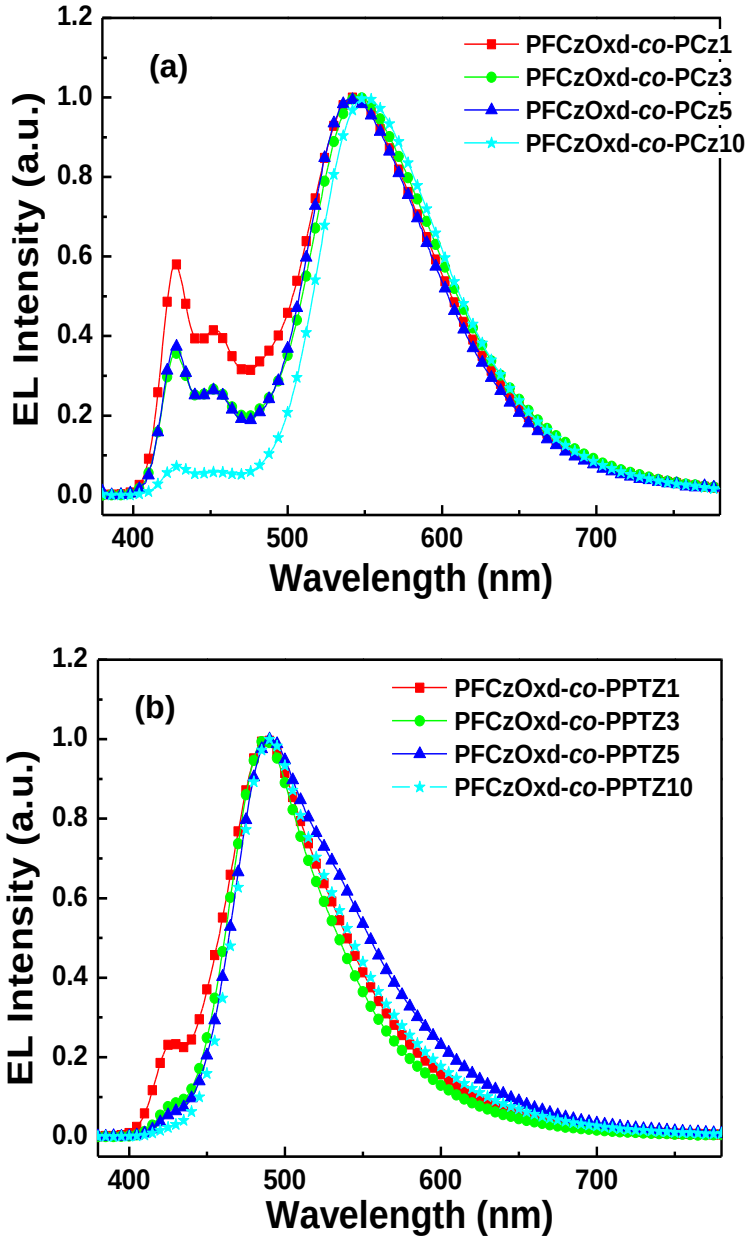

Figure 6. EL spectra of the random copolymers with PCz units (a), and the random copolymer with PTTz units.

corresponding to blue light emission. In case of PFCzCz-*alt*-PCz, there is no oxadiazole unit in any part of the structure. It suggests that the oxadiazole units played an important role in the generation of the long-wavelength peak. The long-wavelength peaks can be attributed to the aggregation caused by the oxadiazole unit with electron withdrawing effect and carbazole unit with electron donating effect. As shown in Figure 6a and b, the effects of the carbazole and phenothiazine units on the EL spectra were also investigated. Typical EL spectra of PFCzOxd-*co*-PCzs and PFCzOxd-*co*-PPTZs were nearly same as compared to the PL of the solid films of the polymers, indicating that the EL and PL phenomena originated from the same excited state. The PFCzOxd-*co*-PCzs and PFCzOxd-*co*-PPTZs showed additional large peak at around 530 and 500 nm, respectively, caused by the aggregation and the excimer formation. The oxadiazole and carbazole pendants in the fluorine unit do not affect the effective conjugation length of the polymers directly, since the oxadiazole and carbazole moieties were introduced as pendants using nonconjugated chain. However, CIE coordinates of synthesized copolymers for white light is not better than that of PFCzOxd caused by more aggregation between pendant unit and carbazole or phenothiazine units in the backbone. The aggregate is formed by aggregation of several neighboring polymer segments at the ground state.[26] The long-wavelength peaks of EL spectra are enhanced by aggregate at ground state, excimer or exciplex at excited state, and electric-field-induced complex (electromer or electroplex).[25] The current density-voltage (*J*–*V*), luminescence-voltage (*L*–*V*), and efficiency characteristics of ITO/PEDOT:PSS/Polymer/Ca/Al devices are shown in Figure 7, 8, and 9, respectively, and summarized in Table 4. The maximum brightness of the devices was in the range of 300–1420 cd/m^2. The luminescence efficiency of the polymers are higher than 0.1 cd/A, except the cases of PFCzCz-*alt*-PCz (0.03 cd/A) and PFCzOxd-*co*-PPTZ10 (0.07 cd/A). Among all the devices, the device fabricated from PFCzOxd-*co*-PCz10 showed the best performance with the efficiency of 0.17 cd/A, caused by the hole transporting ability of the carbazole unit in the polymer backbone.

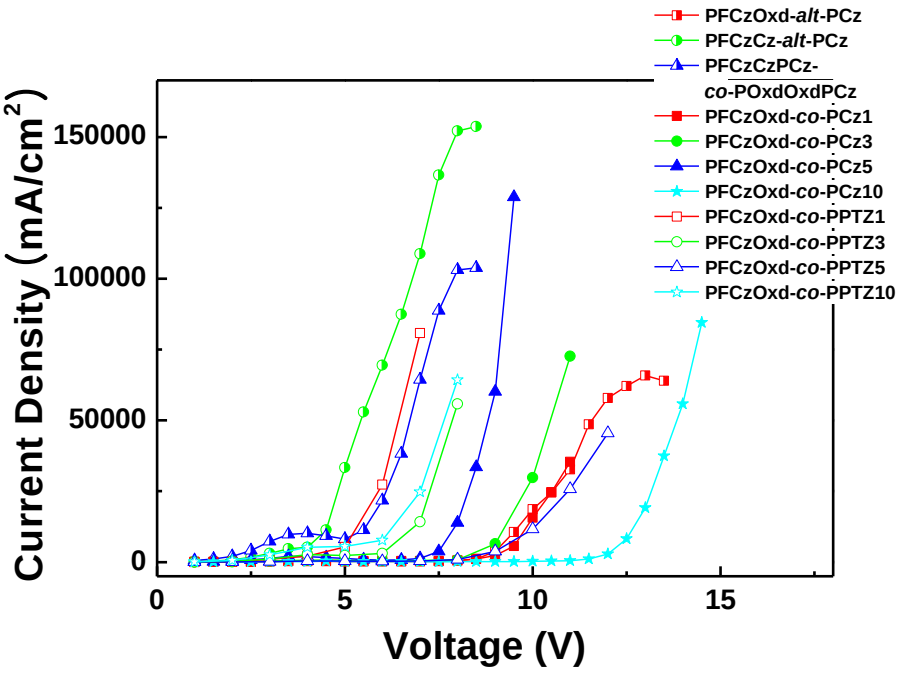

Figure 7. Current density-voltage characteristics of OLED with the configuration of ITO/PEDOT:PSS/Polymer/Ca/Al.

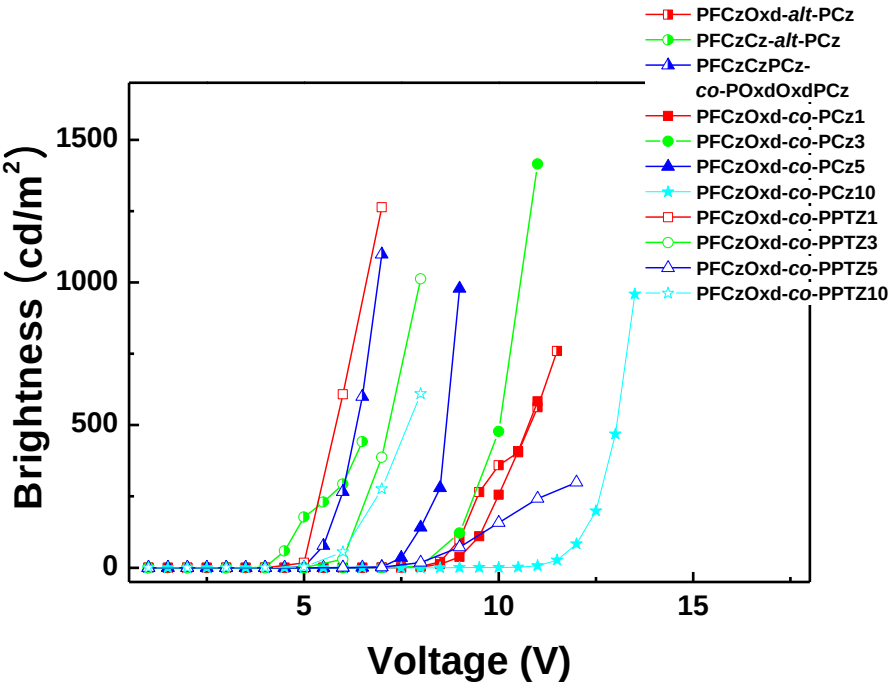

Figure 8. Luminescence-voltage characteristics of OLED with the configuration of ITO/PEDOT:PSS/Polymer/Ca/Al.

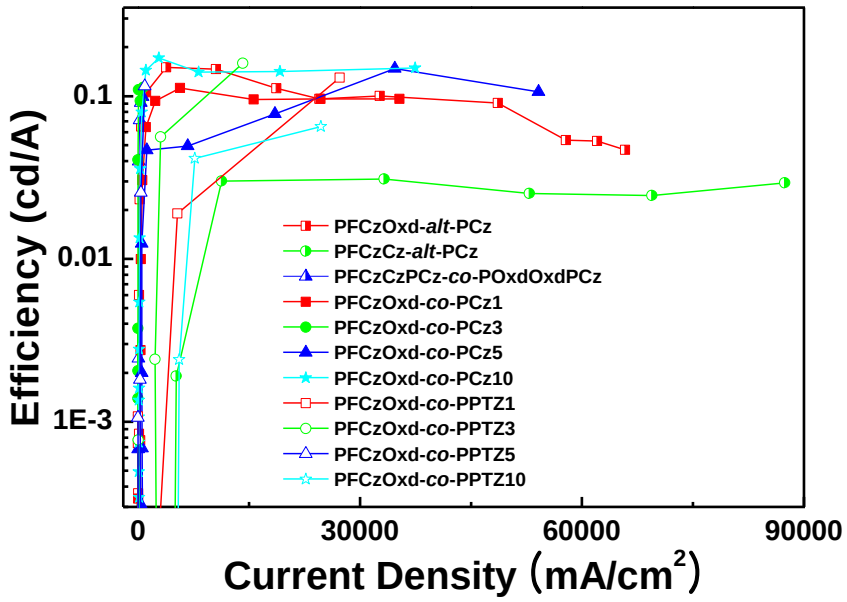

Figure 9. Efficiency-voltage characteristics of OLED with the configuration of ITO/PEDOT:PSS/Polymer/Ca/Al.

Table 4. Device performance characteristics of devices with the configuration of ITO/PEDOT:PSS/Polymer/Ca/Al.

Polymers	Turn-on voltage[a] (V)	Voltage[b]	Current density[b] (mA/cm^2)	Luminance[b] (cd/m^2)	LE_{max}[c] (cd/A)	CIE (x, y)[d]
PFCzOxd-*alt*-PCz	7.5	11.5	48600	760	0.15	(0.28, 0.33)
PFCzCz-*alt*-PCz	3.5	6.5	87400	440	0.03	(0.18, 0.17)
PFCzCzPCz-*co*-POxdOxdPCz	4.5	7.0	64400	1100	0.10	(0.25, 0.32)
PFCzOxd-*co*-PCz1	7.5	11.0	35300	580	0.11	(0.33, 0.42)
PFCzOxd-*co*-PCz3	7.0	11.0	72700	1420	0.11	(0.36, 0.46)
PFCzOxd-*co*-PCz5	4.0	7.0	60200	980	0.15	(0.33, 0.44)
PFCzOxd-*co*-PCz10	10	13.5	37400	960	0.17	(0.41, 0.52)
PFCzOxd-*co*-PPTZ1	4.0	7.0	80800	1260	0.13	(0.21, 0.34)
PFCzOxd-*co*-PPTZ3	4.0	8.0	55800	1000	0.16	(0.20, 0.37)
PFCzOxd-*co*-PPTZ5	6.5	12.0	45400	300	0.12	(0.24, 0.42)
PFCzOxd-*co*-PPTZ10	4.5	8.0	64200	610	0.07	(0.22, 0.41)

[a]Voltages required to achieve a brightness of 1 cd/m^2.

[b]Measured under the condition of maximum brightness.

[c]Maximum luminescence efficiency.

[d]Calculated from the EL spectrum.

4-4. Conclusion

We report here the synthesis, characterization and EL properties of novel conjugated copolymers based on fluorene with carbazole and oxadiazole pendants for the generation of the white emission. The polymers exhibited the absorption peak at around 380–390 nm with both of solutions and thin films. The solid films of PFCzOxd-*co*-PCzs showed PL emission peak at around 430 nm and 530 nm. The peak at 530 nm was increasing with higher contents of carbazole unit in the backbone. The solid films of PFCzOxd-*co*-PPTZs showed major peak at around 500 nm with decreased peak at 430 nm. In the case of PFCzOxd-*alt*-PCz and PFCzCzPCz-*co*-PFOxdOxdPCz, the EL spectra of the polymers showed two distinct peaks comprising the maximum peak at 427 nm and additional one at around 540 and 530 nm, respectively. The CIE coordinates of the devices with PFCzOxd-*alt*-PCz and PFCzCzPCz-*co*-PFOxdOxdPCz were (0.28, 0.33) and (0.25, 0.32), respectively, approaching the value of the standard white of NTSC (0.33, 0.33).

4-5. References

1. Burroughes, J. H.; Jones, C.A.; Friend, R. H.; *Nature* (*London*) **1998**, 335, 137.
2. Yu, G.; Heeger, A. J. *J. Appl. Phys.* **1995**, 78, 4510.
3. Halls, J. J. M.; Walsh, C. A.; Greenham. N. C.; Marseglia, E. A.; Friend, R. H.; Moratti, S. C. et al. *Nature* (*London*) **1995**, 376, 498.
4. Burroughes, J. H.; Bradley, D. D. C.; Brown, A. R.; Marks, R. N.; Mackay, K.; Friend, R. H. et al. *Nature* (*London*) **1990**, 347, 539.
5. Gustafsson, G.; Cao, Y.; Treacy, G. M.; Klavetter, F.; Colaneri, N.; Heeger, A. J. *Nature* (*London*) **1992**, 357, 477.
6. Huang, F.; Hou, L., Wu, H.; Wang, X.; Shen, H.; Cao, W. et al. *J. Am. Chem. Soc.* **2004**, 126, 9845.
7. Cho, H.J.; Jung, B. J.; Cho, N. S.; Lee, J.; Shim, H. K. *Macromolecules* **2003**, 36, 6704.
8. Grisorio, R.; Suranna, G. P.; Mastrorilli, P.; Nobile, C. F. *Org. Lett*. **2007**, 9, 3149.

9. Jin, Y.; Kim, J.; Lee, S.; Kim, J. Y.; Park, S. H.; Lee, K. et al. *Macromolecules* **2004**, 37, 6711.
10. Kido, J.; Kimura, M.; Nagai, K. *Science* **1995**, 267, 1332.
11. Jordan, R. H.; Dodabalapur, A.; Strukelj, M.; Miller, T. M. *Appl. Phys. Lett*. **1996**, 68, 1192.
12. Wang, Y. Z.; Sun, R. G.; Meghdadi, F.; Leising, G.; Epstein, A. *J. Appl. Phys. Lett*. **1999**, 74, 3613.
13. Lee, S. K.; Ahn, T.; Cho, N. S.; Lee, J. I.; Jung, Y. K.; Lee, J. et al. *J. Polym. Sci. Part A Polym. Chem*. **2007**, 45, 1199.
14. Berggren, M.; Inganas, O.; Gustafsson, G.; Rasmusson, J.; Andersson, M. R.; Hjertberg, T. et al. *Nature*, **1994**, 4, 815.
15. Lee, S. K.; Hwang, D. H.; Jung, B. J.; Cho, N. S.; Lee, J.; Lee, J. D. et al. *Adv. Funct. Mater*. **2005**, 15, 1647.
16. Chuang, C. Y.; Shih, P. I.; Chien, C. H.; Wu, F.I.; Shu, C. F. *Macromolecules* **2007**, 40, 247.
17. Park, M. J.; Lee, J.; Park, J. H.; Lee, S. K.; Lee, J. I.; Chu, H. Y. et al. *Macromolecules* **2008**, 41, 3063.
18. Jeong, E.; Kim, S. H.; Jung, I. H.; Xia, Y.; Lee, K.; Suh, H. et al. *J. Polym. Sci. Part A Polym. Chem*. **2009**, 47, 3467.
19. Jin, Y.; Song, S.; Kim, J. Y.; Kim, H.; Lee, K.; Suh, H. *Thin Solid Films* **2008**, 516, 7373.
20. Liao, J. L.; Chen, X.; Liu, C. Y.; Chen, S. A.; Su, C. H.; Su, A. C. *J. Phys. Chem. B* **2007**, 111, 10379.
21. Song, S.; Jin, Y.; Kim, S. H.; Shim, J. Y.; Son, S.; Kim, I. et al. *J. Polym. Sci. Part A Polym. Chem.* **2009**, 47, 6540.
22. Blouin, N.; Michaud, A.; Leclerc, M. *Adv. Mater.* **2007**, 19, 2295.
23. Zou, Y. P.; Wu, W. P.; Sang, G. Y.; Yang, Y.; Liu, Y. Q.; Li, Y. F. *Macromolecules* **2007**, 40, 7231.
24. Sang, G. Y.; Zou, Y. P.; Li, Y. F. *J. Phys. Chem. C* **2008**, 112, 12058.

25. Nguyen, T.Q.; Martini, I. B.; Lei, J.; Schwartz, B. J. *J. Phys. Chem. B* **2000**, 104, 237.
26. Lee, Y.Z.; Chen, X.; Chen, M. C.; Chen, S. A.; Hsu, J. H.; Fann, W. *Appl. Phys. Lett.* **2001**, 79, 308.

LIST OF PUBLICATIONS

Published Articles

1. **Crystallization of Tiatnia Ultra-Fine Particles from Peroxotitanic Acid in Aqueous Solution in the Presence of Polymer and Incorporation into Poly(methyl methacrylate) via Dispersion in Organic Solvent**
   Yamada, S.; Wang, Z.; Mouri, E.; Yoshinaga, K. *Colloid and Polymer Science* **2009**, 287, 139.

2. **Controlled Crystallization of Titanium Dioxide Particles in the Presence of Poly(vinyl alcohol) from Peroxotitanic Acid.**
   Wang, Z.; Yamada, S.; Zhang, M.; Kanzaki, H.; Yoshinaga, K. *Colloid and Polymer Science* **2010**, 288, 433.

3. **Incorporation of TiO_2 Nanoparticles, Formed via Sol-Gel Process in Micelle of Block Copolymer, into Poly(methyl methacrylate) to Fabricate High Refractive and Transparent Hybrid Materials**
   Yamada, S.; Wang, Z.; Yoshinaga, K. *Chemistry Letters* **2009**, 38, 828.

4. **Incorporation of Titanium Dioxide Particles into Polymer Matrix Using Block Copolymer Micelles for Fabrication of High Refractive and Transparent Organic-Inorganic Hybrid Materials**
   Yamada, S.; Mouri, E.; Yoshinaga, K. *Journal of Polymer Science Part A Polymer Chemistry* **2011**, 49, 712.

5. **Synthesis and Characterization of Fluorene-Carbazole and Fluorene-Phenothiazine Copolymers with Carbazole and Oxadiazole Pendants for Organic Light Emitting Diodes**
   Yamada, S.; Park, S.; Song, S.; Heo, M.; Shim, J. Y.; Jin, Y.; Kim, I.; Lee, H.; Lee, K.; Yoshinaga, K.; Kim, J. Y.; Suh, H. *Polymer* **2010**, 51, 6174.

Review Article in Japanese

山田修平，吉永耕二； 総説 エポキシ樹脂 最近の進歩Ⅰ，第4章 硬化物の物性，4. 3 光学的機能，4. 3. 1 高屈折率有機-無機ハイブリッド材料，エポキシ樹脂技術協会，174－179, (2009).

Conference Presentations

1. **Controlled Crystallization of Titania Ultrafine Particles in the Presence of Hydrophilic Polymer and Dispersion into Organic Media**
   Yamada, S.; Karakawa, H.; Mouri, E.; Yoshinaga, K.; Nakai, A. Polymer Preprints, Japan, Vol. 55 No. 1, pp 1148 (2006).

2. **Preparation of Titanium Dioxide Nanoparticles-Dispersed Transparent PMMA Polymer Films**
   Yamada, S.; Mouri, E.; Yoshinaga, K. Polymer Preprints, Japan, Vol. 57 No. 1, pp 1114 (2008).

3. **Synthesis of Titania Particles Using Block Copolymer Micelles Solutions and Fabrication for High Refractive Hybrid Film**
   Yamada, S.; Mouri, E.; Yoshinaga, K. The 2nd International Symposium on Advanced Particles, Abstract, pp 125 (2009).

4. **Preparation of Metal Oxide Particles Using Polymer Micelles and Application for High Refractive and Transparent Films**
   Yamada, S.; Mouri, E.; Yoshinaga, K. KJF International Conference on Organic Materials for Electronics and Photonics, Abstract, pp 149 (2010).

5. **Synthesis of Mono-dispersed TiO_2 Particles from Polymer Micelles and their High Refractive and Transparent Hybrid Films**
   Yamada, S.; Mouri, E.; Yoshinaga, K. 3rd EuCheMS Chemistry Congress, Abstract, pp 519 (2010).

6. **Fabrication of High Refractive and Transparent PMMA/TiO_2 Hybrid Film**
   Yamada, S.; Mouri, E.; Yoshinaga, K. Pacifichem 2010, Macromolecule-1286 (2010).